

HEC-18 Evaluating Scour at Bridges (Richardson and Davis, 2001)

HEC-20 Stream Stability at Highways (Lagasse et al., 2001a)

HEC-23 Bridges Scour and Stream Instability Countermeasures (Lagasse et al., 2001b)

The flow chart in Figure 18.0.4 illustrates the interrelationship between these three documents and emphasizes that they should be used as a set. Another document of interest is the River Engineering for Highway Encroachments, Hydraulic Design Series (HDS) No. 6 (Richardson et al., 2001). All four of these documents (HEC-18, HEC-20, HEC-23, and HDS-6) can be obtained on the Web at: <http://www.fhwa.dot.gov/bridge/hydpub.htm>.

18.1 PROPERTIES OF SEDIMENT

18.1.1 Size and Shape

Grain size is the most important property affecting transportability of sediment. Table 18.1.1 shows the size classification of sediment particles with their corresponding units in millimeters as well as inches, used in the computer code HEC-6 developed by the U.S. Army Corps of Engineers (1991), Hydrologic Engineering Center.

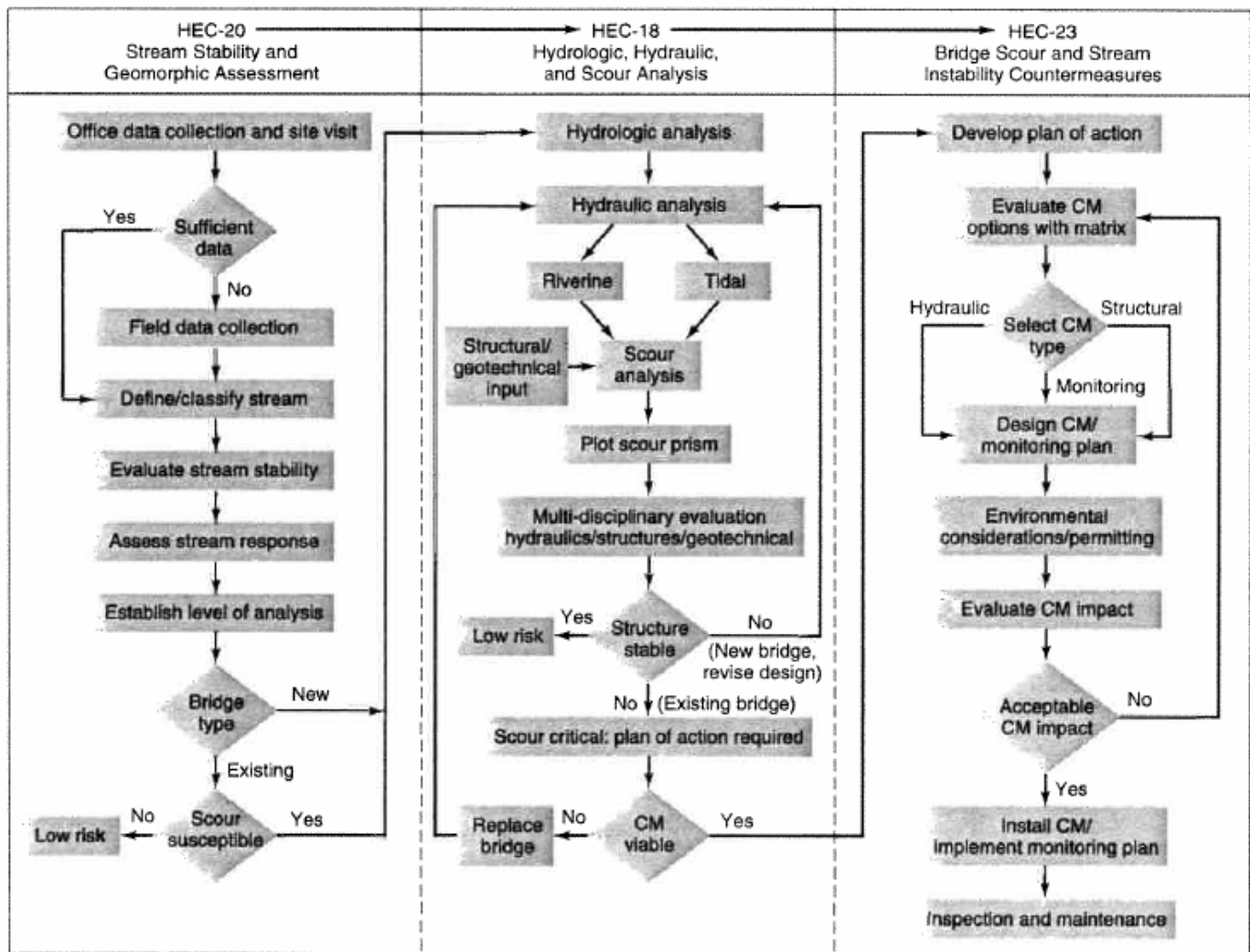


Figure 18.0.4 Flow chart for scour and stream stability analysis and evaluation (Lagasse et al., 1995).

Table 18.1.1 Scale for Size Classification of Sediment Particles (USACE, 1991)

Class Name	Millimeters	Feet	PHI Value
Boulders	>256	–	<–8
Cobbles	256–64	–	–8 to –6
Very Coarse Gravel (VCG)	64–32	.148596	–6 to –5
Coarse Gravel (CG)	32–16	.074216	–5 to –4
Medium Gravel (MG)	16–8	.037120	–4 to –3
Fine Gravel (FG)	8–4	.018560	–3 to –2
Very Fine Gravel (VFG)	4–2	.009279	–2 to –1
Very Coarse Sand (VCS)	2.0–1.0	.004639	–1 to 0
Coarse Sand (CS)	1.0–0.50	.002319	0 to +1
Medium Sand (MS)	0.50–0.25	.001160	+1 to +2
Fine Sand (FS)	0.25–0.125	.000580	+2 to +3
Very Fine Sand (VFS)	0.125–0.0625	.00288	+3 to +4
Coarse Silt	0.0625–0.031	.000144	+4 to +5
Medium Silt	0.031–0.016	.000072	+5 to +6
Fine Silt	0.016–0.008	.000036	+6 to +7
Very Fine Silt	0.008–0.004	.000018	+7 to +8
Coarse Clay	0.004–0.0020	.000009	+8 to +9
Medium Clay	0.0020–0.0010	–	+9 to +10
Fine Clay	0.0010–0.0005	–	+10 to +11
Very Fine Clay	0.0005–0.00024	–	+11 to +12
Colloids	<0.00024	–	>+12

Natural sediments are of irregular shape and therefore any single diameter used to characterize a certain group of grains must be chosen according to some convenient method of measurement. The usually adopted diameters are:

- Triaxial diameters** (a , b , and c): These sizes represent the major, intermediate, and minor dimensions of the particle measured along mutually perpendicular axes.
- Sieve diameter** (D): This size indicates the size of the sieve opening through which the particle will just pass.
- Sedimentation diameter** (D_s): This size represents the diameter of a sphere of the same specific weight and fall velocity as the given particle in the same sedimentation fluid with the same temperature. This is also called the *fall diameter*.
- Nominal diameter** (D_n): This represents the diameter of a sphere having the same volume as the given particle.
- Geometric mean diameter** (D_g): This is the square root of the product of the maximum and minimum size limits in a range. For example, a very coarse sand with size range of 1.00–2.00 mm has a geometric mean of 1.414 mm (i.e., $(1 \cdot 2)^{1/2}$). Table 18.1.1 lists the geometric mean diameters (D_g) that correspond to the grain size classification adopted by the U.S. Army Corps of Engineers (1991).
- Mean diameter** (D_m): This size is the representative grain size computed from the relation:

$$D_m = (p_1 D_1 + p_2 D_2 + \dots + p_n D_n) / (p_1 + p_2 + \dots + p_n) \quad (18.1.1)$$

where p_1, p_2, \dots, p_n are the grain size fractions associated with size classifications 1, 2, \dots , n and D_1, D_2, \dots, D_n are the average diameters for size classifications 1, 2, \dots , n .

- (g) **Median diameter (D_{50}):** This diameter corresponds to the 50 percent finer by weight (or by volume) in the size distribution curve called the *gradation curve*. In general, D_p is used to indicate that p percent (by weight or by volume) of the sample has a diameter smaller than D_p .

18.1.2 Measurement of Size Distribution

Size determination by means of sieving can in principle be used for particles as small as 50 μm , but gives good results for particles down to 75 μm (sand fraction). Sieve sizes (openings) are made in a geometric series with every sieve being $(2)^{1/4}$ larger in size than the preceding. Taking every other sieve gives a $(2)^{1/2}$ series, whereas taking every fourth gives a ratio of 2 between adjacent sieve sizes. When the sand is fairly uniform (i.e., σ_g is fairly small), the $(2)^{1/4}$ series should be used.

18.1.3 Settling Analysis for Finer Particles

18.1.3.1 Grain Size Distribution

By means of sieving, a grain size distribution of the bed-material sample can be obtained, which generally shows a relation between percentages by weight versus grain size, called the *gradation curve*. Figure 18.1.1 shows an example of a gradation curve. The cumulative size distribution of most samples can be approximated by a log-normal distribution, so by using logarithmic probability scale, a more or less straight line is found. For an approximately log-normal distribution, the *geometric mean diameter* can be defined as:

$$D_g = (D_{84} * D_{16})^{1/2} \tag{18.1.2}$$

where D_{84} and D_{16} are the diameters that indicate that 84 percent and 16 percent by weight of the sample has a diameter smaller than D_{84} and D_{16} , respectively. D_g for a log-normal distribution is equal to D_{50} .

The *geometric standard deviation*, σ_g , associated with D_g can be determined as follows:

$$\sigma_g = \frac{1}{2} [D_{84}/D_g + D_g/D_{16}] \tag{18.1.3}$$

For log-normal grain size distribution, the mean diameter, D_m , is determined as follows:

$$D_m = D_g \exp [0.5 \ln \sigma_g^2] \tag{18.1.4}$$

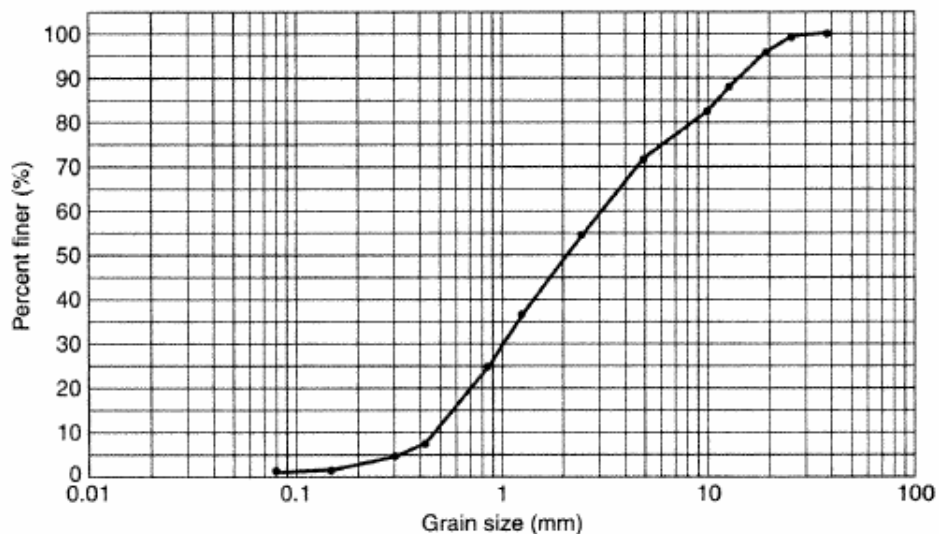


Figure 18.1.1 Gradation curve for the soil aggregates analyzed in Example 18.1.1.

In geological literature, the diameters are often expressed in Φ -units, where $\Phi = -\log 2D_{50}$ (with D_{50} expressed in mm), $\Phi = 0$ for $D_{50} = 1$ mm, and $\Phi = 1$ for $D_{50} = 0.5$ mm.

EXAMPLE 18.1.1

Use the sieve analysis data in column (1) and (2) of Table 18.1.2 to develop a gradation curve.

Table 18.1.2 Sieve Analysis Data for Example 18.1.1

(1) Sieve Size (mm)	(2) Weight of Material Retained (lbs)	(3) % Material Retained	(4) % Material Finer
1.5" (37.5 mm)	0.00	0.00	100.00
1.0" (25.0 mm)	0.25	0.83	99.17
0.75" (19.0 mm)	1.00	3.30	95.87
0.50" (12.5 mm)	2.25	7.44	88.43
0.375" (9.5 mm)	1.75	5.78	82.65
0.25" (4.75 mm)	3.25	10.74	71.91
No. 8 (2.36 mm)	5.20	17.19	54.72
No. 16 (1.20 mm)	5.35	17.68	37.04
No. 20 (0.84 mm)	3.50	11.57	25.47
No. 40 (0.42 mm)	5.45	18.02	7.45
No. 50 (0.30 mm)	0.85	2.81	4.64
No. 100 (0.15 mm)	0.90	2.98	1.55
No. 200 (0.08 mm)	0.25	0.83	0.83
Pan	0.25	0.83	0.00
Total	30.25 lbs	100.00%	

SOLUTION

Column (3) in Table 18.1.2 lists the percent of material retained. Column (4) lists the percent of material finer. For example, 1.5 in. (37.5 mm) is the largest size so that 100 percent of the material is finer. The resulting gradation curve is plotted in Figure 18.1.1.

18.1.3.2 Particle Shape

In addition to the diameter of the grain particles, their shape and roundness is also important. *Shape* describes the form of the particle without reference to the sharpness of its edges, whereas *roundness* depends on the sharpness or radius of curvature of the edges. For example, a flat particle will have a smaller fall velocity than a sphere, but bed load will be more difficult to transport. Several definitions are used to characterize the shape:

- Sphericity:** The ratio of the surface area of a sphere with the same volume as the particle, to the surface area of that particle.
- Roundness:** The ratio of the average radius of curvature of the edges, to the radius of a circle that can be inscribed within the maximum projected area of the particle.
- Shape factor:** $S.F. = c/(ab)^{1/2}$ with a, b, and c being the major, intermediate, and minor dimensions of the particle measured along mutually perpendicular axes. For spheres, $S.F. = 1$; for natural sands, $S.F. \sim 0.7$. Because sphericity and roughness are difficult to determine in practice, the shape factor does have practical application. As an example, the fall velocity of a particle can be expressed in terms of the nominal diameter, shape factor, and Reynolds number.

18.1.4 Fall Velocity

Fall velocity (or *settling velocity*) is the velocity at which a sediment particle falls through a fluid. This velocity reflects the particle size, shape, and weight, as well as the fluid characteristics. Consider a sphere of diameter D that is released at zero velocity in a quiescent fluid (water). As the fall velocity W increases, fluid resistance reduces the acceleration to an equilibrium. At equilibrium, the gravity force is in balance with the drag force and a *terminal velocity* W_T exists.

Relationships for the fall velocity can be developed using the impulse-momentum principle:

$$\sum F_y = \frac{d}{dt} \int_{CV} v_y \rho dV + \sum_{CS} v_y (\rho V \cdot A) \quad (3.4.7)$$

Referring to Figure 18.1.2, the forces are the gravity force, F_g , the buoyant force, F_B , and the resistance or drag force, F_D .

$$\sum F_y = F_g - F_D - F_B \quad (18.1.5)$$

The gravity force is expressed as

$$F_g = \left(\frac{\pi}{6} D^3 \right) \gamma_s \quad (18.1.6)$$

where $\left(\frac{\pi}{6} D^3 \right)$ is the volume of the sphere and γ_s is the specific weight of the sphere. The buoyant force is due to the displaced fluid (see Section 3.5.2).

$$F_B = \frac{\pi}{6} D^3 \gamma \quad (18.1.7)$$

where γ is the specific weight of water. The drag (resistance) force is

$$F_D = C_D \left(\frac{\pi}{4} D^2 \right) \rho \frac{W^2}{2} \quad (18.1.8)$$

where C_D is the *drag coefficient*, which is a function of the Reynolds number for a sphere (see Figure 18.1.3). C_D is the ratio of drag per unit area $\left(\frac{\pi}{4} D^2 \right)$ to the dynamic pressure

$$C_D = \left[F_D / \left(\frac{\pi}{4} D^2 \right) \right] / \left(\frac{1}{2} \rho W^2 \right).$$

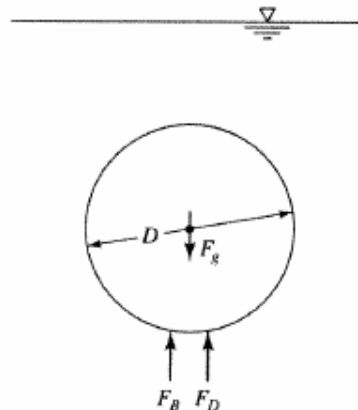


Figure 18.1.2 Fall velocity.

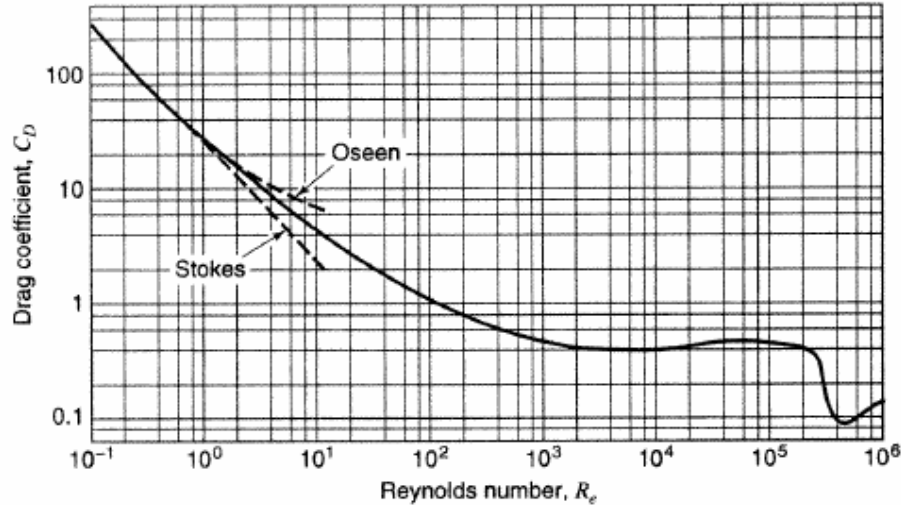


Figure 18.1.3 Drag coefficient of spheres as a function of Reynolds number (Vanoni, 1975).

The change of momentum in the control volume is $\sum_{CS} v_y (\rho V \cdot A) = 0$ and the net rate of momentum outflow is

$$\frac{d}{dt} \int_{CV} v_y \rho dV = \rho_s \left(\frac{\pi}{6} D^3 \right) \frac{dW}{dt} \quad (18.1.9)$$

The momentum equation is derived by substituting equations (18.1.5) through (18.1.9) into (3.4.7) to derive

$$\left(\frac{\pi}{6} D^3 \right) \gamma_s - \left(\frac{\pi}{6} D^3 \right) \gamma - C_D \left(\frac{\pi}{4} D^2 \right) \rho \frac{W^2}{2} = \rho_s \left(\frac{\pi}{6} D^3 \right) \frac{dW}{dt} \quad (18.1.10)$$

Because of the complex nature of the relationship between C_D and the Reynolds number, equation (18.1.10) cannot be directly integrated. The Reynolds number can be expressed as follows:

$$R_e = \frac{WD}{\nu} \quad (18.1.11)$$

For the range of $R_e < 1$, *Stoke's Law* is expressed as

$$C_D = \frac{24}{R_e} \quad (18.1.12)$$

We may then substitute equation (18.1.11) into equation (18.1.12) and use the resulting C_D in equation (18.1.8):

$$\begin{aligned} F_D &= C_D \left(\frac{\pi}{4} D^2 \right) \rho \frac{W^2}{2} \\ &= \left(\frac{24}{\frac{WD}{\nu}} \right) \left(\frac{\pi}{4} D^2 \right) \rho \frac{W^2}{2} \\ &= 3\pi\rho\nu WD \end{aligned} \quad (18.1.13)$$

which is referred to as *Stoke's equation*.

An equation for the fall velocity for $R_e < 1$ can be derived by substituting equation (18.1.13) to replace $C_D \left(\frac{\pi}{4} D^2 \right) \rho \frac{W^2}{2}$ in equation (18.1.10), then integrating to derive

$$W = \frac{D^2 g}{18\nu} \left(\frac{\rho_s}{\rho} - 1 \right) \left\{ 1 - \exp \left[\frac{-18\nu t}{(\rho_s/\rho) D^2} \right] \right\} \quad (18.1.14)$$

When $t \rightarrow \infty$, this fall velocity is the terminal velocity:

$$W_T = \frac{D^2 g}{18\nu} \left(\frac{\rho_s}{\rho} - 1 \right) \quad (18.1.15a)$$

or

$$W_T = \frac{D^2 g}{18\nu} \left(\frac{\rho_s - \rho}{\mu} \right) \quad (18.1.15b)$$

Figure 18.1.4 illustrates the fall velocity as a function of time for equations (18.1.14) and (18.1.15).

Alternatively, we could have used equation (18.1.10) with $dW/dt = 0$ to derive the fall velocity as

$$\left(\frac{\pi}{6} D^3 \right) \gamma_s - \left(\frac{\pi}{6} D^3 \right) \gamma - C_D \left(\frac{\pi}{4} D^2 \right) \rho \frac{W_T^2}{2} = 0 \quad (18.1.16)$$

Solving for W_T :

$$W_T = \left[\frac{4}{3} \frac{D}{C_D} \left(\frac{\rho_s}{\rho} - 1 \right) g \right]^{1/2} \quad (18.1.17)$$

Sediment particles are somewhat less than spherical, and for a given diameter, based on a sieve analysis, they usually have a fall velocity a little less than that of a sphere of the same diameter. Generally speaking, Stoke's Law is applicable to gravity particles in the silt and clay-size range falling in water. Because of the very small velocity of silt and clay, they are usually not found in appreciable quantities in streambeds. They are typically referred to as *wash load* because these fine materials tend to wash on through the system.

There are actually two types of drag:

1. *form drag*, which is due to pressure differences between the front and back of the particle, and
2. *surface drag*, which is due to friction along the surface of the particle.

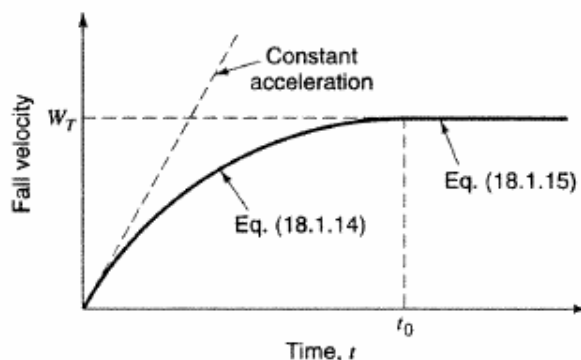


Figure 18.1.4 Velocity vs. function of time.

The two types of forces are the *inertia forces* and the *viscous forces*. Stoke's Law, which is for $R_e < 1$, ignores inertia forces. The Oseen (1927) approximation for C_D is:

$$C_D = \frac{24}{R_e} \left(1 + \frac{3}{16} R_e \right) \quad (18.1.18)$$

and the Goldstein (1929) approximation ($R_e \leq 2$) is:

$$C_D = \frac{24}{R_e} \left(1 + \frac{3}{16} R_e - \frac{19}{1280} R_e^2 + \frac{71}{20,480} R_e^3 + \dots \right) \quad (18.1.19)$$

Refer to Figure 18.1.3 for the drag coefficient as a function of Reynolds number.

When a number of particles are dispersed in a fluid, the fall velocity will differ from that of a single particle because of the mutual interference of the particles. If only a few closely spaced particles are in suspension, they will fall in a group with a velocity that is higher than that of a particle falling alone. On the other hand, if particles are dispersed throughout the fluid, the interference between neighboring particles will tend to reduce the fall velocity. Many investigators have studied the influence of the concentration on the fall velocity.

EXAMPLE 18.1.2

Given a sample of sand with mean particle size of 0.1 mm and density equal to 2.70 g/cm³, compute fall velocity.

SOLUTION

Using equation (18.1.15a), where $D = 0.1 \text{ mm} = 0.0001 \text{ m}$, $\rho = 1.0$, $\rho_s = 2.7$, $\nu = 1.0 \times 10^{-6} \text{ m}^2/\text{s}$, and $g = 9.81 \text{ m/s}^2$, solve for W_T :

$$\begin{aligned} W_T &= \frac{D^2 g}{18\nu} \left(\frac{\rho_s}{\rho} - 1 \right) \\ &= \frac{(0.10 \times 10^{-3})^2 \text{ m}^2 \times 9.81 \text{ m/s}^2}{18 \times 1.0 \times 10^{-6} \text{ m}^2/\text{s}} \left(\frac{2.70}{1.00} - 1 \right) \\ &= 0.0093 \text{ m/s} \\ &= 9.3 \times 10^{-3} \text{ m/s} \end{aligned}$$

The fall velocity is 6.875 mm/s.

18.1.5 Density

Practically all sediments have their origin in rock material and, hence, all constituents of the parent material usually can be found in sediments. For example, fragments of the parent rock are found in boulders and gravels, quartz in sands, silicas in silt, and feldspars and micas in clays. The density of most sediment smaller than 4 mm is 2,650 kg/m³ (specific gravity, $s = 2.65$). The density of clay minerals ranges from 2,500 to 2,700 kg/m³.

18.1.6 Other Important Relations

(a) Relative Density, Δ

$$\Delta = (\rho_s - \rho)/\rho \quad (18.1.20)$$

where ρ_s is the density of sediment and ρ is the density of water

(b) Specific weight of submerged solid particles, γ_s'

$$\gamma_s' = (\gamma_s - \gamma) \quad (18.1.21)$$

where γ_s is the specific weight of sediment particles, lb/ft³, and γ is the specific weight of water, lb/ft³.

- (c) **Grain Reynolds number, R_{NS}**

$$R_{NS} = WD_N/\nu \quad (18.1.22)$$

where D_N is the nominal sediment diameter, ft, and W is the fall velocity associated with D_N , ft/s.

- (d) **Sedimentation parameter**

$$G = (\rho\nu^2)(\gamma_s'D_N^3) \quad (18.1.23)$$

where ν is the kinematic viscosity, ft²/s (or m²/s); D_N is nominal diameter of the grain, ft (or m); and γ_s' is the specific weight of the submerged sediment, lb/ft³ (or N/m³).

- (e) **Porosity, n**

$$n = V_v/V \quad (18.1.24)$$

where V_v is the volume of voids and V is the volume of sediment.

18.2 BED FORMS AND FLOW RESISTANCE

18.2.1 Bed Forms

Free surface flow over erodible sand beds generates a variety of different bed forms and bed configurations. The type and dimensions of a bed form depends on the properties of the flow, fluid, and bed material. Table 18.2.1 is a summary description of bed forms and configurations affecting alluvial channel roughness. Figure 18.2.1 shows bed forms arranged in increasing order of sediment transport rate. Because there is a strong relationship among the flow resistance, the bed configuration, and the rate of sediment transport, it is important to know the conditions under which different bed forms exist. Figure 18.2.2 shows bed form charts from Vanoni (1974) for flow depths up to 10 ft (3 m) and also between 100 and 600 μ m. Bed forms are typically classified into a *lower regime* for subcritical flow, and an *upper regime* for supercritical flow, with a transition zone close to critical flow. The bed forms associated with these flow regimes are as follows:

Table 18.2.1 Summary Description of Bed Forms and Configurations Affecting Alluvial Channel Roughness [Material Taken from ASCE (1966) Task Force on Bed Forms]

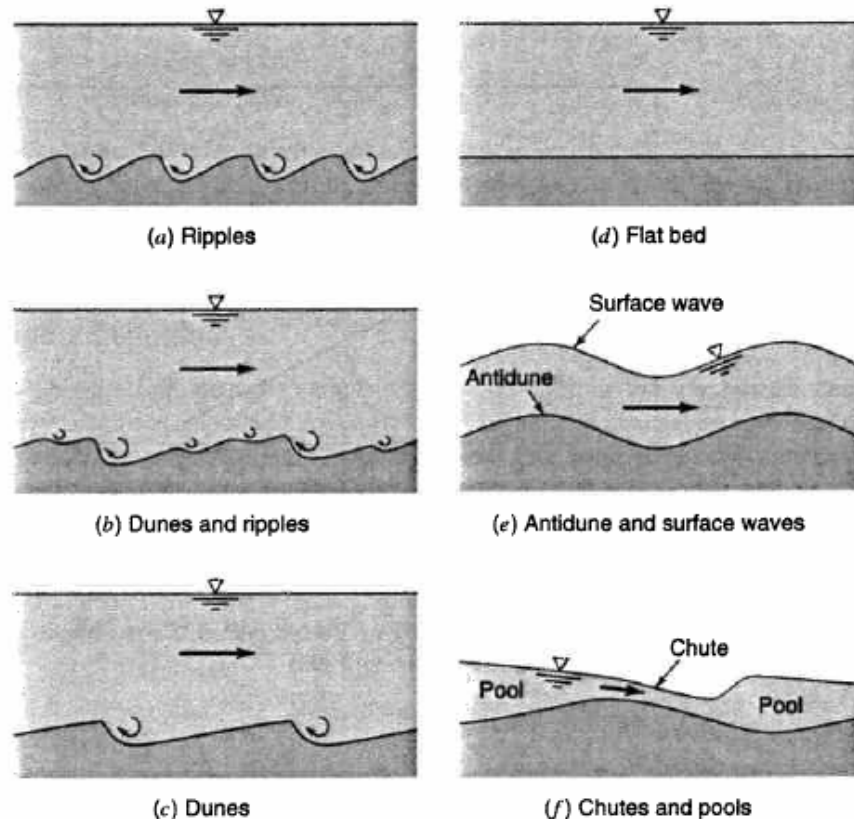
Bed form or configuration (1)	Dimensions (2)	Shape (3)	Behavior and occurrence (4)
Ripples	Wavelength less than approx 1 ft; height less than approx 0.1 ft	Roughly triangular in profile, with gentle, slightly convex upstream slopes and downstream slopes nearly equal to the angle of repose. Generally short-crested and three-dimensional	Move downstream with velocity much less than that of the flow. Generally do not occur in sediments coarser than about 0.6 mm
Bars	Lengths comparable to the channel width. Height comparable to mean flow depth	Profile similar to ripples. Plan form variable	Four types of bars are distinguished: (1) Point, (2) Alternating, (3) Transverse, and (4) Tributary. Ripples may occur on upstream slopes

Table 18.2.1 Summary Description of Bed Forms and Configurations Affecting Alluvial Channel Roughness [Material Taken from ASCE (1966) Task Force on Bed Forms] (*continued*)

Bed form or configuration (1)	Dimensions (2)	Shape (3)	Behavior and occurrence (4)
Dunes	Wavelength and height greater than ripples but less than bars	Similar to ripples	Upstream slopes of dunes may be covered with ripples. Dunes migrate downstream in manner similar to ripples
Transition	Vary widely	Vary widely	A configuration consisting of a heterogeneous array of bed forms, primarily low-amplitude ripples and dunes interspersed with flat regions
Flat bed	—	—	A bed surface devoid of bed forms. May not occur for some ranges of depth and sand size
Antidunes	Wave length = $2\pi v^2/g$ (approx) ^a Height depends on depth and velocity of flow	Nearly sinusoidal in profile. Crest length comparable to wavelength	In phase with and strongly interact with gravity water-surface waves. May move upstream, downstream, or remain stationary, depending on properties of flow and sediment.

^aReported by Kennedy (1969)

Source: Vanoni (1975).

**Figure 18.2.1** Bed forms arranged in increasing order of sediment transport rate. Flow increases consecutively from *a* to *f*. (Vanoni, 1975).

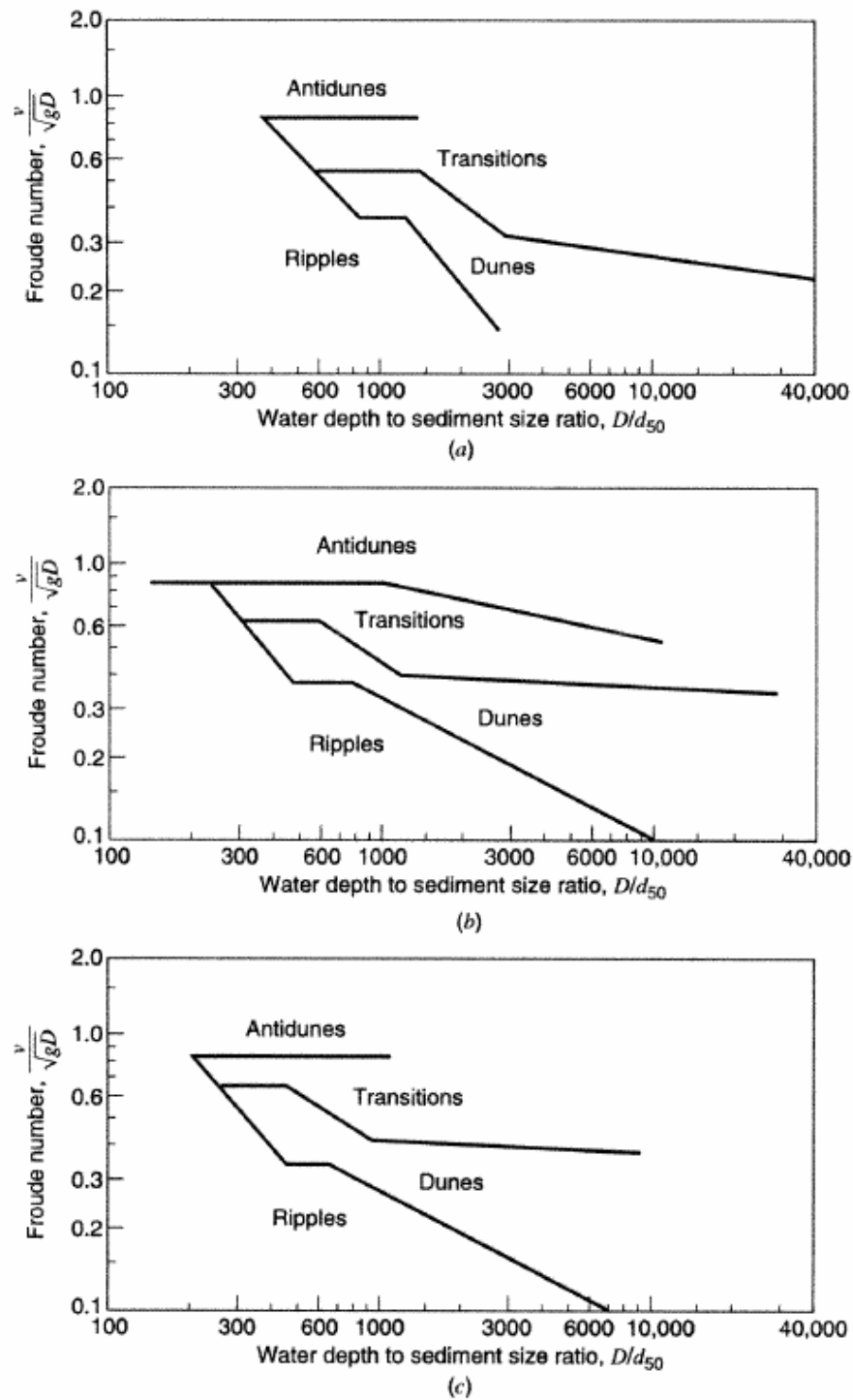


Figure 18.2.2 (a) Bed form chart for fine sand ($d_{50} = 100 \sim 200 \mu\text{m}$). (b) Bed form chart for fine to medium sand ($d_{50} = 200 \sim 300 \mu\text{m}$). (c) Bed form chart for medium sand ($d_{50} = 300 \sim 400 \mu\text{m}$). (d) Bed form chart for medium to coarse sand ($d_{50} = 400 \sim 600 \mu\text{m}$) (Shen and Julien, 1993).

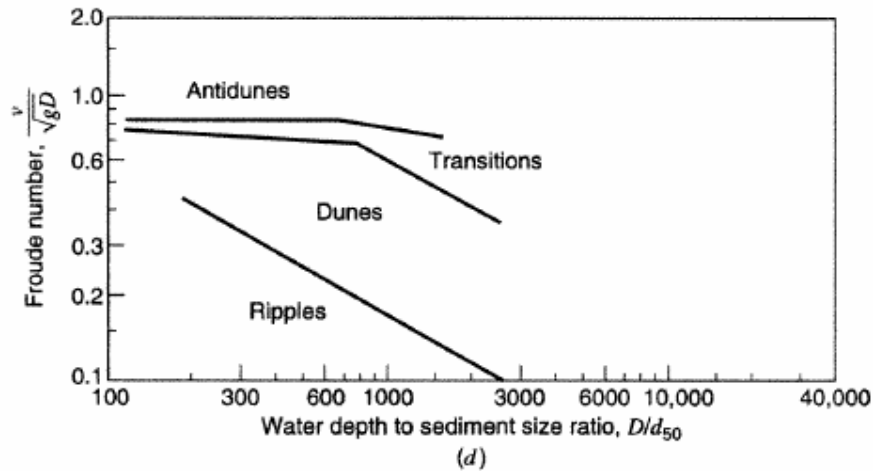


Figure 18.2.2 (continued)

1. Lower regime
 - ripples
 - dunes
2. Transition zone
 - bed configurations range from dunes to antidunes
3. Upper flow regions
 - plane bed with sediment movement
 - antidunes
 - breaking antidunes
 - standing waves
 - chutes and pools

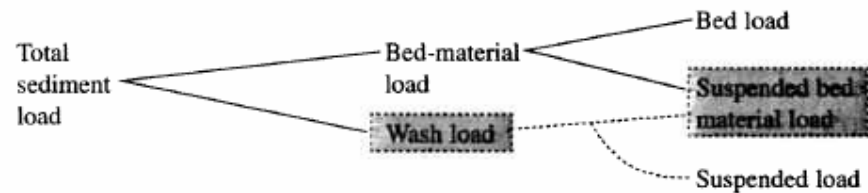
Factors that affect bed forms and resistance to flow include water depth, slope, fluid density, fine material concentration, bed-material size, bed-material gradation, fall velocity of sediment particles, channel cross-sectional shape, seepage force, and others. Refer to Simons and Sentürk (1977) and Yang (1996) for further discussion.

18.2.2 Sediment Transport Definitions

Table 18.2.2 provides the various sediment transport definitions. Finer materials such as silts and clays can be transported very easily once they enter a channel and are washed through with only trace amounts left in the bed. As a result, sediment transport equations do not apply. The so-called *wash load* is that part of the total suspended load that is finer than the bed material. The transport of larger size materials found in the bed material is called the *bed-material load*. *Total load* is the wash load and the bed-material load combined. Under conditions when wash load is not present, bed material and total load are used interchangeably. Bed material is generally expressed on a weight of sediment per unit time tons/day in U.S. customary units (or N/s in SI units).

Table 18.2.2 Sediment Transport Definitions

Transported Sediment:



Nontransported Sediment: Bed material (stationary sediment of the same sizes constituting the bed-material load)

Sediment Load:	Material in suspension and/or in transport
Bed-Material Load:	Total rate at which bed material is transported by a given location on a stream (both bed load and suspended load)
Bed Load:	Material moving on or near the stream bed by rolling, sliding, and sometimes making brief excursions into the flow a few diameters above the bed, (i.e., <i>jumping</i>). (Bed material that moves in continuous contact with the bed.)
Wash Load:	Part of total suspended load that is finer than bed material (wash load limited by supply not hydraulic)
Suspended Load:	Includes both suspended bed material load and wash load. Sediment that moves in suspension

18.2.3 Flow Resistance

Flow resistance varies with different bed forms through the bed roughness, which can be described through Manning's equation as follows:

$$V = \frac{1}{n} R^{2/3} S_f^{1/2} \quad (18.2.1)$$

where V is the average flow velocity (m/s), R is the hydraulic radius (m), and S_f is the dimensionless energy slope. Total roughness can be divided into *grain roughness* or *skin roughness* due to the existence of bed forms. A total Manning's roughness coefficient can be expressed as

$$n = n_g + n_f \quad (18.2.2)$$

where n_g is Manning's coefficient due to grain size roughness and n_f is Manning's coefficient due to form roughness. Einstein and Barbarossa (1952) were the first to separate the total flow resistance into a skin or grain resistance and a form resistance.

Several approaches have been reported in the literature for determining roughness coefficients for sediment-laden channels. See Yen (1996) and Yang (1996) for a review of these. Manning's roughness coefficients provided by Chow (1959), shown in Table 5.1.1, can be used for some bed types as indicated in the table.

Strickler's (1923) equation can be used to estimate Manning's roughness factor for streambeds and banks based on the prevailing sediment sizes on the banks and beds:

$$n = \frac{(D_{50})^{1/6}}{21} \quad (18.2.3)$$

where d_{50} is the median sediment size

$$n = \frac{(D_{50})^{1/6}}{25.6} \quad (18.2.4)$$

EXAMPLE 18.2.1

Compute the Manning's roughness factor for a streambed and banks with a median grain size of $D_{50} = 1$ mm.

SOLUTION

The Manning's roughness factor for the streambed is as follows:

$$n = \frac{(D_{50})^{1/6}}{21} = \frac{(0.001)^{1/6}}{21} = 0.015$$

The Manning's roughness factor for the stream banks is as follows:

$$n = \frac{(D_{50})^{1/6}}{25.6} = \frac{(0.001)^{1/6}}{25.6} = 0.012$$

18.3 SEDIMENT TRANSPORT**18.3.1 Incipient Motion**

Incipient motion of bed particles can be considered as the critical condition between transport and no transport. Consider particle A in Figure 18.3.1 with an objective to evaluate the condition leading to the incipient motion of this particle. Assuming the particle has diameter D_s , the effective surface area is proportional to D_s^2 . The force F_x acting on the particles is considered to be a shear force due to the shear stress, τ_0 , expressed as

$$F_x = C_1 D_s^2 \tau_0 \quad (18.3.1)$$

where C_1 is a constant of proportionality and $(C_1 D_s^2)$ is the effective area.

Assume that the distance y_1 is proportional to D_s so that $y_1 = C_2 D_s$, then the *overturning moment* due to the flow is $\tau_0 C_1 D_s^2 (C_2 D_s)$. The overturning moment is balanced by the submerged weight of the particle that is proportional to $(\gamma_s - \gamma) D_s^3$. The *righting moment* can be expressed as $C_3 (\gamma_s - \gamma) D_s^3 (C_4 D_s)$, where C_3 and C_4 are constants of proportionality. The overturning moment and the righting moment are equal at the *point of incipient motion*. The shear stress associated with the point of incipient motion is the *critical shear stress*, $\tau_c = \tau_0$. Equating the overturning moment and the righting moment,

$$\tau_c C_1 D_s^2 (C_2 D_s) = C_3 (\gamma_s - \gamma) D_s^3 (C_4 D_s) \quad (18.3.2a)$$

$$\tau_c C_1 C_2 D_s^3 = (\gamma_s - \gamma) C_3 C_4 D_s^4 \quad (18.3.2b)$$

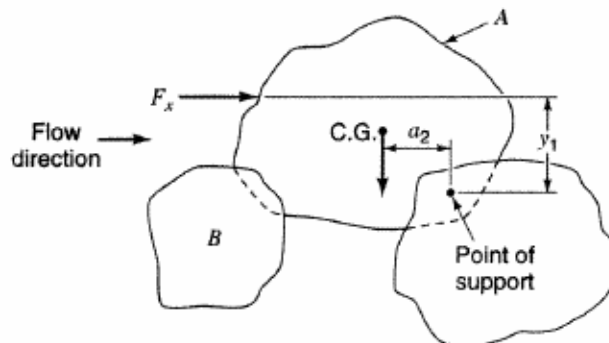


Figure 18.3.1 Incipient motion. Consider (assume) that the hydraulic force acting on the particle is due entirely to shear stress, I_0 , which acts over the surface area (portion of surface area referred to as surface area).

Solving for the critical shear stress

$$\tau_c = \frac{C_3 C_4}{C_1 C_2} (\gamma_s - \gamma) D_s \tag{18.3.3}$$

or

$$\tau_c = C (\gamma_s - \gamma) D_s \tag{18.3.4}$$

where $C = (C_3 C_4) / (C_1 C_2)$.

Dimensional analysis can be used to develop the critical shear stress more completely. A dimensionless shear stress is developed, which is

$$\frac{\tau_c}{(\gamma_s - \gamma) D_s} = \phi \left(\frac{\sqrt{\tau_c / \rho} D_s}{\nu} \right) \tag{18.3.5a}$$

$$= \phi \left(\frac{u_{*c} D_s}{\nu} \right) \tag{18.3.5b}$$

where $\frac{u_{*c} D_s}{\nu}$ is the *shear velocity Reynolds number* and

$$u_{*c} = \sqrt{\tau_c / \rho} \tag{18.3.6}$$

is the *critical shear velocity*. The term on the left side of equations (18.3.5a,b) is a dimensionless shear stress, τ_* ,

$$\tau_* = \frac{\tau_c}{(\gamma_s - \gamma) D_s} \tag{18.3.7}$$

The relationship between τ_* and R_{*c} developed by Shields (1936) is referred to as *Shields diagram*, as shown in Figure 18.3.2. This diagram represents the experimental relationships implied by equation (18.3.5a,b). The Shields diagram can be used to evaluate the *critical shear stress* (the shear stress at incipient motion). To use the Shields diagram, one must first compute the following:

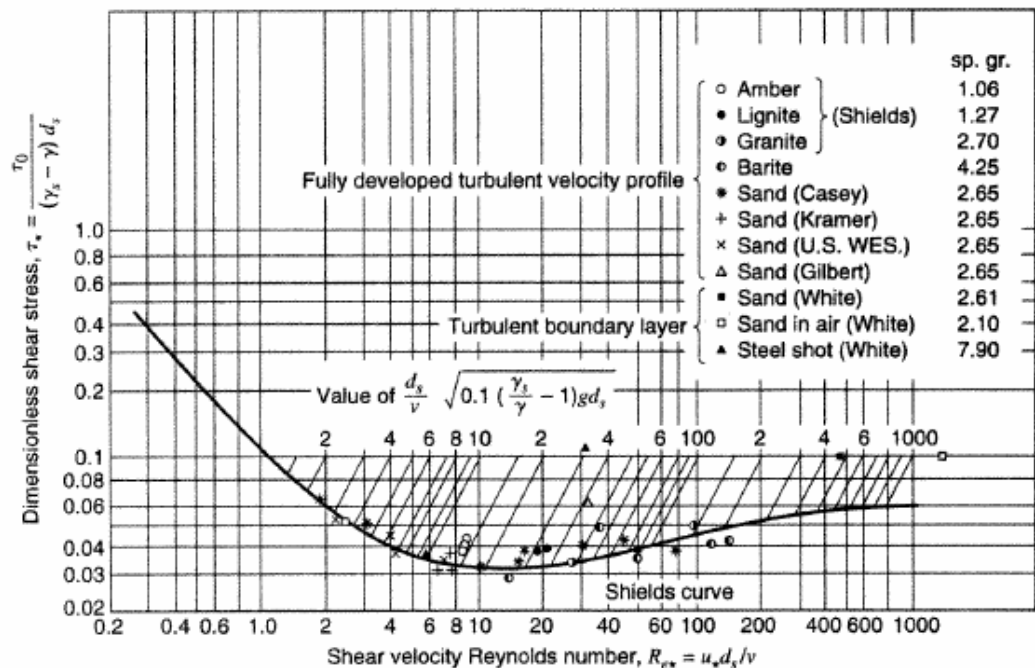


Figure 18.3.2 Shields diagram (Vanoni, 1975, p. 96).

$$\frac{D_s}{\nu} \sqrt{0.1 \left(\frac{\gamma_s}{\gamma} - 1 \right) g D_s}$$

which can then be used to locate τ_* on the curve in the Shields diagram. With τ_* , the critical shear stress can be computed by rearranging equation (18.3.7) to

$$\tau_c = \tau_* (\gamma_s - \gamma) D_s \quad (18.3.8a)$$

$$= \tau_* (\gamma_s / \gamma - 1) \gamma D_s \quad (18.3.8b)$$

The actual shear stress can be computed using

$$\tau_0 = \gamma R S \quad (18.3.9)$$

Then a comparison is made of τ_c and τ_0 . If τ_0 is larger than τ_c , transport is expected. Figure 18.3.3 is a rearrangement of the Shields diagram for quartz sediment in water.

EXAMPLE 18.3.1

Determine whether the critical shear stress is exceeded by the flow for the following situation. A fairly fine sand particle (with a geometric mean of 0.18×10^{-3} m) forms the bed of a wide rectangular channel with a depth of 2.5 m and a slope of 0.0001. The water is at 10°C so that $\nu = 1.308 \times 10^{-6} \text{ m}^2/\text{s}$ and $\gamma_s/\gamma = 2.65$.

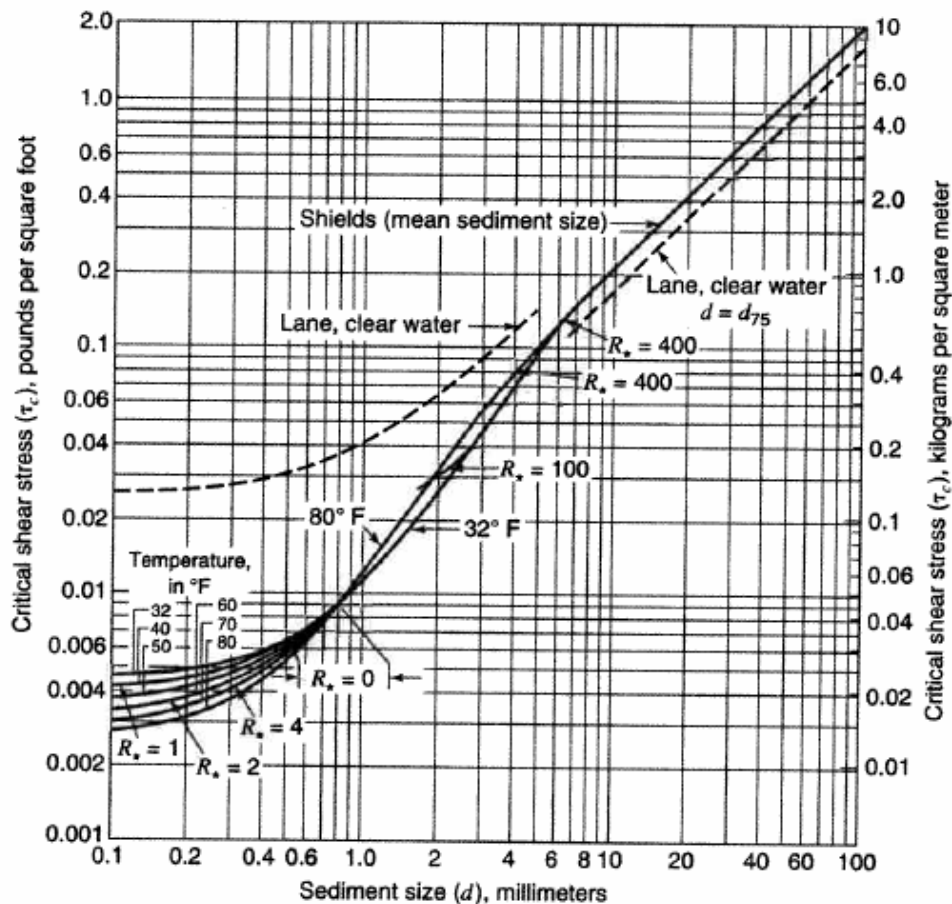


Figure 18.3.3 Critical shear stress for quartz sediment in water as function of grain size (Vanoni, 1975).

SOLUTION

Step 1 Compute

$$\begin{aligned} & \frac{D_s}{V} \sqrt{0.1 \left(\frac{\gamma_s}{\gamma} - 1 \right) g D_s} \\ &= \frac{0.18 \times 10^{-3} \text{ m}}{1.308 \times 10^{-6} \text{ m}^2/\text{s}} \sqrt{0.1(2.65 - 1)9.81 \frac{\text{m}}{\text{s}^2} 0.18 \times 10^{-3} \text{ m}} \\ &= 2.35 \end{aligned}$$

Step 2 Evaluate τ_* from the Shields diagram and compute the critical shear stress using equation (18.3.8b). From the Shields diagram, $\tau_* = 0.065$.

$$\begin{aligned} \tau_c &= \tau_* (\gamma_s/\gamma - 1)\gamma D_s = (0.065)(2.65 - 1)(9810)(0.18 \times 10^{-3}) \\ &= 0.8 \text{ N/m}^2 \end{aligned}$$

Step 3 Compute the actual shear stress τ_0 using equation (18.3.9) where $R = y = 2.5 \text{ m}$

$$\begin{aligned} \tau_0 &= \gamma RS \\ &= 9810 \frac{\text{N}}{\text{m}^3} \times 2.5 \text{ m} \times 0.0001 \\ &= 2.45 \text{ N/m}^2 \\ &= 2.45 \text{ N/m}^2 \end{aligned}$$

Because the actual shear stress $\tau_0 = 2.45 \text{ N/m}^2$ is much larger than the critical shear stress $\tau_c = 0.8 \text{ N/m}^2$, transport of the fine sand particles is expected.

18.3.2 Sediment Transport Functions

Table 18.3.1 lists some of the more common sediment transport functions along with basic information on their development and use.

Table 18.3.1 Basic Information on the Development and Use of Common Sediment Transport Functions

Function Name	Type	Sediment Size Range (mm)	Developed From	Comments
Ackers-White	Total Load	0.04–2.5	Flume Data	Provides good description of movement for lightweight sediments in laboratory flumes and natural rivers.
Colby	Total Load	0.10–0.8	Flume and Stream Data	Temperature at 60°F. The function is recommended for sand rivers with depth less than 10 ft. Effective at velocity range of 1 to 10 fps. Depth range is 0.10–10 ft.
Dubois	Bed Load	0.01–4.0	Small Flumes	The formula is not applicable for sand-bed streams that carry suspended load.
Engelund/Hansen	Total Load	Sizes in excess of 0.15 mm	Large Flume Data	Appears to satisfactorily predict sediment discharge in sand-bed rivers.
Laursen	Total Load	0.01–4.08	Flume Data	Intended to be applied only to natural sediments with specific gravity of 2.65. It is adaptable for shallow rivers with fine sand and coarse silt.
Meyer-Peter/Muller	Bed Load	0.40–30.0	Flume Data	Not valid for flows with appreciable suspended loads. The function was calibrated for coarse sands and gravels. It is recommended for rivers when the bed material is coarser than 5 mm. Depth range is from 1 to 1.2 m.

Table 18.3.1 Basic Information on the Development and Use of Common Sediment Transport Functions (*continued*)

Function Name	Type	Sediment Size Range (mm)	Developed From	Comments
Schoklitsch	Bed Load	0.30–5.0	Small Flume Data	It is a bed load formula that should not be applied to sand-bed streams that carry considerable bed sediments in suspension.
Shields	Bed Load	1.7–2.50	Flume Data	The sediments used in the experiments were coarse and the shear velocities were low. Almost all the sediments moved were bed load.
Toffaletti	Total Load	0.062–16	Stream Data	The bed load portion may be calculated by an bed load function (for example, Schoklitsch, or Meyer-Peter and Muller). It should not be used for lightweight and coarser materials but is adaptable for large sand-bed rivers with specific gravity of 2.65.
Yang's Stream Power Function	Total Load	0.015–1.71	Stream Data	The function is effective for sediments with specific gravity of 2.65. Yang's sand formula is adaptable for sand-bed laboratory flumes and natural rivers—wash load excluded. Yang's gravel formula is for bed material between 2 and 10 mm.

18.3.3 Armoring

Armoring is the process of progressive coarsening of the bed layer by removal of fine particles until a layer is formed that becomes resistant to scour for a particular discharge. The coarse layer that remains on the surface is called the *armoring layer*. Armoring is a temporary condition because larger discharges may destroy an armor layer and the layer may reform as discharges decrease. The formation of a resistant layer of relatively large particles results from removal of finer particles by erosion. Figure 18.3.4 further illustrates the concept of armoring and Figures 18.3.5 a–h show examples of different levels of armoring in the Agua Fria River near Phoenix, Arizona. Section 18.10.2.2 further discusses armoring and presents the equation by Pemberton and Lara (1984) for approximating the thickness of an armoring layer.

18.4 BED LOAD FORMULAS

As previously described, particles can be moved by the flow as bed along the streambed. This section describes several of the more commonly used bed load equations for sand-bed streams. The data in Tables 18.4.1 through 18.4.3 for the Colorado River at Taylor's Ferry are used to apply the bed load formulas.

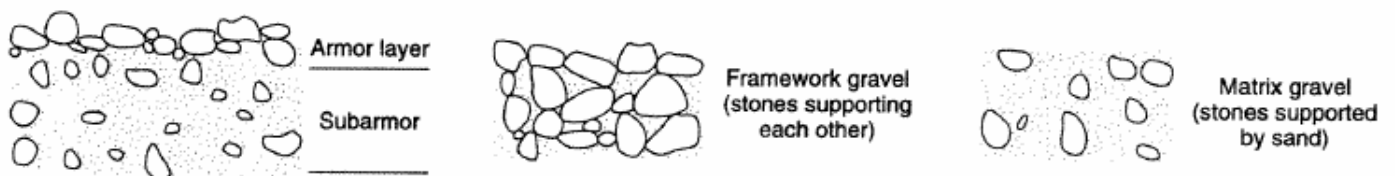


Figure 18.3.4 Patterns of gravel deposition in streambeds, cross-section view. The formation of a surface layer of *armor* or *pavement* about one grain thick protects the finer material in the underlying *subarmor* or *subpavement* zone from hydraulic transport until discharge is sufficient to mobilize the armor layer. Armor layers form frequently in gravel-bed rivers and occur when the bed contains a wide variation in grain sizes, when the supply of the finer grains is small compared to the transport energy, and when the largest grain size is transport-limited.

18.4.1 Duboys Formula

Duboys (1879) developed the following formula:

$$g_s = \psi \tau_0 [\tau_0 - \tau_c] \tag{18.4.1}$$

where ψ is the coefficient depending on the mean size of bed sediment, $\text{ft}^3/\text{lb}/\text{sec}$; τ_0 is the $\gamma dS =$ bed shear stress in lbs per ft^2 ; τ_c is the critical bed shear stress in lb/ft^2 ; γ is the specific weight of water in lb/ft^3 ; d is the water depth in ft ; and S is the slope of the channel.

The parameters ψ and τ_c are given in Figure 18.4.1 as functions of the mean size of sand.

EXAMPLE 18.4.1

Compute the sediment discharge per unit width for the Colorado River at Taylor’s Ferry for a depth of 10 ft and a flowrate of 40 cfs per ft using Duboys formula and the data in Tables 18.4.1 through 18.4.3.

SOLUTION

For a mean size of sand, $D_s = D_m = 0.396 \text{ mm}$ (from Table 18.4.1), τ_c and ψ are found in Figure 18.4.1 as

$$\tau_c = 0.02 \text{ lb}/\text{ft}^2$$

$$\psi = 57 \text{ ft}^3/\text{lb}\cdot\text{s}$$

Using $S = 0.000217$ (given in Table 18.4.1), the bed shear stress is $\tau_0 = \gamma dS = 62.4 (10) (0.000217) = 0.135408 \text{ lb}/\text{ft}^2$.

Substituting these values of ψ , τ_0 , τ_c in equation (18.4.1), results in

$$g_s = 57 (0.135408) (0.135408 - 0.02)$$

$$g_s = 0.8907 \text{ lb}/\text{sec}\cdot\text{ft}$$

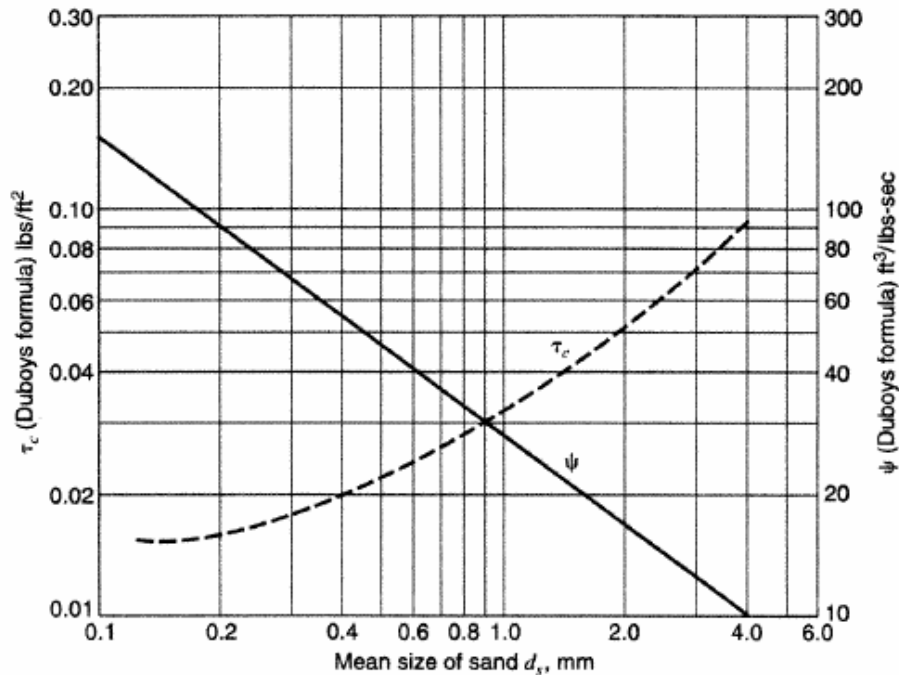


Figure 18.4.1 Graph of coefficient ψ and critical shear stress, τ_c for Duboys.

Table 18.4.1 Properties of the Colorado River (particularly at the site where the sediment discharge measurements were taken)

Depth range d , ft	4–12
Range in q , cfs/ft	8–35
Width, ft	350
Slope, S , ft/ft	0.000217
Temperature, °F	60
Geom. mean sed. size, mm	0.320
Geo. std. deviation	1.44
D_{35} , mm	0.287
D_{50} , mm	0.330
D_{65} , mm	0.378
D_{90} , mm	0.530
Mean size, D_m (mm)	0.396

Table 18.4.2 Size Fractions of Bed Sediment Used in Calculations (Temperature = 60°F)

Items	% by Weight (p_i)		
	20.8	69.6	9.6
Mean Size, D_{si} (mm)	0.177	0.354	0.707
(ft)	0.00058	0.00116	0.00232
Settling Velocity, W_i (cm/sec)	1.9	4.8	9.6
(ft/sec)	0.063	0.158	0.314

Table 18.4.3 Sieve Analysis of Bed Material from the Colorado River

Sieve Opening (mm)	% Finer
0.062	0.22
0.074	
0.125	1.33
0.175	
0.246	
0.250	21.4
0.351	
0.495	
0.500	88.7
0.701	
0.991	
1.000	98.0
1.400	
1.980	
2.000	99.0
3.960	
4.000	99.5

18.4.2 Meyer-Peter and Muller Formula

Meyer-Peter and Muller (1948) developed an empirical formula for the bed load discharge in natural streams, which is expressed as

$$g_s = \left[0.368 \frac{Q_s}{Q} \left[\frac{D_{90}^{1/6}}{n_s} \right]^{3/2} d \cdot S - 0.0698 D_m \right]^{3/2} \quad (18.4.2)$$

where

g_s = bed load discharge, lb/sec-ft width

Q = total water discharge, ft³/s

Q_s = that part of the water discharge apportioned to the bed in ft³/s

D_{90} = particle size for which 90 percent of the bed mixture is finer, mm

D_m = effective diameter of bed-material mixture (mm)

d = mean flow depth, (ft).

S = energy gradient, (ft/ft)

n_s = Manning's roughness value for the bed of the stream

For wide and smooth channels $Q_s/Q = 1$ and

$$n_s = \frac{1.486d^{2/3}S^{1/2}}{V} \quad (18.4.3)$$

where V is the mean flow velocity in ft/sec.

When bank roughness is considered, the following relationships are used:

For rectangular channels:

$$n_s = n_m \left[1 + \frac{2d}{T_w} \left\{ 1 - \left[\frac{n_w}{n_m} \right]^{3/2} \right\} \right]^{2/3} \quad (18.4.4)$$

$$\frac{Q_s}{Q} = \frac{1}{1 + \frac{2d}{T_w} \left(\frac{n_w}{n_s} \right)^{2/3}} \quad (18.4.5)$$

For trapezoidal channels:

$$n_s = n_m \left[1 + \frac{2d(1+z^2)^{1/2}}{B} \left\{ 1 - \left[\frac{n_w}{n_m} \right]^{3/2} \right\} \right]^{2/3} \quad (18.4.6)$$

$$\frac{Q_s}{Q} = \frac{1}{1 + \frac{2d(1+z^2)^{1/2}}{B} \left(\frac{n_w}{n_s} \right)^{2/3}} \quad (18.4.7)$$

where

n_w = roughness value for the channel sides

n_m = roughness value for the total channel

T_w = top width, ft

B = bottom width, ft

Z = channel side slope, hor./vert.

$$D_m = \sum_{i=1}^n D_{si} i_b ; n = \text{number of size fractions}$$

D_{si} = mean grain diameter of the sediment in size fraction i

i_b = fraction by weight of bed material in a given size fraction

EXAMPLE 18.4.2

Compute the sediment discharge per unit width for the Colorado River at Taylor's Ferry for a depth of 10 ft and a flow rate of 40 cfs per ft using the Meyer-Peter and Muller formula.

SOLUTION

First compute the effective diameter of bed-material mixture (mm):

$$D_m = \sum p_i D_{si} = 0.208(0.177) + 0.696(0.345) + 0.096(0.707) \\ = 0.351 \text{ mm}$$

Next compute the Manning's roughness factor, using equation using equation (18.4.3):

$$n_s = \frac{1.486d^{2/3}S^{1/2}}{V} = \frac{1.486(10)^{2/3}(0.000217)^{1/2}}{4} \\ n_s = 0.0254$$

Since the river is wide, $\frac{Q_s}{Q} = 1$. The sediment discharge is computed using equation (18.4.2):

$$g_s = \left[0.368(1) \left[\frac{0.53^{1/6}}{0.254} \right]^{3/2} (10)(0.000217) - 0.0698(0.351) \right]^{3/2} \\ = 0.0545 \text{ lb/sec-ft}$$

18.4.3 Schoklitsch Formula

The Schoklitsch formula (1935) can be expressed as follows:

1. Unigranular material (D_{50}):

$$G_s = \frac{86.7}{\sqrt{D}} S^{3/2} (Q - T_w q_0) \quad (18.4.8)$$

where

$$q_0 = 0.00532d/S^{4/3} \quad (18.4.9)$$

$D \equiv D_0$ (mean grain diameter), inches

G_s = the bedload discharge, lb/s

S = the energy gradient, ft/ft

Q = the discharge ft³/s

T_w = the width in ft

q_c = the critical discharge, ft³/s per ft of width

2. For mixtures of different sizes (D_{si}):

$$g_s = \sum_{i=1}^n g_{s,i} = \sum_{i=1}^n i_b \frac{25}{\sqrt{D_{si}}} S^{3/2} (q - q_0) \quad (18.4.10)$$

where

$$q_0 = 0.0638D_{si}/S^{4/3}$$

n = the number of size fractions in the bed-material mixture

D_{si} = the mean grain diameter, ft

$g_s = G_s/T_w$; bedload discharge, lb/sec-ft

i_b = the fraction, by weight, of bed material in a given size fraction

EXAMPLE 18.4.3

Compute the sediment discharge per unit width for the Colorado River at Taylor's Ferry for a depth of 10 ft and a flowrate of 40 cfs per ft using the Schoklitsch formula.

SOLUTION

1. From Table 18.4.2, $D_{si} = 0.177 \text{ mm} = 0.000581 \text{ ft}$

(i)

$$q_{0i} = \frac{0.0638(0.000581)}{(0.000217)^{4/3}} = 2.84 \text{ cfs/ft}$$

(ii)

$$g_{si} = 0.208 \frac{(25)}{(0.000581)^{1/2}} (0.000217)^{3/2} (40 - 2.84) \\ = 0.0256 \text{ lb/sec-ft}$$

2. For $D_{si} = 0.354 \text{ mm} = 0.00116 \text{ ft}$

(i)

$$q_{0i} = \frac{0.0638(0.000116)}{(0.000217)^{4/3}} = 5.6754 \text{ cfs/ft}$$

(ii)

$$g_{si} = 0.696 \frac{(25)}{(0.00116)^{1/2}} (0.000217)^{3/2} (40 - 5.6754) \\ = 0.05606 \text{ lb/sec-ft}$$

3. For $D_{si} = 0.707 \text{ mm} = 0.00232 \text{ ft}$

(i)

$$q_{0i} = \frac{0.0638(0.00232)}{(0.000217)^{4/3}} = 11.3509 \text{ cfs/ft}$$

(ii)

$$g_{si} = 0.096 \frac{(25)}{(0.00232)^{1/2}} (0.000217)^{3/2} (40 - 11.3509) \\ = 0.00456 \text{ lb/sec-ft}$$

$$g_s = \sum_{i=1}^3 g_{si} = 0.256 + 0.05616 + 0.00456 \\ = 0.0862 \text{ lb/sec-ft}$$

18.5 SUSPENDED LOAD

The suspension of sediment is caused by turbulence, although other factors, such as secondary currents, obstruction, and particle impact, also play a role. In order to calculate the suspended load, the variation of sediment concentration in a vertical section of stream flow must be computed. Figure 18.5.1 illustrates the velocity distribution, the concentration distribution, and the shear stress distribution. At an equilibrium, there is a balance between the rate at which particles are falling due to gravity, W_c , and the rate at which they are being stirred up again by turbulent eddy

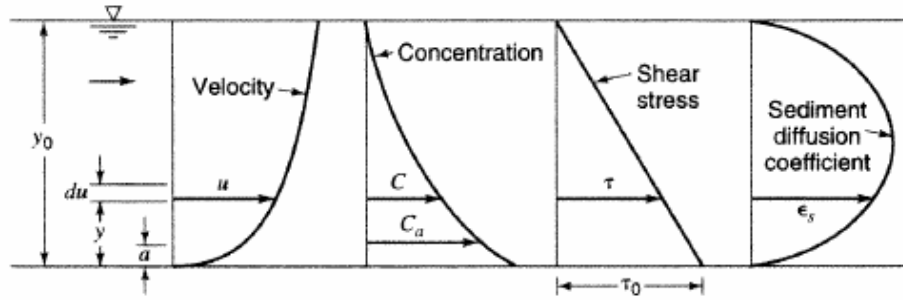


Figure 18.5.1 Definitional sketch for suspension of sediment. (Prasuhn, 1987)

motion, $\epsilon_m \frac{\partial C}{\partial y}$, where W is the fall velocity of sediment particles, C is the concentration of sediment, ϵ_m is the vertical mass transfer coefficient due to eddy motion, and y is the vertical direction. At equilibrium,

$$W \cdot C + \epsilon_m \frac{\partial C}{\partial y} = 0 \quad (18.5.1)$$

which is a diffusion equation.

A solution can be developed for equation (18.5.1) by using the following fluid shear stress relationship:

$$\tau = \epsilon_m \rho \frac{du}{dy} \quad (18.5.2)$$

and a logarithmic vertical velocity distribution such as the *von Karman-Prandtl equation*:

$$\frac{u}{u_*} = \frac{2.303}{k} \log y + A \quad (18.5.3)$$

where $u_* = \sqrt{\tau_0/\rho}$ is the shear velocity, $k \approx 0.4$ for most clear water flows, and A is a constant depending on a smooth or rough boundary.

Differentiating equation (18.5.3) with respect to y gives

$$\frac{du}{dy} = \frac{u_*}{ky} \quad (18.5.4)$$

which can be substituted into equation (18.5.2) and solved for ϵ_m as follows:

$$\begin{aligned} \epsilon_m &= \frac{\tau/\rho}{du/dy} \\ &= \frac{\tau/\rho}{u_*/ky} \end{aligned} \quad (18.5.5)$$

Referring to Figure 18.5.1, the shear stress at the streambed is τ_0 ,

$$\tau_0 = \gamma R S = \gamma y_0 S \quad (18.5.6)$$

where the hydraulic radius $R = y_0$, the depth.

At an intermediate depth y , the shear stress is

$$\tau = \gamma(y_0 - y)S \quad (18.5.7)$$

The ratio τ/τ_0 is

$$\begin{aligned}\frac{\tau}{\tau_0} &= \frac{\gamma(y_0 - y)S}{\gamma y_0 S} \\ &= \frac{(y_0 - y)}{y_0}\end{aligned}\quad (18.5.8)$$

so that

$$\tau = \tau_0 \frac{(y_0 - y)}{y_0} = \tau_0 \left(1 - \frac{y}{y_0}\right) \quad (18.5.9)$$

Equation (18.5.9) can be substituted into equation (18.5.5) to derive the vertical distribution of ϵ_m as follows:

$$\begin{aligned}\epsilon_m &= \frac{\tau_0 k y}{\rho u_*} \left(1 - \frac{y}{y_0}\right) \\ &= u_* k y \left(1 - \frac{y}{y_0}\right)\end{aligned}\quad (18.5.10)$$

Substituting equation (18.5.10) into the diffusion equation (18.5.1)

$$\begin{aligned}CW &= -\epsilon_m \frac{dC}{dy} \\ &= -u_* k y \left(1 - \frac{y}{y_0}\right) \frac{dC}{dy}\end{aligned}\quad (18.5.11)$$

Rearranging

$$\frac{dC}{C} = \frac{W y_0}{u_* k} \frac{dy}{y(y_0 - y)} \quad (18.5.12)$$

and integrating from a reference height a (see Figure 18.5.1) to any arbitrary height y gives

$$\frac{C_y}{C_a} = \left[\left(\frac{y_0 - y}{y} \right) \left(\frac{a}{(y_0 - a)} \right) \right]^z \quad (18.5.13)$$

Figure 18.5.2 is a verification graph of equation (18.5.13) where $z = \frac{W}{u_* k}$. This figure predicts vertical variation of sediment concentration for different values of parameter z .

The sediment discharge per unit width, g_{ss} , through an element of height dy is

$$g_{ss} = \int_a^{y_0} C_y u dy \quad (18.5.14)$$

Einstein (1950) integrated this equation using 18.5.13 for C_y and a logarithmic velocity equation.

EXAMPLE 18.5.1

Compute the sediment discharge per unit width for a depth of 10 ft, with an average flow rate of 0.40 ft/sec for 8~10 ft, 0.38 ft/sec for 6~8 ft, 0.34 ft/sec for 4~6 ft, 0.30 ft/sec for 2~4 ft, and 0.15 ft/sec for 0~2 ft. $C_a = 0.10 \text{ lb/ft}^3$, $z = 0.81$.

SOLUTION

Compute C_y based on equation (18.5.13) and Figure 18.5.2:

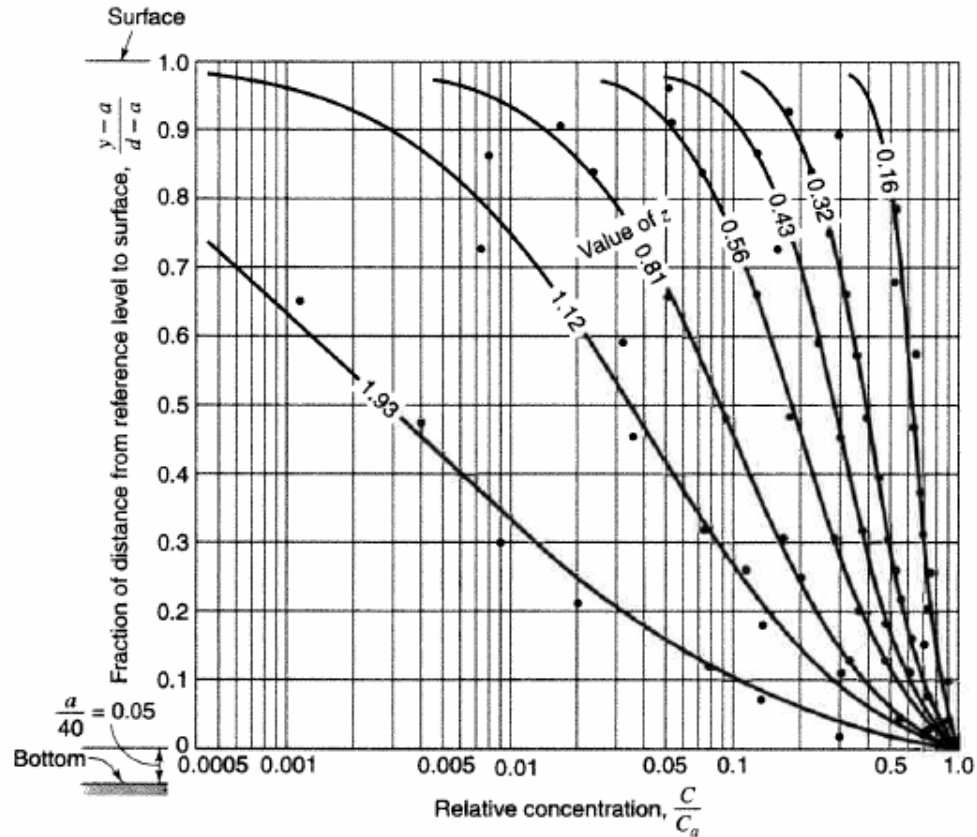


Figure 18.5.2 Vertical distribution of relative concentration C/C_a . Compared with Eq. For wide range of stream size and z values (Vanoni, 1975).

$$C_y = 0.0015 \text{ lb/ft}^3, \text{ for } 8\sim 10 \text{ ft}$$

$$C_y = 0.004 \text{ lb/ft}^3, \text{ for } 6\sim 8 \text{ ft}$$

$$C_y = 0.0085 \text{ lb/ft}^3, \text{ for } 4\sim 6 \text{ ft}$$

$$C_y = 0.016 \text{ lb/ft}^3, \text{ for } 2\sim 4 \text{ ft}$$

$$C_y = 0.035 \text{ lb/ft}^3, \text{ for } 0\sim 2 \text{ ft}$$

Compute g_{ss} based on equation (18.5.14):

$$\begin{aligned} g_{ss} &= \int_a^{y_0} C_y u dy = \sum_{n=1}^5 C_y u \Delta y \\ &= 0.0015 \times 0.40 \times 2 + 0.004 \times 0.38 \times 2 + 0.0085 \times 0.34 \times 2 + 0.016 \times 0.30 \times 2 + 0.035 \times 0.15 \times 2 \\ &= 0.0012 + 0.00304 + 0.00578 + 0.0096 + 0.0105 \\ &= 0.03012 \text{ lb/sec-ft} \end{aligned}$$

EXAMPLE 18.5.2

A sandy channel bed with mean particle size of 0.15 mm and density equal to 2.70 g/cm³ has an elevation of 220.0 m and surface water elevation of 225.60 m. The shear stress at the streambed is 0.75 N/m². At what depth (elevation) does the relative concentration equal 0.1?

SOLUTION

Using equation (18.1.15a), where $D = 0.15 \text{ mm} = 0.00015 \text{ m}$; $\rho = 1.0$; $\rho_s = 2.7$; $\nu = 1.0 \times 10^{-6} \text{ m}^2/\text{s}$; and $g = 9.81 \text{ m/s}^2$, solve for W_T :

$$\begin{aligned}
 W_T &= \frac{D^2 g}{18\nu} \left(\frac{\rho_s}{\rho} - 1 \right) \\
 &= \frac{(0.15 \times 10^{-3})^2 \text{ m}^2 \times 9.81 \text{ m/s}^2}{18 \times 1.0 \times 10^{-6} \text{ m}^2/\text{s}} \left(\frac{2.70}{1.00} - 1 \right) \\
 &= 0.021 \text{ m/s}
 \end{aligned}$$

The shear velocity $u_* = \sqrt{\tau_0/\rho} = (0.75/1000)^{1/2} = 0.0274 \text{ m/s}$

$$\text{Then } z = \frac{W}{u_* k} = \frac{0.021}{0.0274 \times 0.4} = 1.92$$

This is from Figure 18.5.2, where $z = 1.92$ and the relative concentration = 0.1, $y/d = 0.1$, but $d = 225.60 - 220.0 = 5.6 \text{ m}$. Thus, this given relative concentration occurs when the depth is 0.56 m above the bed elevation (i.e., at elevation 220.56).

18.6 TOTAL SEDIMENT LOAD (BED MATERIAL LOAD FORMULAS)

This section presents Colby's formula, the Ackers-White formula, and Yang's formula. These three formulas have been selected in order to illustrate total sediment load (bed material load formula).

18.6.1 Colby's Formula

Colby (1964) recommended the diagrams in Figures 18.6.1 and 18.6.2 based on investigation of sediment transport load as a function of mean flow velocity, depth, viscosity, water temperature, and concentration of the fine sediment of the discharge of sand per ft of channel width. The bed-material discharge can be determined by Colby's formula (Colby, 1964):

$$g_s = A (V - V_c)^B (1 + (AF - 1) CF) 0.672 \quad (18.6.1)$$

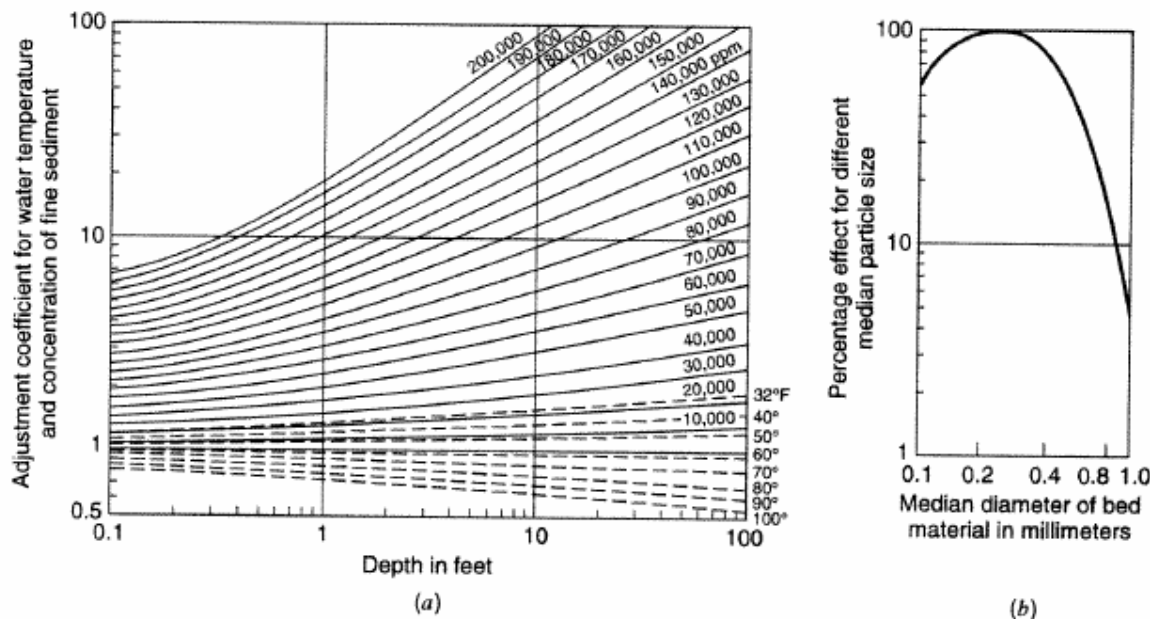


Figure 18.6.1 Approximate effect of water temperature and concentration of fine sediment on the relationship of discharge of sand to mean velocity (Colby, 1964.) Graph (a) is based on sediment sizes 0.2 to 0.3 mm. For other sediment sizes, a correction factor is needed from graph (b) (from Shen and Julien, 1993).

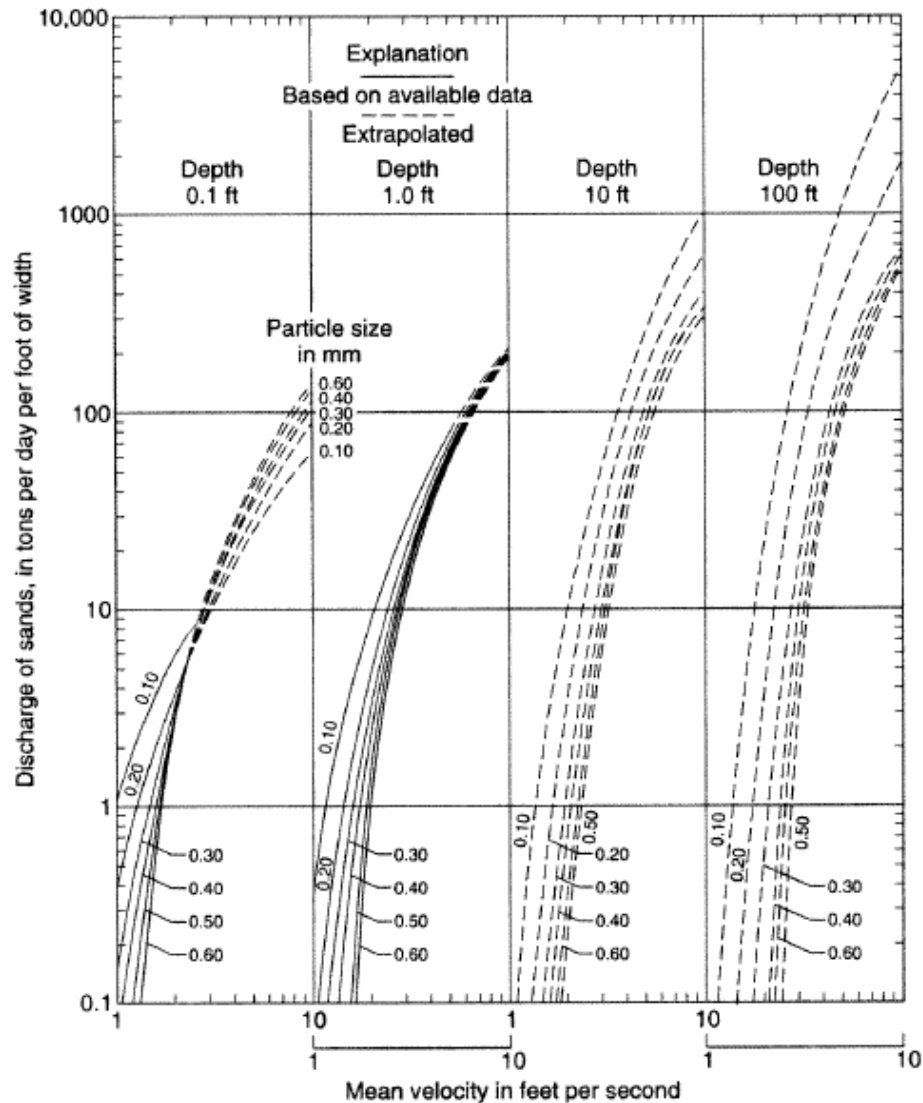


Figure 18.6.2 Relationships of discharge of sands to mean velocity for six median sizes of bed sands, four depths of flow, and a water temperature of 60°F (Colby, 1964.) (from Shen and Julien, 1993).

where

A = coefficient associated with D_{50}

AF = adjustment coefficient for water temperature and concentration of fine sediment (Figure 18.6.1a is based on sediment sizes from 0.2 to 0.3 mm. For other sizes, a correction, CF , from Figure 18.6.1b is needed.)

CF = percentage effect for different medium particle size (Figure 18.6.1b)

V = mean velocity, ft/s

V_c = critical velocity, ft/s

d = mean depth, ft

D_{50} = particle size, mm, at which 50 percent of the bed material by weight is finer

B = an exponent that has the following values:

$$B = 2.5 \text{ for } (V - V_c) < 1.0 \quad (18.6.2a)$$

$$B = 1.453 D_{50}^{-0.138} \text{ for } (V - V_c) \geq 1.0 \quad (18.6.2b)$$

The following procedure is used in the evaluation of the bed-material discharge:

Step 1 Compute the critical velocity, V_c :

$$V_c = 0.4673 d^{0.1} D_{50}^{0.33} \quad (18.6.3)$$

Step 2 Determine exponent B with the value of $(V - V_c)$.

Step 3 Determine the value of A :

$$\text{For } D_{50} = 0.1 \text{ mm} \quad A = 1.453 d^{0.61} \quad (18.6.4a)$$

$$D_{50} = 0.2 \text{ mm} \quad A = 1.329 d^{0.48} \quad (18.6.4b)$$

$$D_{50} = 0.3 \text{ mm} \quad A = 1.4 d^{0.3} \quad (18.6.4c)$$

$$D_{50} = 0.4 \text{ mm} \quad A = 1.26 d^{0.3} \quad (18.6.4d)$$

$$D_{50} = 0.8 \text{ mm} \quad A = 1.099 d^{0.3} \quad (18.6.4e)$$

Step 4 Determine correction factor (CF) from Figure 18.6.1.

Step 5 Determine the coefficient, AF , from the correction curves in Figure 18.6.1a.

Step 6 Compute g_s using equation (18.6.1).

EXAMPLE 18.6.1

Compute the sediment discharge per unit width for the Colorado River at Taylor's Ferry for a depth of 10 ft and a flowrate of 40 cfs/ft using Colby's formula.

SOLUTION

Step 1 Compute V_c for a depth of 10 ft and $D_{50} = 0.33$:

$$V_c = 0.4673 d^{0.1} D_{50}^{0.33}$$

$$V_c = 0.4673 (10.0)^{0.1} (0.33)^{0.33}$$

$$V_c = 0.408 \text{ fps}$$

Step 2 Compute B :

$$\text{Since } (V - V_c) = (4.0 - 0.408) = 3.532 \text{ ft/s}$$

$$B = 1.453 (0.33)^{-0.138} = 1.693$$

Step 3 Compute A :

$$A = 1.4 d^{0.3} \text{ for } D_{50} = 0.3 \text{ mm}$$

$$A = 1.26 d^{0.3} \text{ for } D_{50} = 0.4 \text{ mm}$$

Since $D_{50} = 0.3$ mm, interpolation is necessary:

A	D_{50}
2.793	0.3
x	0.33
2.514	0.40

$$\frac{x - 2.793}{-0.279} = \frac{0.03}{0.1}$$

$$x = 2.7093$$

$$A = 2.7093$$

Step 4 Find $CF = 1$ using Figure 18.6.1b for $D_{50} = 0.33$ mm

Step 5 Find AF using Figure 18.6.1a for 60°F, $AF = 1$

Step 6 Compute g_s using equation (18.6.1) where $(1 + (AF - 1) CF) = 1$:

$$g_s = A(V - V_c)^B (1 + (AF - 1)CF)(0.672)$$

$$g_s = 2.7093(4 - 0.408)^{1.693}(1)(0.672)$$

$$g_s = 15.864 \frac{\text{lbs}}{\text{sec-ft}}$$

18.6.2 Ackers-White Formula

Ackers and White (1973) developed a general sediment discharge function in terms of three dimensionless groups: D_{gr} (size), F_{gr} (mobility), and G_{gr} (discharge). The procedure for the computation of concentration of bed-material discharge is as follows:

Step 1 Compute the dimensionless grain diameter using:

$$D_{gr} = D_{50} \left(\frac{g(S_g - 1)}{\nu^2} \right)^{1/3} \quad (18.6.5)$$

where

D_{50} = particle size, in ft, at which 50 percent of the bed material by weight is finer

g = acceleration of gravity, ft/s²

S_g = specific gravity of the sediment

ν = kinematic viscosity, ft²/s

Step 2 Determine the values of parameters A , C_A , n , and m used in equation (18.6.7) associated with the computed D_{gr} for two size ranges of bed material. For intermediate size, $1 \leq D_{gr} \leq 60$, $D_{gr} = 1$ (0.04 mm silt size) to $D_{gr} = 60$ (2.5 mm sand size):

$$n = 1.00 - 0.56 \log D_{gr}$$

$$A = \frac{0.23}{\sqrt{D_{gr}}} + 0.14$$

$$m = \frac{9.66}{D_{gr}} + 1.34$$

$$\log C_A = 2.86 \log D_{gr} - (\log D_{gr})^2 - 3.53$$

For coarse size, $D_{gr} > 60$:

$$n = 0.00$$

$$A = 0.17$$

$$m = 1.5$$

$$C_A = 0.025$$

Step 3 Compute the particle mobility, F_{gr} :

$$F_{gr} = \frac{u_*^n}{\sqrt{gD_{50}(S_g - 1)}} \left(\frac{V}{\sqrt{32} \log \left(\frac{\alpha d}{D_{50}} \right)} \right)^{1-n} \quad (18.6.6)$$

where

d = mean depth, ft

u_* = shear velocity $(\tau_0/\rho)^{1/2}$, ft/sec

V = mean velocity, ft/sec

α = coefficient in the rough turbulent equation with a value of 10

n = transition exponent depending on sediment size

Step 4 Compute the sediment transport parameter, G_{gr} :

$$G_{gr} = C_A \left[\frac{F_{gr}}{A} - 1 \right]^m \quad (18.6.7)$$

Step 5 Compute the concentration of bed-material discharge:

$$C = 10^6 \left[\frac{G_{gr} S_g D_{50} \left[\frac{V}{u_*} \right]^n}{d} \right] \quad (18.6.8)$$

where

C is the concentration of bed-material discharge, in parts per million (ppm) by weight

Step 6 Convert the concentration to appropriate units:

$$\begin{aligned} g_s &= C(\text{ppm}) \times \frac{8.34 \text{ lbs}/10^6 \text{ gal}}{(1 \text{ ppm})} \times \frac{7.48 \text{ gal}}{1 \text{ ft}^3} \times q \frac{\text{cfs}}{\text{ft}} \\ &= \text{lb}/\text{sec}\text{-ft} \end{aligned}$$

EXAMPLE 18.6.2

Compute the sediment discharge per unit width for the Colorado River at Taylor's Ferry for a depth of 10 ft and a flowrate of 40 cfs/ft using the Ackers-White formula.

SOLUTION

Step 1 Compute dimensionless grain diameter, G_{gr} :

$$D_{50} = 0.33 \text{ mm} = 0.001083 \text{ ft}$$

$$g = 32.2 \text{ ft}/\text{s}^2$$

$$S_g = 2.65$$

$$\nu = 1.22 \times 10^{-5} \text{ for } T = 60^\circ\text{F}$$

$$D_{gr} = 0.001083 \left[\frac{(32.2)(2.65 - 1)}{(1.22 \times 10^{-5})^2} \right]^{1/3} = 7.6825$$

Step 2 Compute A , C_A , n , and m :

$$\text{For } 1 \leq D_{gr} \leq 60$$

$$n = 1.00 - 0.56 \log D_{gr} = 0.504$$

$$A = \frac{0.23}{\sqrt{D_{gr}}} + 0.14 = 0.223$$

$$m = \frac{9.66}{D_{gr}} + 1.34 = 2.597$$

$$\log C_A = 2.86 \log (7.6825) - [\log (7.6825)]^2 - 3.53$$

$$\log C_A = -1.7816$$

$$C_A = 0.01654$$

Step 3 Compute the particle mobility using equation (18.6.6):

First compute shear velocity, $u_* = (\tau_0/\rho)^{1/2}$ for $\rho = 1.94$ at 60°F. Then

$$\tau_0 = \gamma d S = 62.4 (10) (0.000217) = 0.1354$$

and

$$u_* = (0.1354/1.94)^{1/2} = 0.2642 \text{ ft/s:}$$

$$F_{gr} = \frac{0.2642^{0.504}}{\sqrt{(32.2)(0.001083)(2.65-1)}} \left[\frac{4}{\sqrt{32} \log \left(\frac{10 \times 10}{0.001083} \right)} \right]^{0.496}$$

$$F_{gr} = \frac{0.5113}{0.2399} (0.3803) = 0.8106$$

Step 4 Compute G_{gr} using equation (18.6.7):

$$G_{gr} = C_A \left[\frac{F_{gr}}{A} - 1 \right]^m$$

$$G_{gr} = 0.01654 \left[\frac{0.8106}{0.223} - 1 \right]^{2.597} = 0.2048$$

Step 5 Compute concentration of bed-material discharge, ppm, using equation (18.6.8):

$$C = \frac{10^6 G_{gr} S_g D_{50} \left(\frac{V}{u_*} \right)^n}{d}$$

$$C = \frac{10^6 (0.2048) (2.65) (0.001083) \left(\frac{4}{0.2642} \right)^{0.504}}{10}$$

$$C = 231.2 \text{ ppm}$$

Step 5 Convert C from ppm to lb/sec-ft:

$$g_s = 231.2 \text{ ppm} \times \frac{8.34 \text{ lb}}{10^6 \text{ gal}} \times \frac{7.48 \text{ gal}}{1 \text{ ft}^3}$$

$$g_s = 0.0144 \text{ lb/ft}^3 \text{ or } 0.5760 \text{ lb/sec-ft}$$

18.6.3 Yang's Unit Stream Power Formula

18.6.3.1 Yang's Sand Formula

Yang (1973) developed an equation for computing the concentration of bed-material discharge. This equation is for application to sand-bed streams and is based on dimensional analysis and the concept of unit stream power. Yang defined unit stream power as the rate of potential energy dissipated per unit weight of water, expressed by the product of velocity and slope.

Yang's (1973) dimensionless unit stream power for sand transport is as follows:

$$\log C = 5.435 - 0.286 \log \frac{WD_{50}}{\nu} - 0.457 \log \frac{u_*}{W} + \left[1.799 - 0.409 \log \frac{WD_{50}}{\nu} - 0.314 \log \frac{u_*}{W} \right] \log \left[\frac{VS}{W} - \frac{V_{cr}S}{W} \right] \quad (18.6.9)$$

in which the dimensionless critical velocity at incipient motion can be expressed as:

$$\frac{V_{cr}}{W} = \frac{2.5}{\log \frac{u_* D_{50}}{\nu} - 0.06} + 0.66 \quad \text{for } 1.2 < \frac{u_* D_{50}}{\nu} < 70 \quad (18.6.10a)$$

$$\frac{V_{cr}}{W} = 2.05 \quad \text{for } 70 \leq \frac{u_* D_{50}}{\nu} \quad (18.6.10b)$$

where

C = concentration of bed-material discharge (ppm by weight)

W = average fall velocity (fps) of sediment particles of diameter D_{50}

D_{50} = particle size (ft) at which 50 percent of the bed material by weight is finer

ν = kinematic viscosity (ft²/s)

u_* = shear velocity (fps); $u_* = \sqrt{\tau_0/\rho}$

V = average velocity (fps)

S = energy slope (ft/ft)

V_{cr} = average flow velocity (fps) at incipient motion

18.6.3.2 Yang's Gravel Formula

Yang's (1984) dimensionless unit stream power formula for gravel transport is:

$$\log C = 6.681 - 0.633 \log \frac{WD_{50}}{\nu} - 4.816 \log \frac{u_*}{W} + \left[2.784 - 0.305 \log \frac{WD_{50}}{\nu} - 0.282 \log \frac{u_*}{W} \right] \log \left[\frac{VS}{W} - \frac{V_{cr}S}{W} \right] \quad (18.6.11)$$

The dimensionless critical velocity at incipient motion is defined by equations (18.6.10a,b).

For computing the total discharge of graded material (using the gravel or sand formula), the total bed-material discharge concentration can be computed using:

$$C = \sum_{i=1}^n i_b C_i \quad (18.6.12)$$

where

n = number of size fractions in the bed material

i_b = fraction by weight of bed material in a given size fraction

C_i = computed concentration in the size fraction, i (ppm)

EXAMPLE 18.6.3

Compute the sediment discharge per unit width for the Colorado River at Taylor's Ferry for a depth of 10 ft and a flowrate of 40 cfs/ft using Yang's sand formula.

SOLUTION

Step 1 Compute shear velocity, u_* :

$$D_{50} = 0.33 \text{ mm} = 0.001083 \text{ ft}$$

$$\rho = 1.94 \text{ slug/ft}^3 \text{ for } T = 60^\circ\text{F}$$

$$\gamma = 68.4 \text{ lb/ft}^3$$

$$u_* = (\tau_0/\rho)^{1/2}$$

$$\tau_0 = \gamma d S = 62.4 (10) (0.000217) = 0.1354 \text{ lb/ft}^2$$

$$u_* = (0.1354/1.94)^{1/2} = 0.2642 \text{ ft/s}$$

Step 2 Compute $\frac{u_* D_{50}}{\nu}$ for $\nu = 1.22 \times 10^{-5} \text{ ft}^2/\text{sec}$ at $T = 60^\circ\text{F}$

$$\frac{u_* D_{50}}{\nu} = \frac{0.2642(0.001083)}{(1.22 \times 10^{-6})} = 23.45$$

Step 3 Compute V_{cr}/W

$$\text{Since } 1.2 < \frac{u_* D_{50}}{\nu} < 70,$$

$$\frac{V_{cr}}{W} = \frac{2.5}{\log \frac{u_* D_{50}}{\nu} - 0.06} + \frac{2.5}{\log(23.45) - 0.06} + 0.66 = 2.568$$

Step 4 Determine the fall velocity, W , for D_{50} by interpolation. Since $D_{50} = 0.33 \text{ mm}$, interpolation is necessary:

W	D (mm)
1.9	0.177
x	0.33
4.8	0.354

$$\frac{x - 1.9}{2.9} = \frac{0.153}{0.177}$$

$$x = 4.407 \text{ cm/sec}$$

$$W = 0.1446 \text{ fps for } D_{50} = 0.33 \text{ mm}$$

Step 5 Compute V_{cr} :

$$\frac{V_{cr}}{W} = 2.568; V_{cr} = 0.3713 \text{ ft/s}$$

Step 6 Compute concentration using equation (18.6.9):

$$\begin{aligned} \log C = & 5.435 - 0.268 \log \left[\frac{0.1446(0.001083)}{1.22 \times 10^{-5}} \right] - 0.457 \left[\frac{0.2642}{0.1446} \right] + \\ & \left[1.799 - 0.409 \log \left[\frac{0.1446(0.001038)}{1.22 \times 10^{-5}} \right] - 0.314 \log \left[\frac{0.2642}{0.1446} \right] \right] \times \\ & \log \left[\frac{(4 - 0.3713)(0.000217)}{0.1446} \right] \end{aligned}$$

$$\log C = 2.13784$$

$$C = 137.354 \text{ ppm or } 0.00857 \text{ lb/ft}^3 \text{ or } 0.343 \text{ lb/sec-ft}$$

Table 18.6.1 summarizes the resulting sediment discharge per unit width for the Colorado River at Taylor's Ferry. Figure 18.6.3 presents the sediment rating curves for the Colorado River at Taylor's Ferry using several sediment discharge formulas for the condition specified in the figure.

Table 18.6.1 Sediment Transport for a Discharge of ($q=40$ cfs/ft width) the Functions Used

Formula	Sediment Transport (lbs/sec per foot width)
(a) Schoklitsch Formula	0.086
(b) Duboys Formula	0.891
(c) Meyer-Peter-Muller [English]	0.054
Meyer-Peter-Muller [Metric]	0.105
(d) Laursen Formula	5.442
(a) Yang's Sand Formula	0.343
(b) Tofalleti Formula	3.039
(c) Ackers-White [D_{50} Option]	0.576
Ackers-White [D_{35} Option]	0.704
(d) Einstein Bed-Load Function	0.140
(e) Colby Formula [Graph]	0.718

18.7 WATERSHED SEDIMENT YIELD

Watershed erosion is characterized by the detachment and entrainment of solid particles from the land surface. Erosion occurs under the influence of water, gravity, wind, and ice. *Water erosion* can be classified as *sheet erosion* and *channel erosion*. Sheet erosion is the detachment caused by raindrop impact and the thawing of frozen grounds and the subsequent removal by overland flow.

The *universal soil loss equation* (USLE) was developed to predict the long-term average soil losses in runoff from field areas under specified cropping and management systems (U.S. DA-ARS, 1961). The USLE equation is:

$$A = RKLSCD \quad (18.7.1)$$

where

A is the computed soil loss in tons/acre

R is the rainfall-erodibility factor (see Figure 18.7.1)

K is the soil-erodibility factor (see Table 18.7.1)

L is the slope-length factor normalized to a plot length of 72.6 ft

S is the slope-steepness factor normalized to a field slope of 9 percent

C is the cropping-management factor normalized to a tilled area with continuous fallow (see Table 18.7.2)

D is the conservation practice factor normalized to straight-row farming up and down the slope

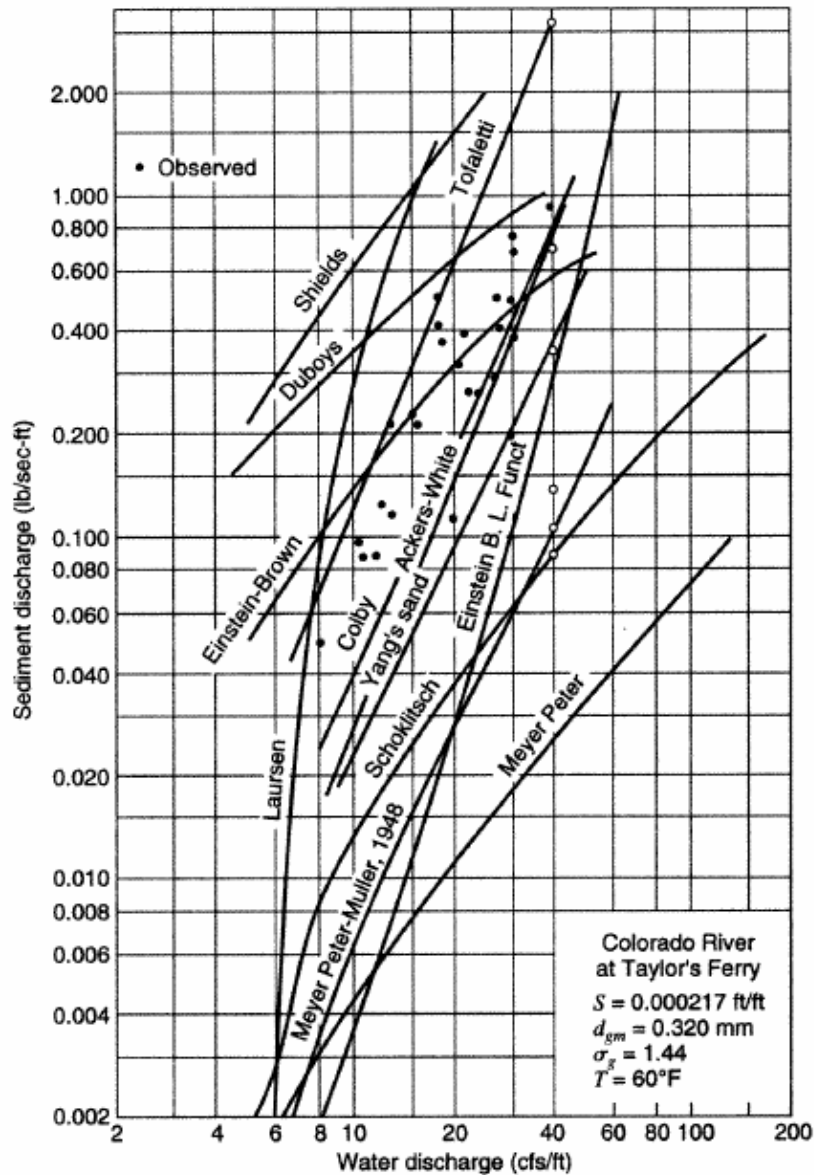


Figure 18.6.3 Sediment rating curves for the Colorado River at Taylor's Ferry according to several formulas, compared with measurements.

Table 18.7.1 Soil Erodibility Factor K in tons/acre

Textural class	Organic matter content, %	
	0.5	2
Fine sand	0.16	0.14
Very fine sand	0.42	0.36
Loamy sand	0.12	0.10
Loamy very fine sand	0.44	0.38
Sandy loam	0.27	0.24
Very fine sandy loam	0.47	0.41
Silt loam	0.48	0.42
Clay loam	0.28	0.25
Silty clay loam	0.37	0.32
Silty clay	0.25	0.23

Source: From Schwab et al. (1981).

The value of the *rainfall erodibility factor*, R , on an annual basis is shown in Figure 18.7.1 for use in computing average annual erosion losses. R also can be computed for each storm (summed over hours) using

$$R = 0.01 \sum EI \quad (18.7.2)$$

where the summation is for the time increments of the storm and E , the kinetic energy per foot-tons per acre-inch, is given by

$$E = (916 + 331 \log I) \quad (18.7.3)$$

where I is the rainfall intensity in inches per hour.

K , the *soil-erodibility factor*, describes the inherent erodibility (intrinsic susceptibility) of a given soil to erode, expressed in tons/acre (see Table 18.7.1). The slope length-steepness factor LS is a topographic factor relating the erosion losses from a field of given slope and length when compared with soil losses of a standard plot 72.6 ft long inclined at 9 percent slope. The LS factor can be computed using:

$$LS = \left(\frac{\lambda}{72.6} \right)^m (65.41 \sin^2 \theta + 4.56 \sin \theta + 0.065) \quad (18.7.4)$$

where λ is the actual slope length in ft, θ is the angle of the slope, and m is an exponent ranging from 0.5 for slopes ≥ 5 percent to 0.2 for slopes ≤ 1 percent. The graphical representation of equation (18.7.4) is presented in Figure 18.7.2.

The *cropping management factor*, C , accounts for the crop rotation, tillage method, crop residue treatment, productivity level, and other cultural practice variables (see Table 18.7.2).

Table 18.7.2 Cropping Management Factor C

Undisturbed forest land							
Percent of area covered by canopy of trees and undergrowth		Percent of area covered by duff at least 2 in deep		Factor C			
100–75		100–90		0.0001–0.001			
70–45		85–75		0.002–0.004			
40–20		70–40		0.003–0.009			
Permanent pasture, range, and idle land*							
Cover that contacts the soil surface							
Vegetative canopy		Percent ground cover					
Type and height [†]	Type [‡]	0	20	40	60	80	95+
No appreciable canopy	G	0.45	0.20	0.10	0.042	0.013	0.003
	W	0.45	0.24	0.15	0.091	0.043	0.011
Tall weeds or short brush with average drop fall height of 20 in.	G	0.17–0.36	0.10–0.17	0.06–0.09	0.032–0.038	0.011–0.013	0.003
	W	0.17–0.36	0.12–0.20	0.09–0.13	0.068–0.083	0.038–0.041	0.011
Appreciable brush or bushes, with average drop fall height of 6 1/2 ft	G	0.28–0.40	0.14–0.18	0.08–0.09	0.036–0.040	0.012–0.013	0.003
	W	0.28–0.40	0.17–0.22	0.12–0.14	0.078–0.087	0.040–0.042	0.011
Trees, but no appreciable low brush. Average drop fall height of 13 ft	G	0.36–0.42	0.17–0.19	0.09–0.10	0.039–0.041	0.012–0.013	0.003
	W	0.36–0.42	0.20–0.23	0.13–0.14	0.084–0.089	0.041–0.042	0.011

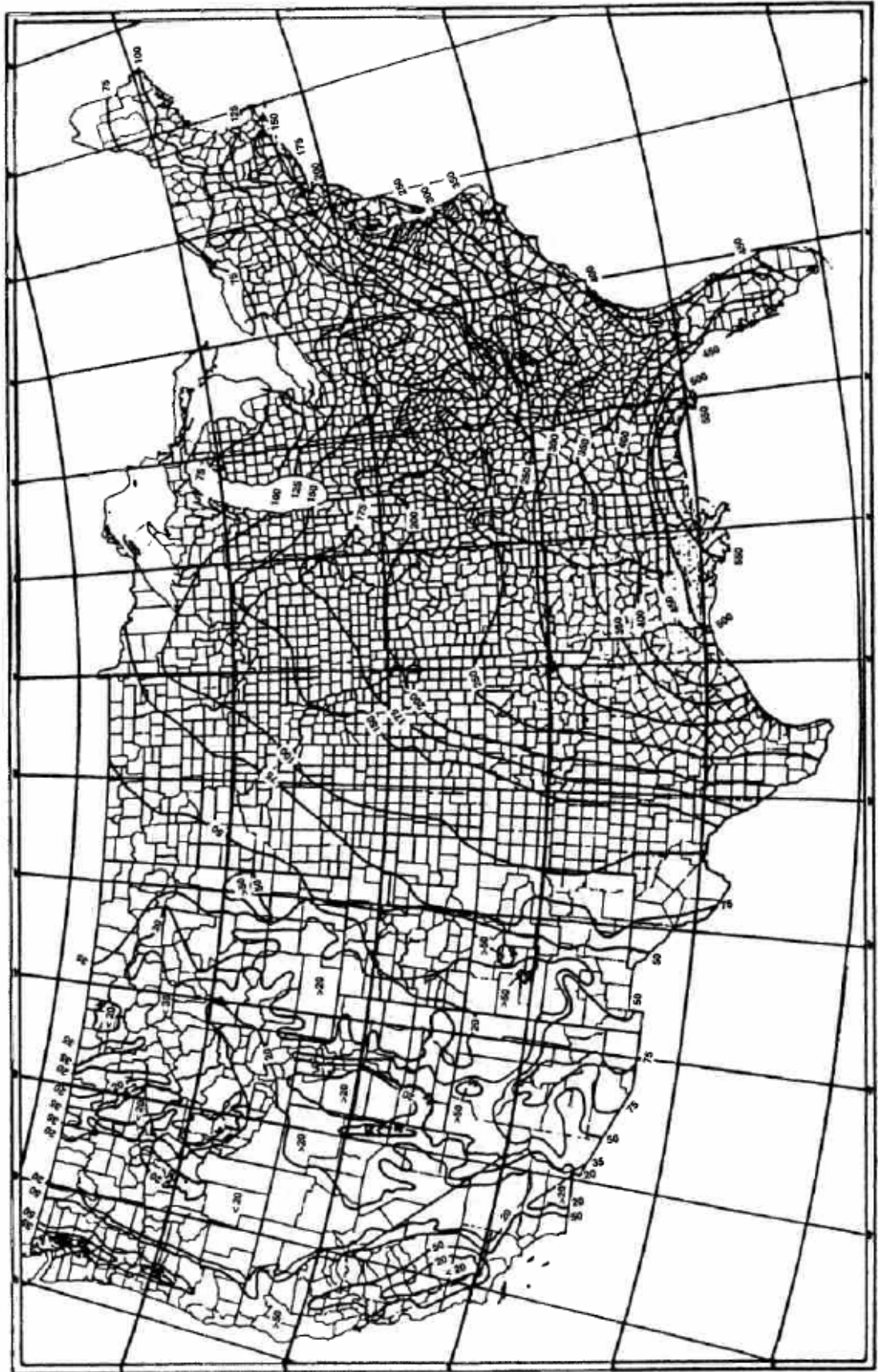


Figure 18.7.1 Average annual values of the rainfall erosion index R (Wischmeier and Smith, 1978).

Table 18.7.2 Cropping Management Factor C (continued)

Construction slopes		
Type of mulch	Mulch rate (tons/acre)	Factor C
Straw	1.0–2.0	0.06–0.20
Crushed stone, 1/4–1.5 in	135	0.05
	240	0.02
Wood chips	7	0.08
	12	0.05
	25	0.02

*The listed C values assume that the vegetation and mulch are randomly distributed over the entire area.

†Canopy height is measured as the average fall height of water drops falling from the canopy to the ground. Canopy effect is inversely proportional to drop fall height and is negligible if fall height exceeds 33 ft.

‡G: cover at surface is grass, grasslike plants, decaying compacted duff, or litter at least 2 in deep. W: cover at surface is mostly broadleaf herbaceous plants (as weeds with little lateral-root network near the surface) or undecayed residues or both.

Source: Shen and Julien (1993).

EXAMPLE 18.7.1

Compute soil loss in Phoenix, Arizona for a very fine sand with 0.5 percent organic matter content. $C = 0.006$, $D = 1.5$. $S = 5$ percent, $L = 300$ ft.

SOLUTION

Use equation 18.7.1 to compute the soil loss

$$A = RKLSCD$$

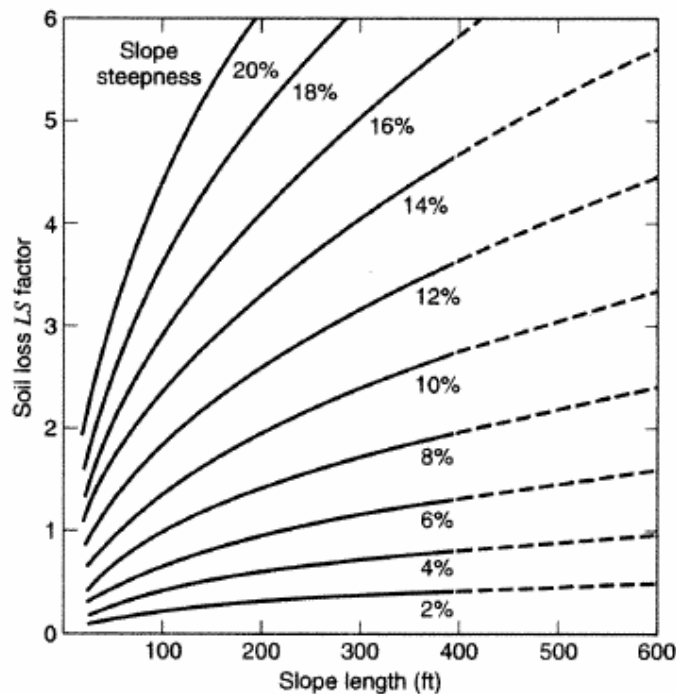


Figure 18.7.2 Topographic-effect graph used to determine LS -factor values for different slope-steepness–slope-length combinations (Wischmeier and Smith, 1965).

where

$$\begin{aligned}
 R &= 50 \text{ from Figure 18.7.1} \\
 K &= 0.42 \text{ from Table 18.7.1} \\
 LS &= 0.928 \text{ from Figure 18.7.2} \\
 C &= 0.006 \\
 D &= 1.5 \\
 A &= RKLSCD \\
 &= 50 \times 0.42 \times 0.928 \times 0.006 \times 1.5 \\
 &= 0.1754 \text{ tons/acre}
 \end{aligned}$$

8.8 RESERVOIR SEDIMENTATION

Accumulation of sediment in reservoirs may have the following effects (Shen and Julien, 1993):

1. reducing the useful storage volume for water in the reservoir,
2. changing the water quality near the dam,
3. increasing flooding level upstream of the dam because of sediment aggradation,
4. influencing the stability of the stream downstream of the dam,
5. affecting stream ecology in the dam region, and
6. causing other environmental impacts by changing the water quality.

This section briefly outlines a method that can be used to estimate the potential sediment accumulation in a reservoir.

Step 1 Construct a *flow duration curve*, which is the cumulative distribution curve of stream runoff passing the dam (see Figure 18.8.1a).

Step 2 Construct a *sediment rating curve*, which relates sediment concentration to stream discharge (see Figure 18.8.1b).

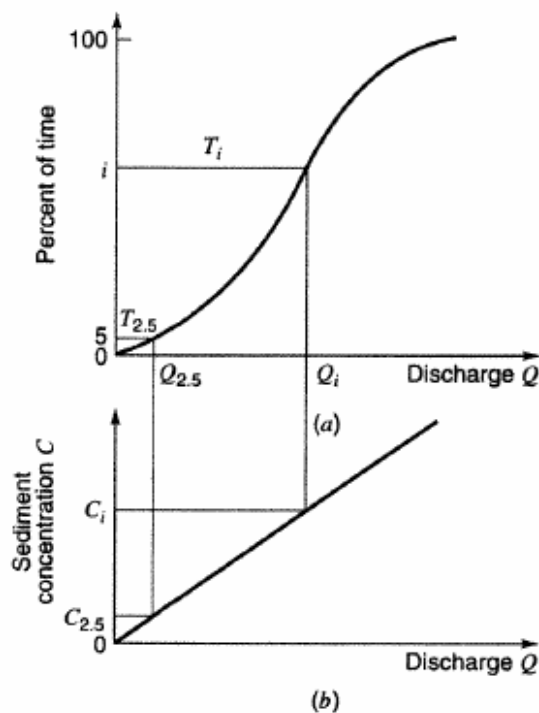


Figure 18.8.1 Flow and sediment discharge. (Shen and Julien, 1993)

Step 3 Divide the flow duration curve into equally spaced sections of percentage, Δp (e.g., 20 sections, $\Delta p = 0.05$). Read average discharge, Q_i , from the flow duration curve. Read the corresponding sediment concentration, C_i , from the sediment rating curve. Repeat for each of the sections.

Step 4 Compute the average total sediment load in weight per unit time, q_t , using

$$\begin{aligned}
 q_t &= \sum_i C_i Q_i \Delta P \\
 &= \Delta P \sum_i C_i Q_i
 \end{aligned}
 \tag{18.8.1}$$

Step 5 Determine the percentage of sediment trapped in the reservoir, which is a function of the fall velocity of sediment and the allowable time for settling. The more important factors to determine the amount of sediment trapped include: the relative size of the reservoir, the reservoir shape, the reservoir operation, and the sediment particle size. Brune (1953) developed a commonly used relation for determining sediment trapping, as illustrated in Figure 18.8.2. *Trap efficiency* is the ratio between sediment trapped in the reservoir and the total sediment entering the reservoir. Reservoir capacity is the reservoir volume at the normal operation pool level for the period considered.

The U.S. Bureau of Reclamation (1987) classifies reservoir operation according to the following:

Operation	Reservoir Operation
1	Sediment always submerged or nearly submerged
2	Normally moderate to considerable reservoir drawdown
3	Reservoir normally empty
4	Riverbed sediments

The selection of the proper operation number can usually be made from the operation study prepared for the reservoir. The density of the sediment deposits is estimated using:

$$W = W_c P_c + W_m P_m + W_s P_s
 \tag{18.8.2}$$

where W is the unit weight in lb/ft^3 (or density in kg/m^3); P_c , P_m , and P_s are the percentages of clay, silt, and sand, respectively, of the inflowing sediment; and W_c , W_m , and W_s are the coefficients of unit weight for clay, silt, and sand, respectively, in lb/ft^3 (kg/m^3), obtained from Table 18.8.1.

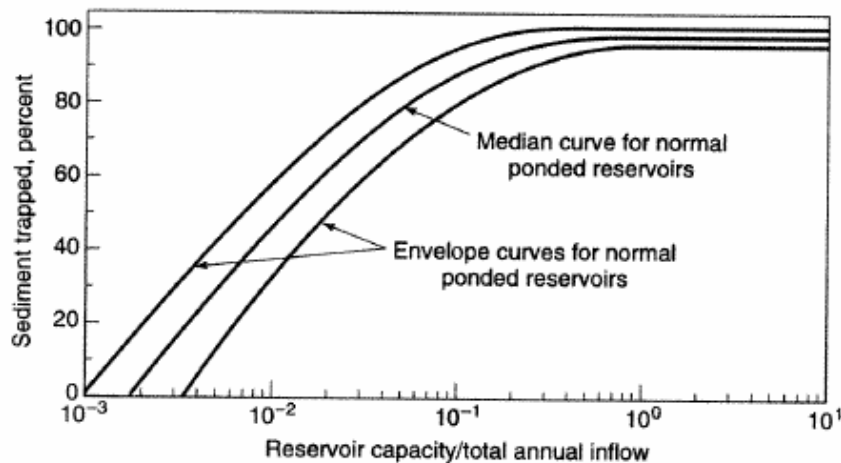


Figure 18.8.2 Sediment trap efficiency in a reservoir (after Brune, 1953) (from Shen and Julien, 1993).

Table 18.8.1 Reservoir Operation Number

Operation	Initial weight (initial mass in lb/ft ³ (kg/m ³))		
	W_c	W_m	W_s
1	26 (416)	70 (1120)	97 (1550)
2	35 (561)	71 (1140)	97 (1550)
3	40 (641)	72 (1150)	97 (1550)
4	60 (961)	73 (1170)	97 (1550)

Source: Yang (1996).

EXAMPLE 18.8.1

Determine the density of sediment deposits for a reservoir operation 2 with 23 percent clay, 40 percent silt, and 37 percent sand.

SOLUTION

$$\begin{aligned}
 W &= W_c P_c + W_m P_m + W_s P_s \\
 &= 561(0.23) + 1140(0.40) + 1550(0.37) \\
 &= 1158 \text{ kg/m}^3
 \end{aligned}$$

Miller (1953) developed an approximation for the average density of sediment deposited, W_T , in T years as follows:

$$W_T = W_0 + 0.4343K \left[\frac{T}{T-1} (\ln T) - 1 \right] \quad (18.8.3)$$

where W_0 is the initial unit weight (density) derived from equation (18.8.2) and K is a constant based on the type of reservoir operation and sediment size analysis. K is expressed as:

$$K = K_c P_c + K_m P_m + K_s P_s \quad (18.8.4)$$

where K_s , K_m , and K_c are found in Table 18.8.2.

Table 18.8.2 K Values of Sand, Silt, and Clay

Reservoir operation	K for inch-pound units (metric units)		
	Sand	Silt	Clay
1	0	5.7 (91)	16 (256)
2	0	1.8 (29)	8.4 (135)
3	0	0 (0)	0 (0)

Source: Yang (1996).

EXAMPLE 18.8.2

For data given in Example 18.8.1, determine the average density of sediments deposited after 100 years.

SOLUTION

First determine K :

$$\begin{aligned}
 K &= K_c P_c + K_m P_m + K_s P_s \\
 &= 0(0.23) + 29(0.40) + 135(0.37) \\
 &= 62
 \end{aligned}$$

Determine W_{100} using equation (18.8.3):

$$\begin{aligned} W_T &= W_0 + 0.4343K \left[\frac{T}{T-1} (\ln T) - 1 \right] \\ &= 1158 + 0.4343(62) \left[\frac{100}{100-1} (\ln 100) - 1 \right] \\ &= 1256.3 \text{ kg/m}^3 \end{aligned}$$

18.9 STREAM STABILITY AT HIGHWAY STRUCTURES

18.9.1 Factors that Affect Stream Stability

The factors that affect stream stability and potentially bridge stability at highway stream crossings can be classified as geomorphic factors (see Figure 18.9.1) and hydraulic factors (see Figure 18.9.2). FHWA Hydraulic Engineering Circular (HEC) No. 20 (Lagasse et al., 2001a) presents detailed descriptions of the various factors and how they affect stream stability. Much of the material presented in this section is adapted from HEC No. 20.

18.9.2 Basic Engineering Analysis

FHWA HEC No. 20 recommends a three-level procedure for analyzing stream stability:

Level 1 Qualitative and Other Geomorphic Analysis

- Step 1 Stream characteristics
- Step 2 Land use changes
- Step 3 Overall stability
- Step 4 Lateral stability
- Step 5 Vertical stability
- Step 6 Stream response

Level 2 Basic engineering analysis (steps illustrated in Figure 18.9.3)

Level 3 Mathematical and physical model studies

The remaining discussion will focus on the steps in Level 2, basic engineering analysis. Evaluating the flood history (step 1) is an integral step in characterizing watershed response and morphologic evaluation, particularly in arid regions. It is important to study flood records and corresponding stream responses using aerial photography or other physical information. Developing of the rainfall-runoff relation is important in understanding watershed conditions and historical changes in the watershed.

To evaluate the hydraulic conditions (Step 2), it is common practice to compute water surface profiles and hydraulic conditions using a computer code. For the analysis and design of bridge crossings, the U.S. Dept. of Transportation Federal Highway Administration (1990) WSPRO computer program is recommended because the computational procedure for evaluating bridge losses is superior to other models such as the U.S. Army Corps of Engineers HEC-2 and HEC-RAS River Analysis System (see Section 5.4.3). The input structure for WSPRO was specifically developed to facilitate bridge design.

Step 3 involves performing an analysis of the bed and bank materials to determine particle size gradation and other properties and a shape, fall velocity, and so on (see Section 18.1).

Step 4 involves evaluating the watershed sediment yield using a method such as the universal soil loss equation (USLE) (see Section 18.7).


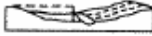



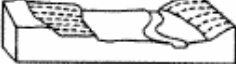

























Stream size (Sect. 2.2.1)	Small (< 30 m wide)	Medium (30–150 m)		Wide (> 150 m)
Flow habit (Sect. 2.2.2)	Ephemeral	(Intermittent)	Perennial but flashy	Perennial
Bed material (Sect. 2.2.3)	Silt-Clay	Silt	Sand	Gravel Cobble or Boulder
Valley setting (Sect. 2.2.4)	 No valley; alluvial fan	 Low relief valley (< 30 m deep)	 Moderate relief (30–300 m deep)	 High relief (> 300 m deep)
Floodplains (Sect. 2.2.5)	 Little or none (< 2 × channel width)	 Narrow (2–10 × channel width)		 Wide (> 10 × channel width)
Natural levees (Sect. 2.2.6)	 Little or none	 Mainly on concave		 Well developed on both banks
Apparent incision (Sect. 2.2.7)	 Not incised		 Probably incised	
Channel boundaries (Sect. 2.2.8)	 Alluvial	 Semi-alluvial		 Non-alluvial
Tree cover on banks (Sect. 2.2.8)	< 50 percent of bankline	50–90 percent of bankline		> 90 percent of bankline
Sinuosity (Sect. 2.2.10)	 Straight sinuosity (1–1.05)	 Sinuous (1.06–1.25)	 Meandering (1.25–2.0)	 Highly meandering (> 35 percent)
Braided streams (Sect. 2.2.10)	 Not braided (< 5 percent)	 Locally braided (5–35 percent)		 Generally braided (> 35 percent)
Anabranching streams (Sect. 2.2.11)	 Not anabranching (< 5 percent)	 Locally anabranching (5–35 percent)		 Generally anabranching (> 35 percent)
Variability of width and development of bars (Sect. 2.2.12)	 Narrow point bars	 Equiwidth	 Wider at bends	 Random variation
		 Wide point bars	 Irregular point and lateral bars	

Figure 18.9.1 Geomorphic factors that affect stream stability (adapted from Brice and Blodgett, 1978a, as presented in Lagasse et al., 2001a).

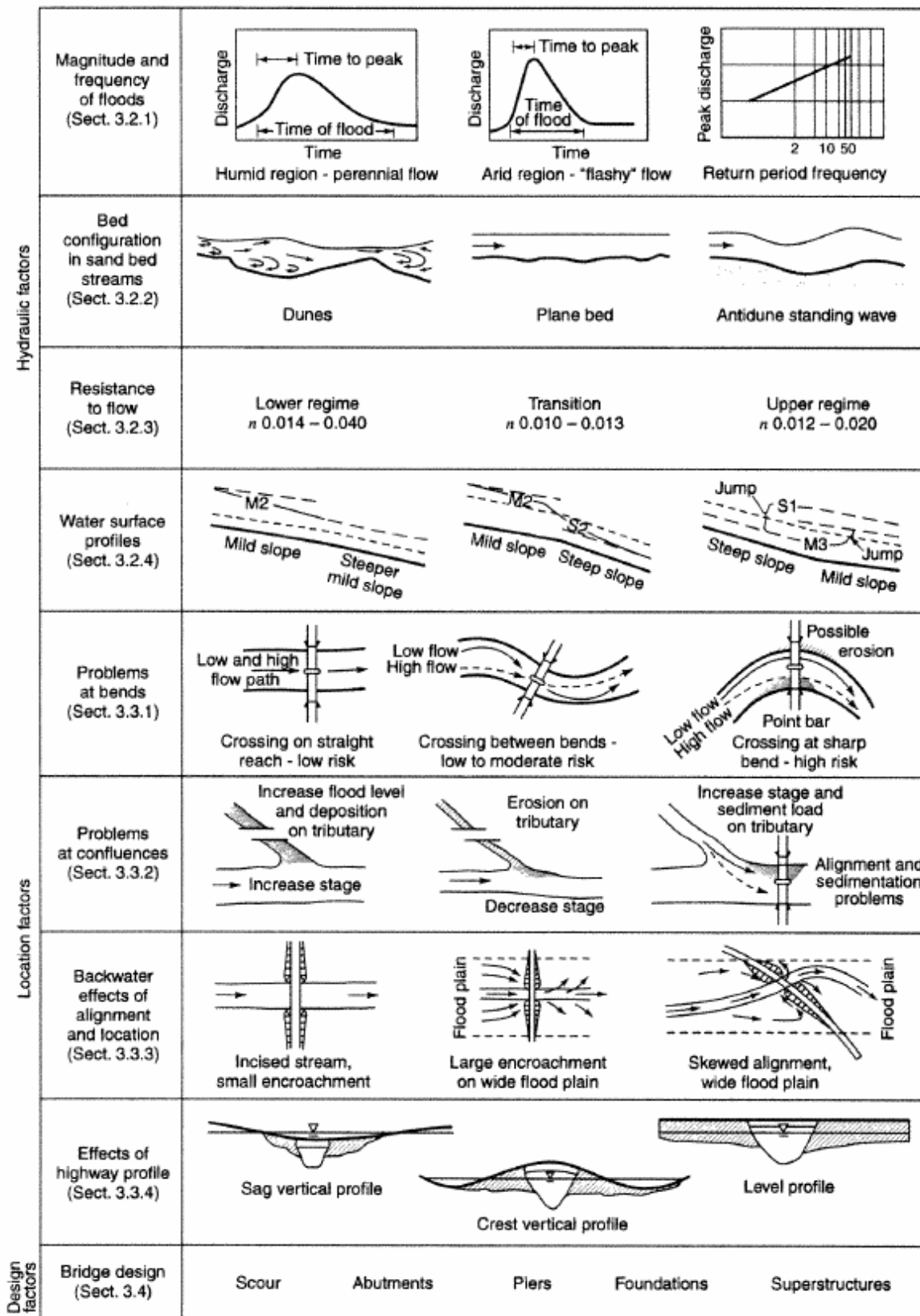


Figure 18.9.2 Hydraulic and location factors that affect stream stability (from Lagasse et al., 2001a).

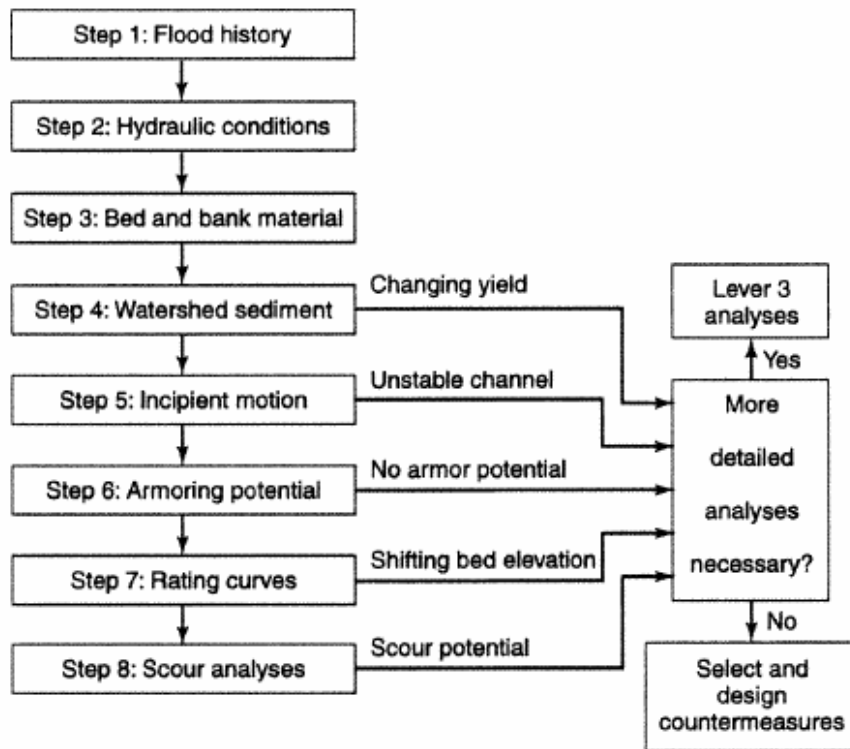


Figure 18.9.3 Flow chart for Level 2: Basic Engineering Analyses (from Lagasse et al., 2001a).

Step 5 involves performing an *incipient motion analysis* to evaluate the relative channel stability. Incipient motion was defined in Section 18.3. For most river conditions, the following equation derived from the Shields diagram can be used (Lagasse et al., 2001a):

$$D_c = \frac{\tau}{0.047(\gamma_s - \gamma)} \quad (18.9.1)$$

where D_c is the diameter of the sediment particle at incipient motion condition in (m); τ is the boundary shear stress in N/m^2 (pa); γ_s and γ are the specific weights of the sediment and water, respectively in N/m^3 ; and 0.047 (for sand bed channels) is the dimensionless coefficient often referred to as Shields critical parameter.

Step 6 involves evaluating the *armoring potential*. Armoring is the natural process whereby an erosion-resistant layer of relatively large particles is formed on a streambed because of the removal of finer particles by the stream flow. An armoring layer that is sufficient to protect the bed against moderate discharges can be disrupted during high discharges and then may be restored as flows diminish. By determining the percentage of bed material equal to or larger than the armor size, D_c , computed using equation (18.9.1) for incipient motion, the depth of scour necessary to establish an armor layer can be determined using the following (Pemberton and Lara, 1984):

$$y_s = y_a \left[\frac{1}{P_c} - 1 \right] \quad (18.9.2)$$

where y_a is the thickness of the armoring layer and P_c is the decimal fraction of material coarser than the armoring size. y_a ranges from one to three times the armor size, P_c , depending on the value of D_c (Lagasse et al., 2001a). Stable armoring conditions require a minimum of the layer of armoring particles.

Step 7 involves evaluating stage-discharge rating curve shifts. Scour and fill is the most common cause of rating curve shifts. Rating curves that continually shift indicate channel instability.

Step 8 involves evaluating the scour condition at bridge crossings. Section 18.10 provides a detailed description of procedures based upon the FHWA-HEC No. 18 (Richardson and Davis, 2001). Calculation of the three components of scour (local scour, contraction scour, and aggradation/degradation) quantifies the potential instability at a bridge crossing.

Once the above steps have been completed, if a more detailed analysis is needed, Level 3 analysis is performed. In Level 3 analysis, mathematical and/or physical models are used to evaluate and assess the stream stability. If a more detailed analysis is not needed, countermeasures are selected and designed. Historically, the need for a Level 3 analysis has been for high-risk locations and for extraordinarily complex problems; however, because of the importance of stream stability to the safety and integrity of bridges, Level 3 analysis should be computed routinely according to Lagasse et al., (2001a).

18.9.3 Countermeasures (Flow Control Structure) for Stream Instability

Countermeasures are measures incorporated into a highway stream crossing system to monitor, control, inhibit, change, delay, or minimize stream and bridge stability problems or action plans for monitoring structures during and/or after flood events (Lagasse et al., 2001a). Selection of a countermeasure for a bank erosion problem depends on the erosion mechanism, stream characteristic, construction and maintenance requirements, potential for vandalism, and costs.

Of particular interest in this section are *flow control structures*, which are defined as structures, either within or outside a channel, that act as countermeasures by controlling the direction, velocity, or depth of flowing water (Richardson et al., 1990, 2001). These types of structures are also referred to as *river training works*. Figure 18.9.4 shows various types of flow control structures.

18.9.4 Spurs

Spurs are structures or embankments that are projected into streams at an angle in order to deflect flowing water away from critical zones, to prevent erosion of the banks, and to establish a more desirable channel alignment or width (Richardson et al., 1990, 2001). Spurs have several functions:

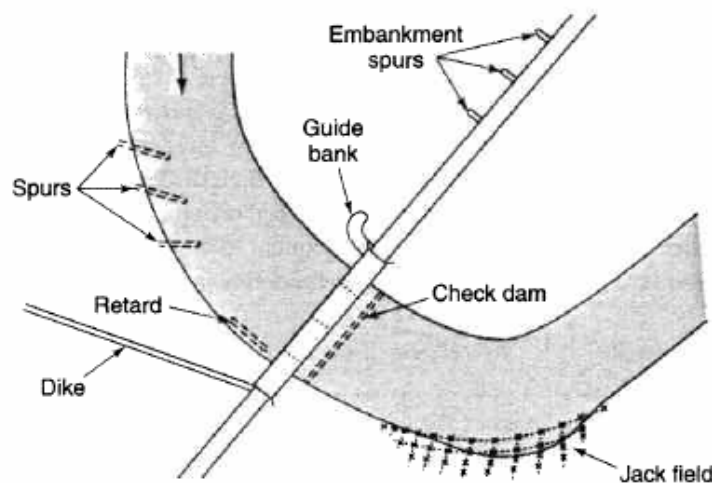


Figure 18.9.4 Placement of flow control structures relative to channel banks, crossing, and floodplain. Spurs, retards, dikes, and jack fields may be either upstream or downstream from the bridge (from Brice and Blodgett, 1978a).

1. to protect highway embankments that form approaches to bridge crossings,
2. to channelize wide, poorly defined streams into well-defined channels,
3. to establish and maintain new alignments through deposition of sediments, and
4. to halt meander migration at banks.

Spurs are classified as retarder spurs, retarder/deflector spurs, and deflector spurs, based on their permeability, which is defined as the percentage of the spur surface area facing the streamflow that is open. Accordingly, *retarder spurs* are permeable and function by retarding flow velocities near stream banks. *Retarder/deflector spurs* are permeable and function by retarding flow velocities at stream banks and direct flow away from the banks. *Deflector spurs* are impermeable, basically deflecting flow currents away from banks.

18.9.5 Guide Banks (Spur Dikes)

Guide banks (spur dikes) are placed at or near the ends of approach embankments to guide the streamflow through a bridge opening. They are used to prevent erosion of the approach embankments by cutting off the flow adjacent to the embankment. By guiding flow through the opening, they transfer scour away from abutments. Guide banks reduce separation of flow at the upstream abutment face and reduce abutment scour as a result of less turbulence at the abutment face.

Figure 18.9.5 illustrates a typical guide bank plan view. Figure 18.9.6 can be used to determine guide bank length, L_s , for designs greater than 15 m and less than 75 m. Lagasse et al. (2001a) recommend 15 m as the minimum length of guide banks; if the figure indicates length larger than 75 m, the design should be set at 75 m. FHWA practice has shown that a standardized length of 46 m has performed well (Lagasse et al., 2001a). Other guidelines for design include the following:

- A minimum freeboard of 0.6 m above the design water surface elevation should be used.
- Generally, top widths of 3 to 4 m are used.
- The upstream end of the guide bank should be round-nosed.
- Side slopes should be 1V:2H or less.
- Rock riprap should be placed on the stream side face and around the end of the guide bank.
- A gravel, sand, or fabric filter may be required to protect the underlying embankment material.

Refer to Lagasse et al. (2001a) for more detailed design concerns.

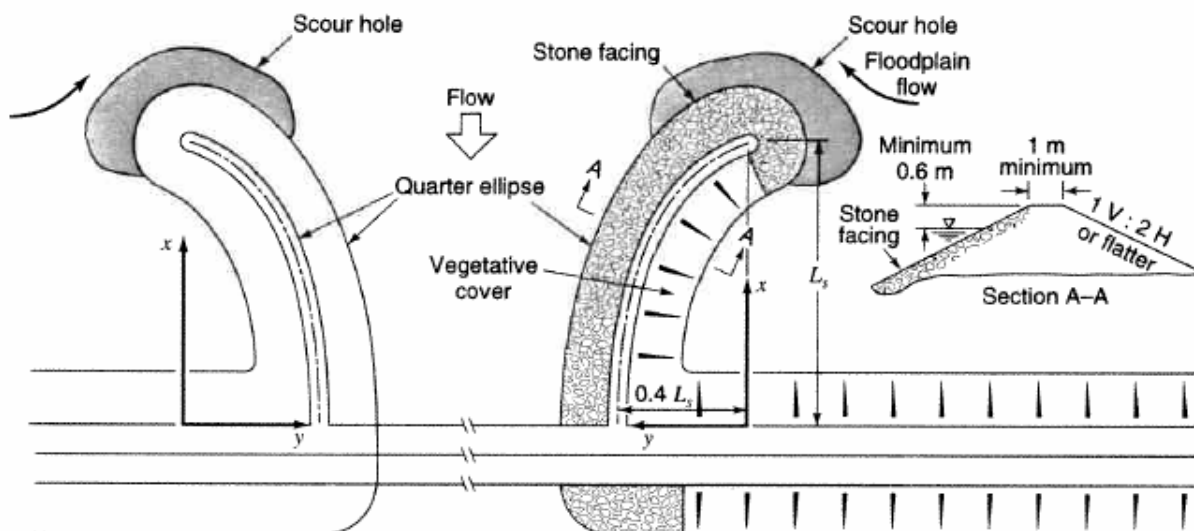


Figure 18.9.5 Typical guide bank (modified from Bradley, 1978) (as presented in Lagasse et al., 2001a).

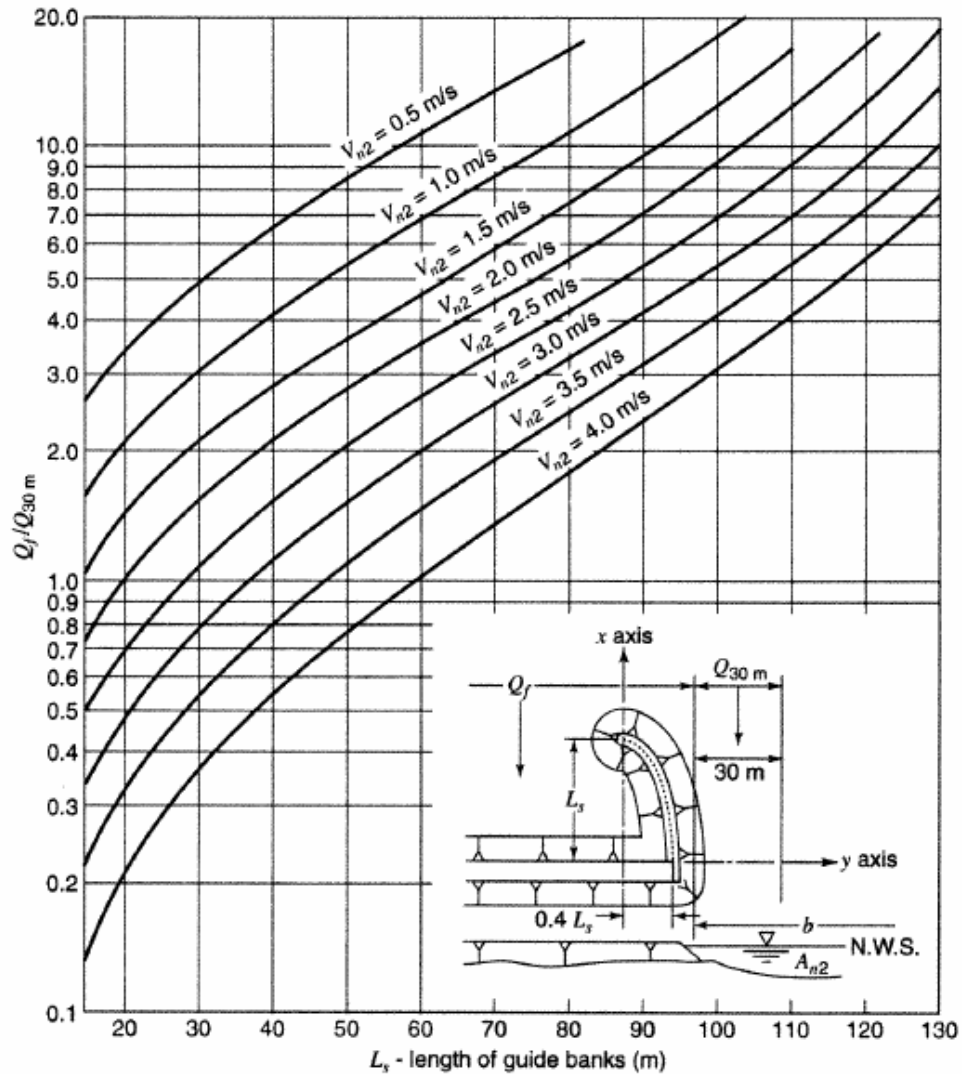


Figure 18.9.6 Nomograph to determine guide bank length (after Bradley, 1978) (as presented in Lagasse et al., 2001a).

To use Figure 18.9.6, the following parameters are needed:

Q_f = the lateral or floodplain discharge of either floodplain intercepted by the embankment, m^3/s

Q_{30m} = the discharge in 30 m of stream adjacent to the abutment, m^3/s

Q = the total discharge of the stream, m^3/s

A_{n2} = the cross-sectional flow area at the bridge opening at normal stage, m^2

$V_{n2} = Q/A_{n2}$ = the average velocity through the bridge opening, m/s

Q_f/Q_{30m} = the guide bank discharge ratio

18.9.6 Check Dams (Channel Drop Structures)

Check dams or channel drop structures are downstream of highway crossings to arrest head cutting and to maintain stable streambed elevation in the vicinity of the bridge. They are typically constructed of rock riprap, concrete, sheet piles, gabions, or treated timber piles. Figure 18.9.8 shows a typical vertical drop structure with a free overfall.

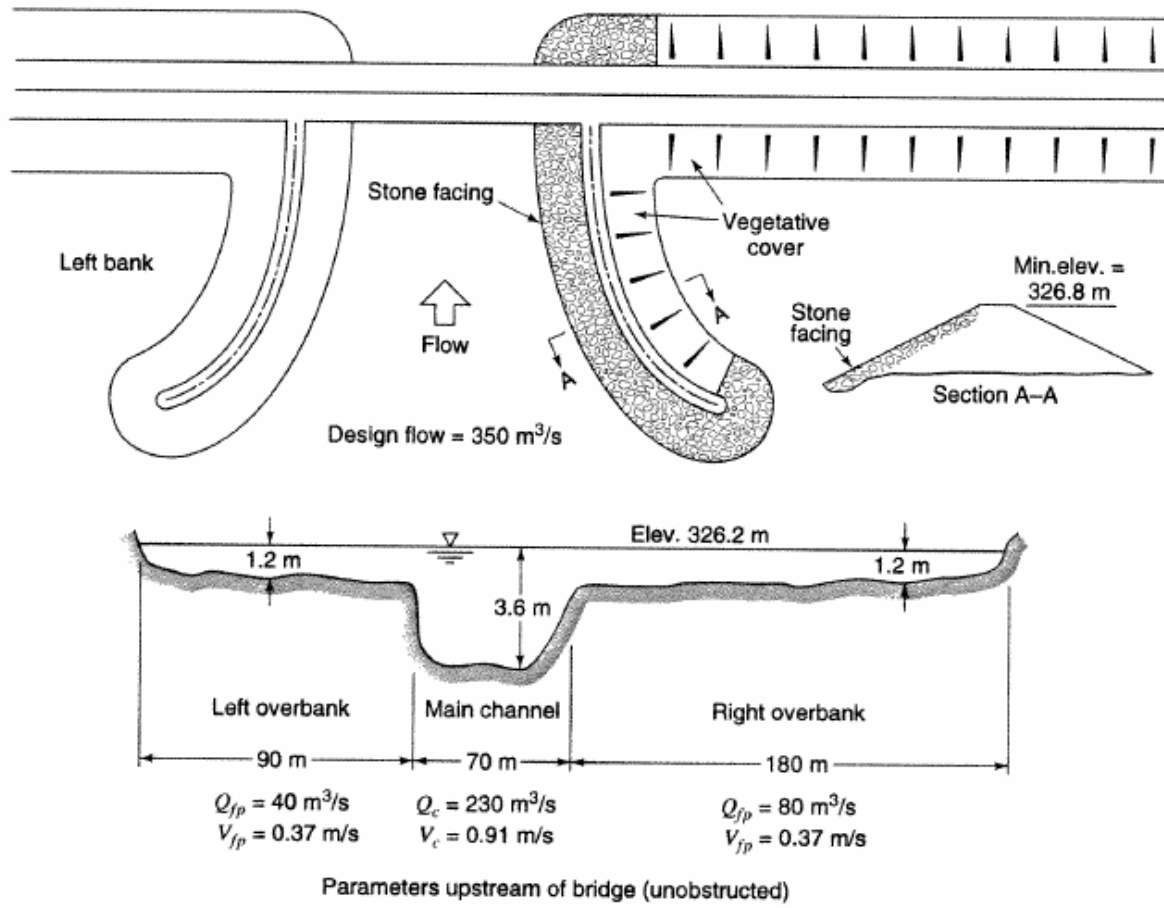


Figure 18.9.7 Example guide bank design (from Lagasse et al., 2001a).

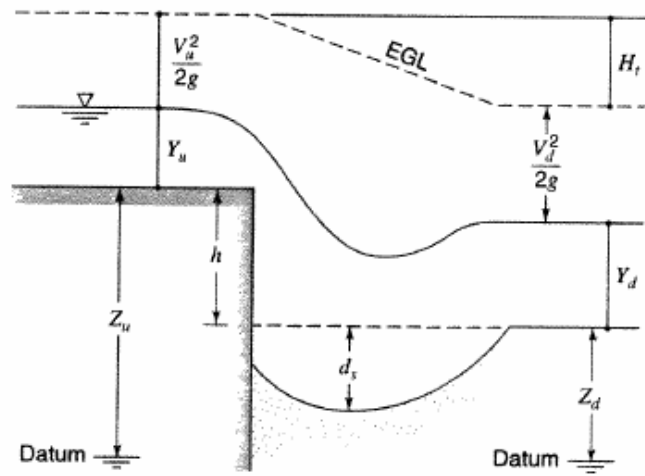


Figure 18.9.8 Schematic of a vertical drop caused by a check dam (from Lagasse et al., 2001a).

Pemberton and Lara (1984) recommended the following equation to estimate the depth of scour downstream of a vertical drop:

$$d_s = KH_t^{0.225} q^{0.54} - d_m \quad (18.9.3)$$

where d_s is the local scour depth for a free overfall, measured from the streambed downstream of the drop in m; q is the discharge per unit width in $\text{m}^3/\text{s}/\text{m}$; H_t is the total drop in head, measured from the upstream to the downstream energy grade line in m; d_m is the tail water depth in m; and $K = 1.90$. Equation (18.9.3) is independent of grain size of the bed material and acknowledges that the bed will scour regardless of the type of material.

Based upon the energy equation,

$$H_t = \left(Y_u + \frac{V_u^2}{2g} + Z_u \right) - \left(Y_d + \frac{V_d^2}{2g} + Z_d \right) \quad (18.9.4)$$

where Y is the depth in m; V is the velocity in m/s; Z is the bed elevation in m; and g is the acceleration due to gravity (9.81 m/s^2). Subscript u and d refer to upstream and downstream of the channel drop, as shown in Figure 18.9.8.

EXAMPLE 18.9.1

Determine the depth of scour for the following hydraulic parameters. Design discharge = $167 \text{ m}^3/\text{s}$; channel width = 32 m ; $Y_u = 3.22 \text{ m}$; $d_m = 2.9 \text{ m}$; $Y_d = 2.9 \text{ m}$; unit discharge (q) = $5.22 \text{ m}^3/\text{s}/\text{m}$; $V_u = 1.62 \text{ m/s}$; $V_d = 1.80 \text{ m/s}$; drop height (h) = 1.4 m .

SOLUTION

Compute H_t using equation (18.9.2):

$$\begin{aligned} H_t &= \left(3.22 + \frac{1.62^2}{2(9.81)} + 1.4 \right) - \left(2.9 + \frac{1.80^2}{2(9.81)} + 0 \right) \\ &= 1.69 \text{ m} \end{aligned}$$

Compute d_s using equation (18.9.3):

$$\begin{aligned} d_s &= 1.90(1.69)^{0.225}(5.22)^{0.54} - 2.9 \\ &= 2.3 \text{ m} \end{aligned}$$

The unsupported height of the structure is $h + d_s = 3.7 \text{ m}$.

18.10 BRIDGE SCOUR

This section presents methods and equations for determining total scour at a bridge (i.e., long-term aggradation or degradation, contraction scour, and local scour). *Bridge scour* is the erosion or removal of streambed or bank material from bridge foundations caused by flowing water, usually considered as long-term bed degradation caused by contraction scour and local scour. Much of the material in this section has been adapted from the FHWA, Hydraulic Engineering Circular No. 18 by Richardson and Davis (2001).

18.10.1 Design Approach

Before applying the various methods for estimating scour, it is necessary to

1. determine the fixed-bed channel hydraulics,
2. determine the long-term impact of degradation or aggradation on the bed profile,
3. if degradation occurs, adjust the fixed-bed hydraulics to reflect this change, and
4. compute the bridge hydraulics (Richardson and Davis, 2001).

The seven steps recommended in "Evaluating Scour at Bridges," FHWA Hydraulic Engineering Circular No. 18 (Richardson and Davis, 2001) are:

1. Determine the scour analysis variables.
2. Analyze long-term bed elevation change.

3. Evaluate the scour analysis method.
4. Compute the magnitude of contraction scour.
5. Compute the magnitude of local scour of pier.
6. Compute magnitude of local scour at abutments.
7. Plot and evaluate the total scour depths.

Many of the hydraulic variables used in estimating scour can be obtained from computer models for water profile computation such as WSPRO developed by the U.S. Department of Transportation (1990).

The following definitions are from the FHWA Hydraulic Engineering Circular No. 18 by Richardson and Davis (2001).

Aggradation and degradation are long-term streambed elevation changes due to natural or man-induced causes. These changes can affect the reach of the river on which the bridge is located. Aggradation involves the deposition of material eroded from the channel or watershed upstream of the bridge, whereas degradation involves the lowering or scouring of the streambed because of a deficit in sediment supply from upstream.

Contraction scour in a natural channel or at a bridge crossing involves the removal of material from the bed and banks across all or most of the channel width. This component of scour can result from a contraction of the flow area, an increase in discharge at the bridge, or both. It can also result from a change in downstream control of the water surface elevation. The scour is the result of increased velocities and shear stress on the channel bed. Contraction of the flow by bridge approach embankments encroaching onto the floodplain and/or into the main channel is the most common cause of contraction scour. Contraction scour can be either clear-water or live-bed.

Live-bed contraction scour occurs when there is transport of bed material in the approach reach, whereas *clear-water contraction scour* occurs when there is no bed material transport in the approach reach or the bed material being transported in the upstream reach is so fine that it washes through the contracted section. Live-bed contraction scour typically occurs during the rising stage of a runoff event, whereas refilling of the scour hole occurs during the falling stage. Also, clear-water scour at low or moderate flows can change to live-bed scour at high flows. This cyclic nature creates difficulties in measuring contraction scour after a flood event.

Local scour involves removal of material from around piers, abutments, spurs, and embankments. It is caused by an acceleration of flow and resulting vortices induced by the flow obstructions. Local scour can also be either clear-water or live-bed scour. Live-bed local scour is cyclic in nature; that is, the scour hole that develops during the rising stage refills during the falling stage.

Lateral stream migration of the main channel of a stream within a floodplain may increase pier scour, erode abutments or the approach roadway, or change the total scour by changing the flow angle of attack at piers. Factors that affect lateral stream movement also affect the stability of a bridge. These factors are the geomorphology of the stream, location of the crossing on the stream, flood characteristics, and the characteristics of the bed and bank materials.

18.10.2 Contraction Scour

18.10.2.1 Live-Bed Contraction Scour

Live-bed contraction scour occurs at a bridge when there is transport of bed material in the upstream reach into the bridge cross-section. With live-bed contraction scour, the area of the contracted section increases until, in the limit, the transport of sediment out of the contracted section equals the sediment transported in (Richardson and Davis, 2001). Normally, the width of the contracted section is constrained, and depth increases until the limiting conditions are reached. Laursen (1960) derived the following live-bed contraction scour equation based on a simplified transport function, transport of sediment in a long contraction, and other simplifying assumptions:

$$\frac{y_2}{y_1} = \left(\frac{Q_2}{Q_1} \right)^{6/7} \left(\frac{W_1}{W_2} \right)^{k_1} \left(\frac{n_2}{n_1} \right)^{k_2} \quad (18.10.1)$$

The average scour depth in m is $y_s = y_2 - y_0$
where

y_1 = average depth in the upstream main channel, m

y_2 = average depth in the contracted section, m

y_0 = existing depth in the contracted section before scour, m

Q_1 = flow in the upstream channel transporting sediment, m³/s

Q_2 = flow in the contracted channel, m³/s, which is often equal to the total discharge unless the total flood flow is reduced by relief bridges, water overtopping the approach roadway, or in the setback area

W_1 = bottom width of the upstream main channel, m

W_2 = bottom width of the main channel in the contracted section, m

n_2 = Manning's n for the contracted section

n_1 = Manning's n for the upstream main channel

k_1 & k_2 = exponents depending on the mode of bed-material transport (see Table 18.10.1a)

$u_* = (gyS_1)^{1/2}$ shear velocity in the upstream section, m/s

ω = median fall velocity of the bed material based on the D_{50} , m/s (see Figure 18.10.1)

g = acceleration of gravity (9.81 m/s²)

S_1 = slope of the energy grade line of the main channel, m/m

D_{50} = median diameter of the bed material, m

Table 18.10.1 Exponents for Live-Bed Contraction Scour Equation

(a) For Long Section			
$\frac{u_*}{w}$	k_1	k_2	Mode of bed material transport
<0.50	0.59	0.066	Mostly contact bed material discharge
0.50–2.0	0.64	0.21	Some suspended bed material discharge
>2.0	0.69	0.37	Mostly suspended bed material discharge
(b) For Contracted Section			
$\frac{u_*}{w}$	k_1		Mode of bed material transport
<0.50	0.59		Mostly contact bed material discharge
0.50–2.0	0.64		Some suspended bed material discharge
>2.0	0.69		Mostly suspended bed material discharge

Source: From Laursen (1960).

The location of the upstream section for y_1 , Q_1 , W_1 , and n_1 needs to be located with engineering judgment. If WSPRO is used to obtain the values of the quantities, the upstream channel section is located a distance equal to one bridge opening from the upstream face of the bridge.

A modified version of Laursen's (1960) equation for live-bed scour at a long contraction is recommended to predict the depth of scour in a *contracted section*. The original equation (18.10.1) is modified by eliminating the ratio of Manning's n . The equation assumes that bed material is being transported in the upstream section, and is given as:

$$\frac{y_2}{y_1} = \left(\frac{Q_2}{Q_1} \right)^{6/7} \left(\frac{W_1}{W_2} \right)^{k_1} \quad (18.10.2)$$

and the average scour depth in m is $y_s = y_2 - y_0$ and k_1 is obtained from Table 18.10.1b.

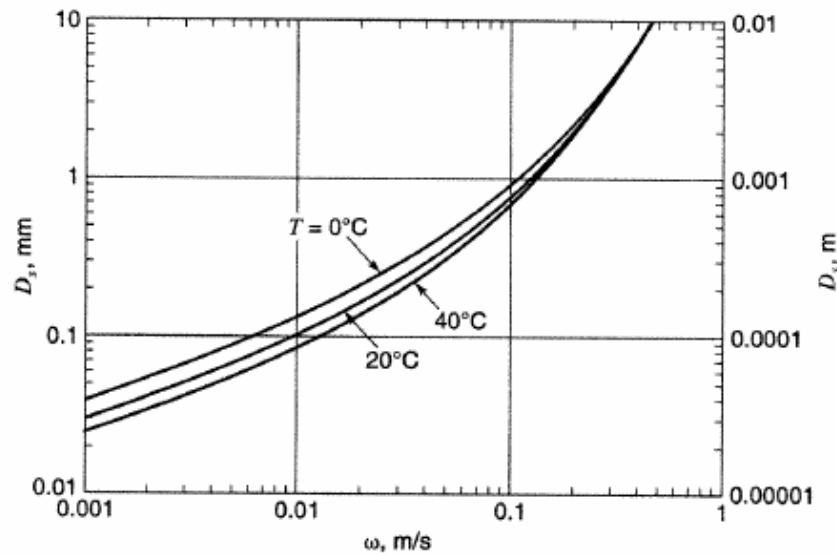


Figure 18.10.1 Fall velocity of sand-sized particles (from Richardson et al., 2001).

The Manning's n ratio in equation (18.10.1) can be significant for the condition of a dune bed in the main channel and a corresponding plane bed, washed out dunes, or antidunes in the contracted channel (Richardson and Davis, 2001). However, equation (18.10.1) does not adequately account for the increase in transport which occurs as the result of the bed planing out (which decreases resistance to flow and increases the velocity and the transport of bed material at the bridge). Laursen's equation (18.10.1) results in a decrease in scour for this case, whereas in reality, there would be an increase in scour depth. In addition, at flood flows, a plain bedform will usually exist upstream and through the bridge waterway, and the values of Manning's n will be equal. Consequently, the n value ratio is not recommended by Richardson and Davis (2001) or presented in the recommended equation (18.10.2).

Scour depths with live-bed contraction scour may be limited by coarse sediments in the bed material armoring the bed. Where coarse sediments are present, Richardson and Davis (2001) recommend that scour depths be calculated for live-bed scour conditions using the clear-water scour equation (given in Section 18.10.2.2) in addition to the live-bed equation, and that the smaller calculated scour depth be used.

18.10.2.2 Clear-Water Contraction Scour

Clear-water contraction scour occurs in a long contraction when (1) there is no bed material transport from the upstream reach into the downstream reach or (2) the material being transported in the upstream reach is transported through the downstream reach mostly in suspension and at less than capacity of the flow. The area of the contracted section increases until, in the limit, the velocity of the flow (V) or the shear stress (τ_0) on the bed is equal to the critical velocity (V_c) or the critical shear stress (τ_c) of a certain particle size (D) in the bed material. Normally, the width (W) of the contracted section is constrained and the depth (y) increases until the limiting conditions are reached. Following the development given by Laursen (1960), equations for determining the clear-water contraction scour in a *long contraction* were developed in metric units. For equilibrium in the contracted reach, $\tau_0 = \tau_c$ where τ_0 is the average bed shear stress, contracted section, Pa (N/m^2), and τ_c is the critical bed shear stress at incipient motion, Pa (N/m^2):

The average bed shear stress based on the hydraulic radius ($R = y$) and Manning's equation to determine the slope (S_f) is expressed as:

$$\tau_0 = \gamma y S_f = \frac{\rho g n^2 V^2}{y^{1/3}} \quad (18.10.3)$$

For noncohesive bed materials and fully developed clear-water contraction scour, the critical shear stress can be determined using Shields relation (Laursen, 1960):

$$\tau_c = K_s (\rho_s - \rho) g D \quad (18.10.4)$$

The bed in a long contraction scours until $\tau_0 = \tau_c$ so that using equation (18.10.3) and (18.10.4):

$$\frac{\rho g n^2 V^2}{y^{1/3}} = K_s (\rho_s - \rho) g D \quad (18.10.5)$$

Solving for the depth (y) in the contracted section gives:

$$y = \left[\frac{n^2 V^2}{K_s (S_s - 1) D} \right]^3 \quad (18.10.6)$$

and in terms of discharge (Q), the depth is:

$$y = \left[\frac{n^2 Q^2}{K_s (S_s - 1) D W^2} \right]^{3/7} \quad (18.10.7)$$

where

y = average depth in the contracted section after contraction scour, m

S_f = slope of the energy grade line, m/m

V = average velocity in the contracted section, m/s

D = diameter of the smallest nontransportable particle in the bed material, m

Q = discharge, m³/s

W = bottom width of the contracted section, m

g = acceleration of gravity (9.81 m/s²)

n = Manning's roughness coefficient

K_s = Shields coefficient

S_s = specific gravity (2.65 for quartz)

γ = unit weight of water (9800 N/m³)

ρ = density of water (100 kg/m³)

ρ_s = density of sediment (quartz, 2647 kg/m³)

Equations (18.10.6) and (18.10.7) are the basic equations for the clear-water scour depth (y) in a long contraction. Laursen used a value of 4 (in English units) for $K_s(\rho_s - \rho)g$; D_{50} for the size (D) of the smallest nonmoving particle in the bed material and Strickler's approximation for Manning's n ($n = 0.034 D_{50}^{1/6}$). Laursen's assumption that $\tau_c = 4D_{50}$ with $S_s = 2.65$ is equivalent to assuming a Shields parameter $K_s = 0.039$. Shields coefficient (K_s) to initiate motion ranges from 0.01 to 0.25 is a function of particle size, Froude number, and size distribution. Some typical values for K_s for $Fr < 0.8$ and as a function of bed material size are $K_s = 0.047$ for sand (D_{50} from 0.065 to 2.0 mm); $K_s = 0.03$ for median coarse bed material (2 mm $< D_{50} < 40$ mm) and $K_s = 0.02$ for coarse-bed material ($D_{50} > 40$ mm).

In metric units, Strickler's equation for n as given by Laursen is $0.041 D_{50}^{1/6}$, where D_{50} is in meters. Richardson et al. (1990) recommend the use of the effective mean bed material size (D_m) in place of the D_{50} size for the beginning of motion ($D_{50} = 1.25D_m$). Changing D_{50} to D_m in the

Strickler's equation gives $n = 0.040 D_m^{1/6}$. Substituting $K_s = 0.039$ into equations (18.10.6) and (18.10.7) gives the following equation for y :

$$y = \left[\frac{V^2}{40D_m^{2/3}} \right]^3 \quad (18.10.8)$$

$$y = \left[\frac{V^2}{40D_m^{2/3}W^2} \right]^{3/7} \quad (18.10.9)$$

$$y_s = y - y_0 = (\text{average scour depth, m}) \quad (18.10.10)$$

where

Q = discharge through contraction, m^3/s

D_m = diameter of the bed material ($1.25 D_{50}$) in the contracted section, m

W = bottom width in contraction, m

y_0 = existing depth in the contracted section before scour, m

The clear-water contraction scour equations assume homogeneous bed materials. For clear-water scour in stratified materials, using the layer with the finest D_{50} would result in the most conservative estimate of contraction scour. Alternatively, the clear-water contraction scour equations could be used sequentially for stratified bed materials.

Equations (18.10.8) and (18.10.9) do not give the distribution of the contraction scour in the cross-section. In many cases, assuming a uniform contraction scour depth across the opening would not be in error (e.g., short bridges, relief bridges, and bridges with simple cross-sections and on straight reaches). However, for wide bridges, bridges on bends, bridges with large overbank flow, or crossings with a large variation in bed-material size distribution, the contraction scour depths will not be uniformly distributed across the bridge opening. In these cases, equations (18.10.6) and (18.10.8) can be used if the distribution of the velocity and/or the bed material is known. The computer program WSPRO uses stream tubes to give the discharge and velocity distribution in the cross-section. Using this distribution, equations (18.10.6) and (18.10.8) can be used to estimate the distribution of the contraction scour depths. Equations (18.10.7) and (18.10.9) are used to determine the average contraction scour depth in the section.

The velocity and depth given in equation (18.10.6) are associated with initiation of motion of the indicated particle size (D). Rearranging equation (18.10.6) to give the critical velocity (V_c) for beginning of motion of bed material of size D results in:

$$V_c = \frac{K_s^{1/2}(S_s - 1)^{1/2} D^{1/2} y^{1/6}}{n} \quad (18.10.11)$$

Using $K_s = 0.039$, $S_s = 2.65$, and $n = 0.041 D^{1/6}$, equation (18.10.11) reduces to

$$V_c = 6.19^{1/6} D^{1/3} \quad (18.10.12)$$

where

V_c = critical velocity above which bed material of size D and smaller will be transported, m/s

K_s = Shields parameter

S_s = specific gravity of bed material

D = size of bed material, m

y = depth of flow, m

n = Manning's roughness coefficient

EXAMPLE 18.10.1 This example problem and the succeeding examples in Section 18.10 are based on the examples taken from Arneson et al. (1991) and also used by Richardson and Davis (2001) in FHWA Hydraulic Engineering Circular No. 18. FHWA's computer code WSPRO was used to obtain the hydraulic variables listed in Tables 18.10.2 through 18.10.6.

A 198.12-m long bridge (see Figure 18.10.2) is to be constructed over a channel with spill-through abutments (slope of 1V:2H). The left abutment is set approximately 60.5 m back from the channel bank. The right abutment is set at the channel bank. The bridge deck is set at elevation 6.71 m and has a girder depth of 1.22 m. Six round-nose piers are evenly spaced in the bridge opening. The piers are 1.52 m thick, 12.19 m long, and are aligned with the flow. The 100-year design discharge is 849.51 m³/s. The 500-year flow of 1444.16 m³/s was estimated by multiplying the Q_{100} by 1.7 since no hydrologic records were available to predict the 500-year flow.

Determine whether the flow condition in the main channel is a live-bed or a clear-water condition (see Figure 18.10.3a,b,c).

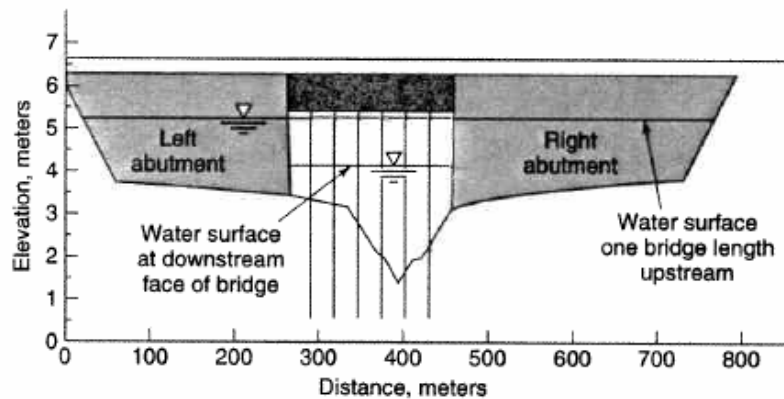


Figure 18.10.2 Cross-section of proposed bridge (from Richardson et al., 2001).

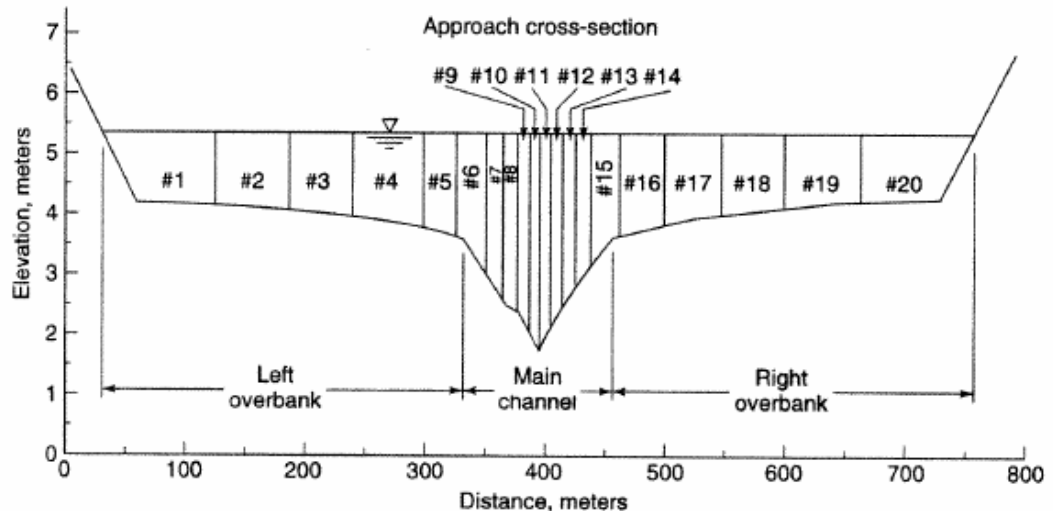


Figure 18.10.3a Equal conveyance tubes of approach section (from Richardson et al., 2001).

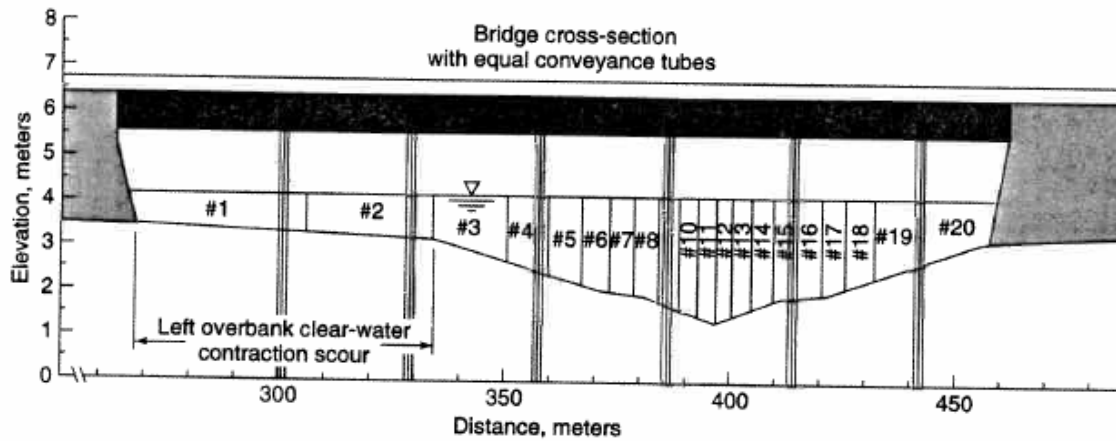


Figure 18.10.3b Equal conveyance tubes of bridge section (from Richardson et al., 2001).

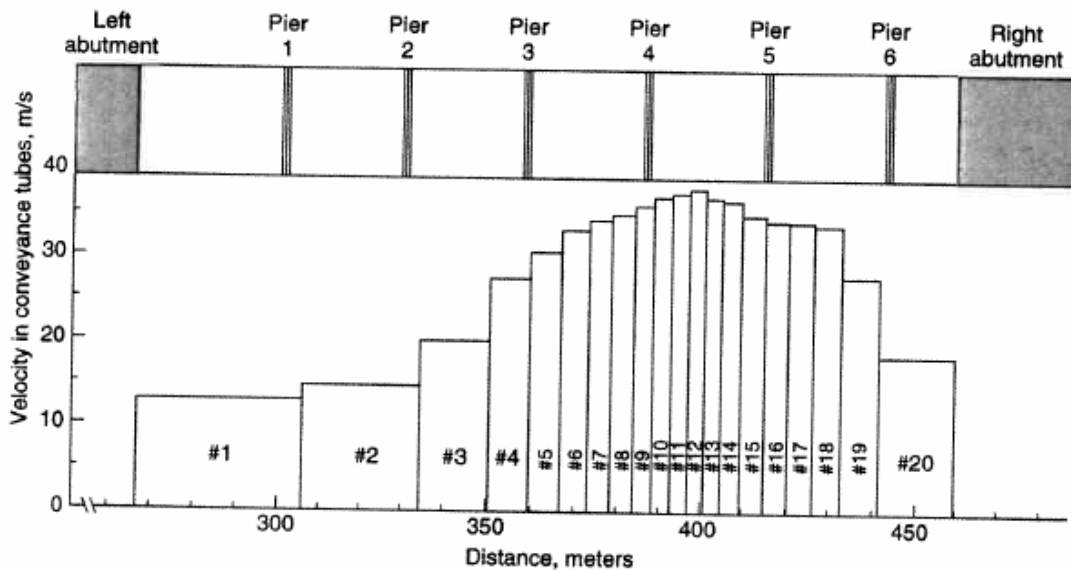


Figure 18.10.3c Velocity distribution at bridge crossing (from Richardson et al., 2001).

SOLUTION

First determine whether the flow condition in the main channel is live-bed or clear-water by comparing the critical velocity for sediment movement and the average channel velocity at the approach section. The discharge in the main channel at the approach section, Q_1 , is computed as:

$$Q_1 = Q \left(\frac{K_1}{K_{\text{total}}} \right) = 849.51 \left(\frac{\text{m}^3}{\text{s}} \right) \left[\frac{19,000}{39,150} \right] = 412.28 \text{ m}^3/\text{s}$$

where K_1 and K_{total} are the conveyance of the main channel of approach and the total conveyance of the approach section, respectively, from Table 18.10.2. The average velocity in the main channel of the approach section is:

$$V_1 = Q_1/A_c = 412.28/320 = 1.29 \text{ m/s}$$

Table 18.10.2 Hydraulic Variables from WSPRO for Estimation of Live-Bed Contraction Scour

		Remarks
Q (m ³ /s)	849.51	Total discharge
K_1 (approach)	19,000	Conveyance of main channel of approach
K_{total} (approach)	39,150	Total conveyance of approach section
W_1 or TOPW (approach) (m)	121.9	Top width of flow (TOPW). Assumed to represent active live bed width of approach
A_c (approach) (m ²)	320	Area of main channel approach section
WETP (approach) (m)	122.0	Wetted perimeter of main channel approach section
K_c (bridge)	11,330	Conveyance through bridge
K_{total} (bridge)	12,540	Total conveyance through bridge
A_c (bridge) (m ²)	236	Area of the main channel, bridge section
W_c (bridge) (m)	122	Channel width at the bridge. Difference between subarea break-points defining banks at bridge
W_2 (bridge) (m)	115.9	Channel width at the bridge, less four channel pier widths (6.08 m)
S_f (m/m)	0.002	Average unconfined energy slope (SF)

Source: From Richardson et al. (2001).

Table 18.10.3 Hydraulic Variables from WSPRO for Estimation of Clear-Water Contraction Scour on Left Overbank

		Remarks
Q (m ³ /s)	849.51	Total discharge (see Table 18.10.2).
Q_{chan} (bridge)	767.54	Flow in main channel at bridge. Determined in live-bed computation of Step 5A.
Q_2 (bridge)	81.97	Flow in left overbank through bridge. Determined by subtracting Q_{chan} (listed above) from total discharge through bridge.
D_m (bridge overbank) (m)	0.0025	Grain size of left overbank area. $D_m = 1.25 D_{50}$.
W_{setback} (bridge) (m)	68.8	Top width of left overbank area. (SA #1) at bridge
$W_{\text{contracted}}$ (bridge) (m)	65.8	Setback width less two pier widths (3.04 m).
A_{left} (bridge) (m ²)	57	Area of left overbank at the bridge.

Source: From Richardson et al. (2001).

Table 18.10.4 Hydraulic Variables from WSPRO for Estimation of Pier Scour (Conveyance Tube Number 12)

		Remarks
V_1 (m)	3.73	Velocity in conveyance tube #12
V_1 (m)	2.84	Mean depth of tube #12

Table 18.10.5 Hydraulic Variables from WSPRO for Estimation of Abutment Scour Using Froehlich's Equation for Left Abutment

		Remarks
Q (m ³ /s)	849.51	Total discharge (see Table 18.10.2).
q_{tube} (m ³ /s)	42.48	Discharge per equal conveyance tube, defined as total discharge divided by 20.
# Tubes	3.5	Number of approach section conveyance tubes that are obstructed by left abutment. Determined by superimposing abutment geometry onto the approach section.
Q_e (m ³ /s)	148.68	Flow in left overbank obstructed by left abutment. Determined by multiplying # tubes and q_{tube} .
A_e (left abut) (m ²)	264.65 (m ²)	Area of approach section conveyance tubes number 1, 2, 3, and half of tube number 4.
L' (m)	232.80	Length of abutment projected into flow, determined by adding top widths of approach section conveyance tubes number 1, 2, and 3, and half of tube number 4.

Source: From Richardson et al. (2001)

Table 18.10.6 Hydraulic Variables from WSPRO for Estimation of Abutment Scour Using HIRE Equation for Left Abutment

		Remarks
V_{tube} (m/s) (bridge section)	1.29	Mean velocity of conveyance tube #1, adjacent to left abutment
y_1 (m) (bridge section)	0.83	Average depth of conveyance tube #1

Source: Richardson et al. (2001).

where A_c is the area of the main channel approach section from Table 18.10.2. The average depth of flow y_1 in the approach section is:

$$y_1 = A_1/W_1 = 320/121.9 = 2.63 \text{ m}$$

where W_1 is the top width of flow.

The critical velocity for D_{50} size sediment is computed using equation (18.10.12):

$$\begin{aligned} V_c &= 6.19y_1^{1/6}D_{50}^{1/3} \\ &= 6.19(2.63 \text{ m})^{1/6}(0.002 \text{ m})^{1/3} \\ &= 0.92 \text{ m/s} \end{aligned}$$

Comparing V_1 and V_c , $V_1 > V_c$ indicating that the flow condition is live-bed.

EXAMPLE 18.10.2

Compute the live-bed contraction scour for the main channel for the Example 18.10.1 problem.

SOLUTION

Equation 18.10.2 is used to compute y_2/y_1 , and the scour depth is computed using $y_s = y_2 - y_0$, so:

$$\begin{aligned} y_s &= \left(\frac{y_2}{y_1}\right)y_1 - y_0 \\ &= \left(\frac{Q_2}{Q_1}\right)^{6/7} \left(\frac{W_1}{W_2}\right)^{k_1} y_1 - y_0 \quad (\text{a}) \end{aligned}$$

The first step is to compute all the parameters in this equation to evaluate y_s . Q_1 was evaluated as 412.28 m³/s in Example 18.10.1 and Q_2 , the discharge in the main channel at the bridge, is:

$$Q_2 = Q \left(\frac{K_2}{K_{\text{total}}} \right) = 849.51 \left(\frac{\text{m}^3}{\text{s}} \right) \left[\frac{11,330}{12,540} \right] = 767.54 \text{ m}^3/\text{s}$$

The channel widths are $W_1 = 121.9$ m and $W_2 = 115.9$ m in Table 18.10.2, $y_1 = 2.63$ m was computed in Example 18.10.1. The bridge channel flow depth is the area divided by the top width $y_0 = 236 \text{ m}^2/122 \text{ m} = 1.93$ m.

The only remaining unknown is K_1 , which can be obtained from Table 18.10.1b for u_* / ω . To compute u_* / ω , first compute the shear velocity u_* using $u_* = \sqrt{\tau_0 / \rho}$, where $\tau_0 = \gamma R S = 9810 \text{ (N/m}^3)(2.63 \text{ m})(0.002 \text{ m/m}) = 51.4 \text{ N/m}^2 = 51.4 \text{ Pa}$. The shear velocity is then $u_* = \sqrt{51.4/1000} = 0.227 \text{ m/s}$. The bed material is sand with $D_{50} = 0.002$ m (2mm). Fall velocity $\omega = 0.21$ m/s from Figure 18.10.1. Then $u_* / \omega = 0.227/0.21 = 1.08$. From Table 18.10.1b, $k_1 = 0.64$, which indicates that the mode of bed transport is a mixture of suspended and contact bed-material discharge.

The live-bed contraction scour of the channel is computed using (a) from above:

$$\begin{aligned} y_s &= (767.54/412.28)^{6/7} (121.9/115.9)^{0.64} (2.63) - 1.93 \\ &= 2.7 \text{ m} \end{aligned}$$

This scour is large and could be minimized through a larger bridge opening by building relief bridges in the overbank, or possibly in some cases providing for highway approach overtopping (Richardson and Davis, 2001).

EXAMPLE 18.10.3

Clear-water contraction scour will occur in the overbank area between the left abutment and the left bank of the bridge opening of Example 18.10.1. Compute the clear-water contraction scour in the left bank based on the discharge and depth of flow passing under the bridge and use the hydraulic variables from the example in Table 18.10.3.

SOLUTION

Using equation (18.10.9):

$$\begin{aligned} y &= \left[\frac{Q^2}{40 D_m^{2/3} W_{\text{contracted}}^2} \right]^{3/7} \\ &= \left[\frac{0.025 (81.97 \text{ m}^3/\text{s})^2}{(0.0025 \text{ m})^{2/3} (65.8 \text{ m})^2} \right]^{3/7} \\ &= 1.38 \text{ m} \end{aligned}$$

Average flow depth (y_0) in the left overbank bridge section is $y_0 = A_{\text{left}} / W_{\text{setback}} = (57.0 \text{ m}^2) / (68.8 \text{ m}) = 0.83$ m. The clear-water contraction scour in the left overbank of the bridge opening is $y_s = y_2 - y_0 = 1.38 \text{ m} - 0.83 \text{ m} = 0.55$ m.

18.10.3 Local Scour at Piers

The basic mechanism causing local scour at piers or abutments is the formation of horseshoe vortices at their base (see Figure 18.10.4). The *horseshoe vortex* results from the increased head water on the upstream surface of the obstruction and subsequent acceleration of the flow around the nose of the pier or abutment. The action of the vortex removes bed material from around the base of the obstruction, where the transport rate of sediment away from the base region is greater than the

transport rate into the region; consequently, a scour hole develops. With an increase in depth of scour, the strength of the horseshoe vortex is reduced, thereby reducing the transport rate from the base region. Eventually, for live-bed local scour, equilibrium is reestablished between bed material inflow and outflow, and scouring ceases. For clear-water scour, scouring ceases when the shear stress caused by the horseshoe vortex equals the critical shear stress of the sediment particle at the bottom of the scour hole (Richardson and Davis, 2001).

In addition to the horseshoe vortex around the base of a pier, there are also vertical vortices called *wake vortices* downstream of the pier (see Figure 18.10.4). Wake vortices also remove material from the pier base region. However, the intensity of wake vortices diminishes rapidly as the distance downstream of the pier increases, so that immediately downstream of a long pier there is often deposition of material.

Factors that affect the magnitude of local scour depth at piers and abutments are (1) velocity of the approach flow, (2) depth of flow, (3) width of the pier, (4) discharge intercepted by the abutment and returned to the main channel at the abutment, (5) length of the pier if skewed to flow, (6) size and gradation of bed material, (7) angle of attack of the approach flow to a pier or abutment, (8) shape of a pier or abutment, (9) bed configuration, and (10) ice formation or jams and debris (Richardson and Davis, 2001).

There have been many scour equations reported in the literature for live-bed scour in cohesionless sand-bed streams. The only equation presented here is recommended for both live-bed and clear-water pier scour, given by Richardson et al. (1990):

$$\frac{y_s}{y_1} = 2.0K_1K_2K_3K_4 \left[\frac{a}{y_1} \right]^{0.65} F_{r1}^{0.43} \quad (18.10.13)$$

In terms of y_1/a , where a is the pier width, equation (18.10.13) is:

$$\frac{y_s}{a} = 2.0K_1K_2K_3K_4 \left[\frac{y_1}{a} \right]^{0.35} F_{r1}^{0.43} \quad (18.10.14)$$

where

y_s = scour depth, m

y_1 = flow depth directly upstream of the pier, m

K_1 = correction factor for pier nose shape (see Figure 18.10.5 and Table 18.10.7)

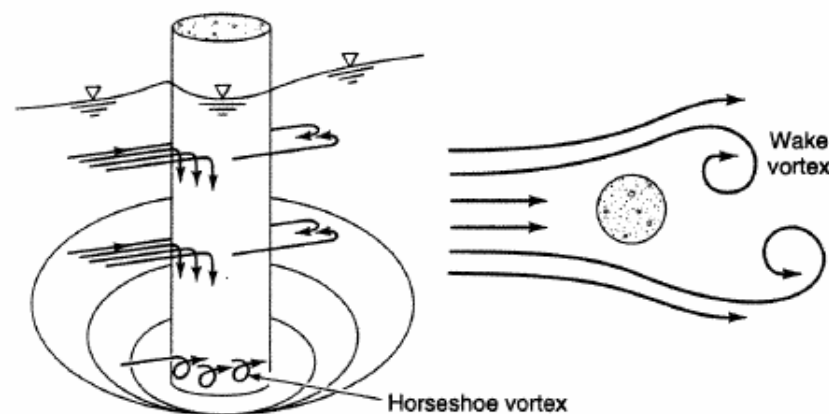


Figure 18.10.4 Schematic representation of scour at a cylindrical pier (from Richardson et al., 2001).

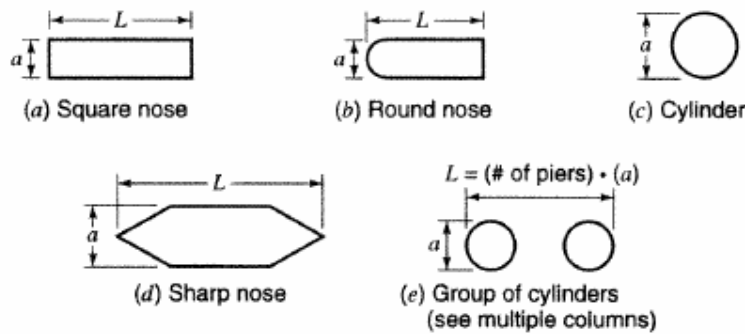


Figure 18.10.5 Common pier shapes (from Richardson, et al., 2001).

Table 18.10.7 Correction Factor, K_1 , for Pier Nose Shape*

Shape of pier nose	K_1
(a) Square nose	1.1
(b) Round nose	1.0
(c) Circular cylinder	1.0
(d) Group of cylinders	1.0
(e) Sharp nose	0.9

*The correction factor K_1 for pier nose should be determined using Table 18.10.7 for angles of attack up to 5° . For greater angles, K_2 dominates and K_1 should be considered as 1.0. If L/a is larger than 12, use the values for $L/a = 12$ as a maximum in Table 18.10.8.

Source: Richardson et al. (2001).

K_2 = correction factor for angle of attack of flow from Table 18.10.8

Table 18.10.8 Correction Factor, K_2 , for Angle of Attack, θ of the Flow*

Angle	$L/a = 4$	$L/a = 8$	$L/a = 12$
0	1.0	1.0	1.0
15	1.5	2.0	2.5
30	2.0	2.75	3.5
45	2.3	3.3	4.3
90	2.5	3.9	5.0

Source: From Richardson and Davis (1995)

*The value of the correction factor K_2 should be applied only when the field conditions are such that the entire length of the pier is subject to the angle of attack of the flow. Use of this factor directly from the table will result in a significant overprediction of scour if (1) a portion of the pier is shielded from the direct impingement of the flow by an abutment or another pier, or (2) an abutment or another pier redirects the flow in a direction parallel to the pier. For such cases, judgment must be exercised to reduce the value of the K_2 factor by selecting the effective length of the pier actually subjected to the angle of attack of the flow (Richardson et al., 2001).

K_3 = correction factor for bed condition from Table 18.10.9

Table 18.10.9 Increase in Equilibrium Pier Scour Depths, K_3 for Bed Condition*

Bed Condition	Dune Height (m)	K_3
Clear-water scour	NA	1.1
Plane bed and antidune flow	NA	1.1
Small dunes	$3 > H \geq 0.6$	1.1

Table 18.10.9 Increase in Equilibrium Pier Scour Depths, K_3 for Bed Condition* (continues)

Bed Condition	Dune Height (m)	K_3
Medium dunes	$9 > H \geq 3$	1.2–1.1
Large dunes	$H \geq 9$	1.3

Source: From Richardson et al. (2001)

Abbreviations: NA, not applicable.

*The correction factor K_3 results from the fact that for plane-bed conditions, which is typical of most bridge sites for the flood frequencies employed in scour design, the maximum scour may be 10 percent greater than computed with Eq. (18.10.13). In the unusual situation where a dune bed configuration with large dunes exists at a site during flood flow, the maximum pier scour may be 30 percent greater than the predicted equation value. This may occur on very large rivers, such as the Mississippi. For smaller streams that have a median dune configuration at flood flow, the dunes will be smaller and the maximum scour may be only 10 to 20 percent larger than equilibrium scour. For antidune bed configuration, the maximum scour depth may be 10 percent greater than the computed equilibrium pier scour depth (Richardson et al., 2001).

K_4 = correction factor for armoring by bed material size from Table 18.10.10

Table 18.10.10 Correction Factor for Armoring by Bed Material Size

Minimum Bed Material Size	Minimum K_4 Value	$V_R > 1.0$
$D_{50} > 0.06$	0.7	1.0

a = pier width, m

L = length of pier, m

F_{r1} = Froude number directly upstream of the pier = $v_1/(gy_1)^{1/2}$

V_1 = mean velocity of flow directly upstream of the pier, m/s

g = acceleration of gravity (9.81 m/s²)

EXAMPLE 18.10.4

For Example 18.10.1, compute the magnitude of the local scour at the pier. Anticipating that any pier under the bridge could be subject to the maximum flow depth and velocities, only one computation of pier scour of the side pier is needed. This assumption is acceptable because the thalweg is prone to shift and there is a possibility of lateral channel migration.

SOLUTION

This solution requires the parameters in equation (18.10.13):

$$\frac{y_s}{y_1} = 2.0K_1K_2K_3K_4 \left[\frac{a}{y_1} \right]^{0.65} F_{r1}^{0.43}$$

The Froude number, F_{r1} , for the pier scour computation is based on the hydraulic characteristics of conveyance tube number 12. The velocity $V_1 = 3.73$ m/s, and $y_1 = 2.84$ m are from Table 18.10.4, so:

$$F_{r1} = \frac{V_1}{(gy_1)^{0.5}} = \frac{3.73 \text{ m/s}}{[(9.81 \text{ m/s}^2)(2.84 \text{ m})]^{0.5}} = 0.71$$

For a round-nose pier aligned with the flow and sand-bed material (see Tables 18.10.7, 18.10.8, and 18.10.10), $K_1 = K_2 = K_4 = 1.0$.

For plane-bed condition (see Table 18.10.9), then $K_3 = 1.1$. Using equation (18.10.14):

$$\frac{y_s}{2.84} = 2.0(1)(1)(1.1)(1) \left[\frac{1.52 \text{ m}}{2.84 \text{ m}} \right]^{0.65} (0.71)^{0.43}$$

$$y_s = 3.6 \text{ m}$$

The maximum local pier scour depth will be 3.6 m.

18.10.4 Live-Bed Scour at Abutments

When abutments obstruct flow, local scour occurs as a result of a horizontal vortex that starts at the upstream end of the abutment and runs along the toe of the abutment, similar to the horizontal vortex that forms at piers. A vertical wake vortex forms at the downstream end of an abutment, similar to that which forms downstream of a pier or downstream of any flow separation. Figure 18.10.6 is a definition sketch for abutment scour. There are three general abutment shapes, as indicated in Figure 18.10.7.

The potential for lateral channel migration, long-term degradation, and contraction scour should be considered in determining abutment foundation depths near the main channel. FHWA HEC-18 recommends that abutment scour equations be used to develop insight as to the scour potential of an abutment. Then, the abutment may be designed to resist the computed scour, or, as an alternative, riprap and guide banks can be used to protect the abutment from scour and erosion (Richardson and Davis, 2001).

Two approaches, Froelich's live-bed scour equation and a U.S. Army Corps of Engineers equation, are discussed in this section. In order to check the potential depth of scour for the design of the foundation and placement of rock riprap or guide banks, Froelich's live-bed scour equation can be used. Froelich (1989) analyzed 170 live-bed scour measurements in laboratory flumes and developed the following regression equation:

$$\frac{y_s}{y_a} = 2.27 K_1 K_2 \left[\frac{L'}{y_a} \right]^{0.43} F_{r1}^{0.61} + 1 \quad (18.10.15)$$

where

K_1 = coefficient for abutment shape (see Table 18.10.11)

Table 18.10.11 Abutment Shape Coefficients

Description	K_1
Vertical-wall abutment	1.0
Vertical-wall abutment with wing walls	0.82
Spill-through abutment	0.55

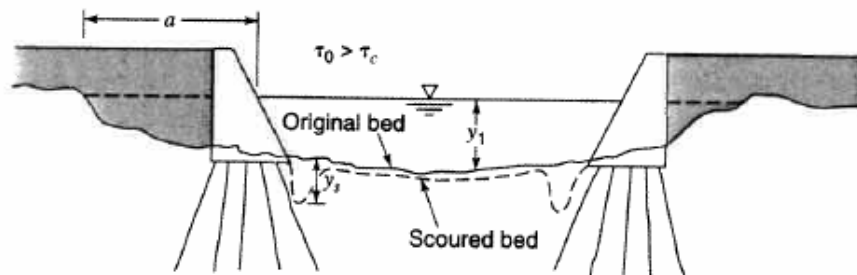


Figure 18.10.6 Definition sketch for abutment scour (from Richardson et al., 1990).

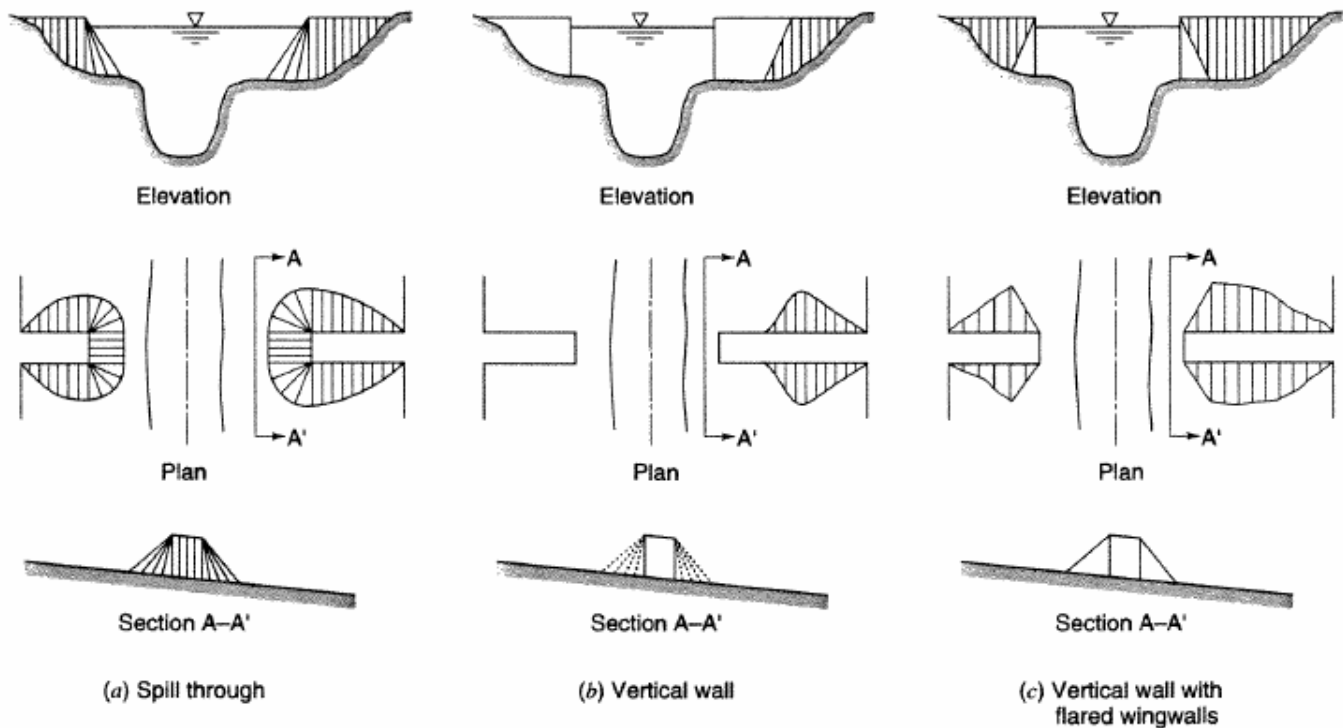


Figure 18.10.7 Abutment shape (from Richardson et al., 2001).

K_2 = coefficient for angle of embankment to flow

$$K_2 = (\theta/90)^{0.13} \text{ (see Figure 18.10.8 for definition of } \theta \text{)}$$

$\theta < 90^\circ$ if embankment points downstream

$\theta > 90^\circ$ if embankment points upstream

L' = length of abutment (embankment) projected normal to flow, m

A_e = flow area of the approach cross-section obstructed by the embankment, m^2

F_r = Froude number of approach flow upstream of the abutment = $V_e / (gy_a)^{1/2}$

$V_e = Q_e / A_e$, m/s

Q_e = flow obstructed by the abutment and approach embankment, m^3/s

y_a = average depth of flow on the floodplain, m

y_s = scour depth, m

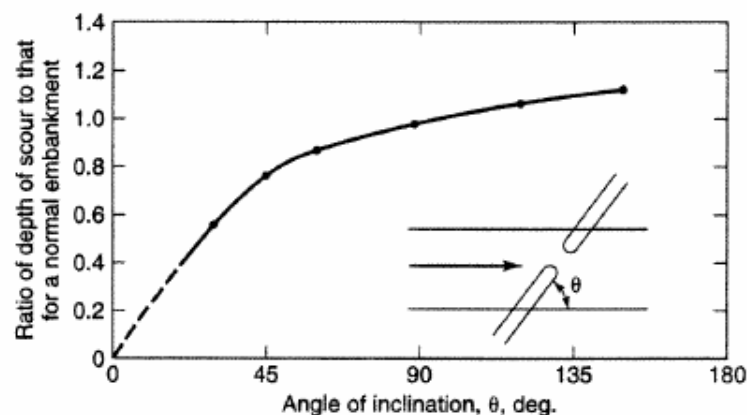


Figure 18.10.8 Adjustment of abutment scour estimate for skew (from Richardson et al., 2001).

It should be noted that equation (18.10.15) is not consistent because as L' tends to 0, y_s also tends to 0. The 1 was added to the equation so as to envelope 98 percent of the data.

Field data of scour at the end of spurs in the Mississippi River (obtained by the U.S. Army Corps of Engineers) can also be used for estimating abutment scour. This field situation closely resembles the laboratory experiments for abutment scour in that the discharge intercepted by the spurs was a function of the spur length. Equation (18.10.16), referred to as the HIRE (Highway in the River Environment) equation (Richardson et al., 1990), is applicable when the ratio of projected abutment length (L') to the flow depth (y_1) is greater than 25. This equation can be used to estimate scour depth (y_s) at an abutment where conditions are similar to the field conditions from which the equation was derived (Richardson and Davis, 2001):

$$\frac{y_s}{y_1} = 4F_{r1}^{0.33} \frac{K_1}{0.55} \quad (18.10.16)$$

where

y_1 = depth of flow at the abutment on the overbank or in the main channel, m

F_r = Froude number based on the velocity and depth adjacent to and upstream of the abutment

K_1 = abutment shape coefficient (from Table 18.10.11)

To correct equation (18.10.16) for abutments skewed to the stream, use Figure 18.10.8.

For clear-water scour at an abutment, use either equation (18.10.15) or (18.10.16) because clear-water scour equations potentially decrease scour at abutments because of the presence of coarser material. This decrease is unsubstantiated by field data (Richardson and Davis, 2001).

Froelich's equation will generally result in deeper scour predictions than experienced in the field, according to Richardson and Davis (2001). These scour depths could occur if the abutments protruded into the main channel flow, or when a uniform velocity field is cut off by the abutment in such a manner that most of the returning overbank flow is forced to return to the main channel at the abutment end. All of the abutment scour computations (left and right abutments) assumed that the abutments were set perpendicular to the flow. If the abutments were angled to the flow, a correction utilizing K_2 would be applied to Froelich's equation or, using Figure 18.10.8, would be applied to equation (18.10.16). However, the adjustment for skewed abutments is minor when compared to the magnitude of the computed scour depths.

EXAMPLE 18.10.5

Compute the magnitude of the local scour at the left abutment for Example 18.10.1. Use Froelich's live-bed scour equation for the computation.

SOLUTION

First determine all the parameters for Froelich's equation (18.10.15):

$$\frac{y_s}{y_a} = 2.27K_1K_2 \left[\frac{L'}{y_a} \right]^{0.43} F_{r1}^{0.61} + 1$$

For spill-through abutments, $K_1 = 0.55$, and for abutments perpendicular to the flow, $K_2 = 1.0$. Abutment scour can be estimated using Froelich's equation with data derived from the WSPRO output (see Table 18.10.5). y_a at the abutment is assumed to be the average flow depth in the overbank area, computed as the cross-sectional area of the left overbank cut off by the left abutment divided by the distance the left abutment protrudes into the overbank flow:

$$y_a = A/L' = 264.65 \text{ m}^2/232.80 \text{ m} = 1.14 \text{ m}$$

The average velocity of the flow in the left overbank that is cut off by the left abutment is computed as the discharge cut off by the abutment divided by the area of the left overbank cut off by the left abutment:

$$V_e = \frac{Q_e}{A_e} = \frac{148.68 \text{ m}^3/\text{s}}{264.65 \text{ m}^2} = 0.56 \text{ m/s}$$

The Froude number of the overbank flow is:

$$F_r = \frac{V_e}{(gy_a)^{1/2}} = \frac{0.56 \text{ m/s}}{\left[(9.81 \text{ m/s}^2)(1.14 \text{ m}) \right]^{0.5}} = 0.17$$

$$\frac{y_s}{1.14} = 2.27(0.55)(1.0) \left[\frac{232.8}{1.14} \right]^{0.43} (0.17)^{0.61} + 1$$

$$\frac{y_s}{1.14} = 5.17$$

$$y_s = 5.9 \text{ m}$$

The abutment scour at the left abutment based upon Froelich's equation is 5.9 m.

EXAMPLE 18.10.6

Compute the magnitude of the local scour at the left abutment for Example 18.10.1 using the HIRE equation (18.10.16).

SOLUTION

The HIRE equation is:

$$\frac{y_s}{y_1} = 4F_{r1}^{0.33} \frac{K_1}{0.55}$$

which is based on the velocity and depth of flow passing through the bridge opening adjacent to the abutment listed in Table 18.10.6. The Froude number is:

$$F_{r1} = \frac{V_{\text{tube}}}{(gy_1)^{0.5}} = \frac{1.29 \text{ m/s}}{\left[(9.81 \text{ m/s}^2)(0.83 \text{ m}) \right]^{0.5}} = 0.45$$

and from Table 18.10.11, $K_1 = 0.55$, using equation (18.10.16):

$$\frac{y_s}{0.83 \text{ m}} = 4F_{r1}^{0.33} \left(\frac{0.55}{0.55} \right) = 4(0.45)^{0.33} = 3.07$$

$$y_s = 2.6 \text{ m}$$

The depth of scour at the left abutment as computed using the HIRE equation is 2.6 m.

EXAMPLE 18.10.7

Use the HIRE equation and the data below to compute the magnitude of the local scour at the right abutment using $V_{\text{tube}} = 2.19 \text{ m/s}$ and $y_1 = 1.22 \text{ m}$.

SOLUTION

The HIRE equation is also applicable to the right abutment since L/y_1 is greater than 25. The HIRE equation is based on the velocity and depth of the flow passing through the bridge opening adjacent to the end of the right abutment listed above. The Froude number is:

$$F_{r1} = \frac{2.19 \text{ m/s}}{\left[(9.81 \text{ m/s}^2)(1.22 \text{ m}) \right]^{0.5}} = 0.63$$

and $K_1 = 0.55$ (see Table 18.10.11), using the HIRE equation:

$$\frac{y_s}{1.22 \text{ m}} = 4F_{r1}^{0.33} \left(\frac{0.55}{0.55} \right) = 4(0.63)^{0.33} = 3.43$$

$$y_s = 4.2 \text{ m}$$

The depth of scour at the right abutment is 4.2 m.

EXAMPLE 18.10.8

For the Examples 18.10.1 through 18.10.7, the final step is to plot the results of the scour computation.

SOLUTION

Figure 18.10.9 is a plot of the total scour on the bridge cross-section. Only the computation for pier scour with piers aligned with the flow and the abutment scour computation for equation (18.10.16) were used. The top width of the local scour holes suggested is $2.0 y_s$ (Richardson and Davis, 2001).

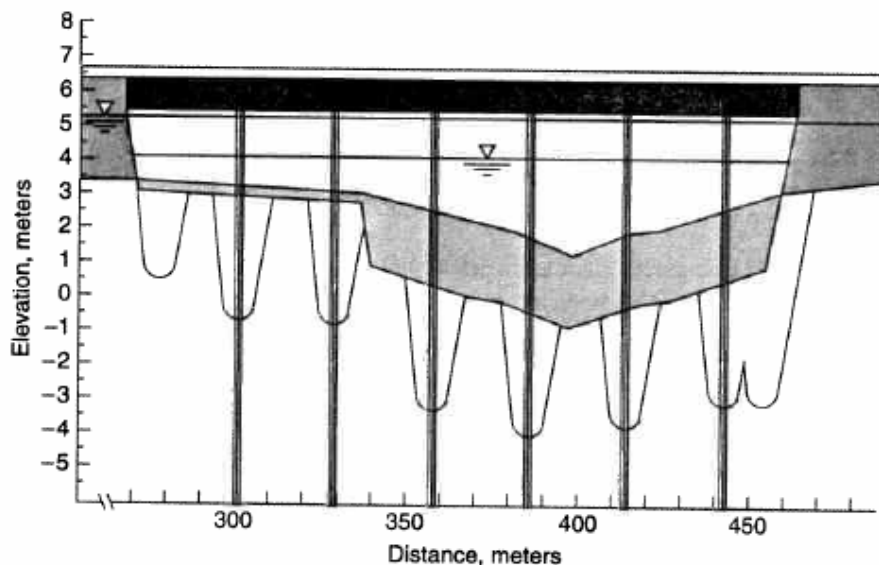


Figure 18.10.9 Plot of total scour for example problem (from Richardson, et al., 2001).

PROBLEMS

18.1.1. Given a sample of sand with D_{50} of 0.205 mm and sand density of $2,650 \text{ kg/m}^3$, with ν being $1.308 \times 10^{-6} \text{ m}^2/\text{s}$, compute fall velocity and plot the velocity with time.

18.3.1 A fine sand particle with a mean size of 0.25 mm forms the bed of a wide rectangular channel with a depth of 5.0 m and a slope of 0.0003. ν is $1.308 \times 10^{-6} \text{ m}^2/\text{s}$, $\gamma_s/\gamma = 2.7$. Compute the critical shear stress and the actual shear stress, and explain what will happen under this flow condition.

18.4.1 Using the Meyer-Peter and Muller formula, compute the sediment discharge per unit width for a rectangular channel with the following characteristics:

Water depth: 12 ft

Total flow rate: $8500 \text{ ft}^3/\text{s}$

Channel surface width: 170 ft

D_{50} and D_{90} : 2.0 mm and 2.9 mm, respectively

Gradation coefficient: 1.4

Manning's resistance coefficient for the channel bed and the channel walls 0.04 and 0.058, respectively

Friction slope: 0.0003 ft/ft

Effective mean diameter of sediment $D_m = 2.1 \text{ mm}$

18.5.1 For a certain river with total water depth of 4.30 m and mean flow velocity of 1.0 m/s, calculate and plot the vertical suspended sediment concentration profile for the D_{50} sediment size in mg/l. Given $D_{50} = 0.00026 \text{ m}$, falling velocity of the sediment particle is 0.04 m/s, kinematics viscosity of a fluid is $10^{-6} \text{ m}^2/\text{s}$, and the concentration just above the bed is 666,000 mg/l.

18.6.1 Using Colby's formula, compute the sediment discharge per unit width for the rectangular channel described in Problem 18.4.1.

18.6.2 Using Yang's gravel formula, calculate total bed-material discharge for a channel with total water flow $331.39 \text{ m}^3/\text{s}$, surface water width 150.4 m , water depth 2.39 m , $D_{50} = 0.32 \text{ mm}$, $\nu = 1.16 \times 10^{-6} \text{ m}^2/\text{s}$, particle falling velocity 0.096 m/s , mean flow velocity 1.05 m/s , and friction slope 0.0003 m/m .

18.8.1 Using Table 18.8.1, determine the density of sediment deposits for a reservoir operation 1 with 33 percent clay, 40 percent silt, and 27 percent sand.

18.8.2 For data given in Problem 18.8.1 and Table 18.8.2, determine the average density of sediments deposited after 150 years.

18.9.1 Determine the unsupported height of the structure by using the following hydraulic parameters: design discharge = $210 \text{ m}^3/\text{s}$, channel width = 42 m, $Y_u = 5.2 \text{ m}$, $Y_d = 4.7 \text{ m}$, drop height = 1.5 m.

REFERENCES

- Ackers, P., and W. R. White. "Sediment Transport: New Approach and Analysis," *Journal of Hydraulic Engineering*, vol. 99, no. HY-11, pp. 2041-2060, 1973.
- American Society of Civil Engineers (ASCE), "Nomenclature for Bed Forms in Alluvial Channels," by the Task Force on Bed Forms in Alluvial Channels, John F. Kennedy, Chmn, *Journal of the Hydraulics Division*, ASCE, vol. 92, No. HY3, Proc. Paper 4823, pp. 51-64, May 1966.
- Arneson, L., J. O. Shearman, and J. S. Jones, "Evaluating Scour at Bridges Using WSPRO," unpublished paper presented at the 71st Annual Transportation Research Board meeting, Washington, D.C., January, 1991.
- Bradley, J. N., "Hydraulics of Bridge Waterways," Hydraulic Design Series No. 1, Federal Highway Administration, U.S. Department of Transportation, Washington, D.C., 1978.
- Brady, N. S., *The Nature and Properties of Soils*, 8th ed., Macmillan, New York, 1974.
- Brice, J. C., and J. C. Blodgett, "Countermeasures for Hydraulic Problems at Bridges, vol. 1, Analysis and Assessment, FHWA/RD-78-162," Federal Highway Administration, U.S. Department of Transportation, Washington, D.C., 1978a.
- Brice, J. C., and J. C. Blodgett, "Countermeasures for Hydraulic Problems at Bridges, vol. 2, Case Histories for Sites 1-283, FHWA/RD-78-163," Federal Highway Administration, U.S. Department of Transportation, Washington, D.C., 1978b.
- Brune, G. M., "Trap Efficiency of Reservoirs," *Trans. Am. Geophys. Union*, vol. 34, no. 3, pp. 407-418, 1953.
- Chow, V. T., *Open Channel Hydraulics*, McGraw-Hill, New York, 1959.
- Colby, B., "Practical Computations of Bed Material Discharge," *Journal of Hydraulic Engineering*, vol. 90, HY2, pp. 217-246, 1964.
- deVries, J., "Altgermanische Religionsgeschichte," Berlin, Germany, 1970.
- duBoys, P., "The Rhone and Streams with Movable Beds," *Annales des ponts et chaussees*, section 5, vol. 18, pp. 141-195, 1879.
- Einstein, H. A., "The Bedload Function for Bedload Transportation in Open Channel Flows," Technical Bulletin No. 1026, U.S.D.A. Soil Conservation Service, 1950.
- Einstein, H. A., and N. L. Barbarossa, "River Channel Roughness," *Trans. ASCE*, vol. 117, pp. 1121-1146, 1952.
- Exner, F. M., "Über die wechselwirkung zwischen wasser und geschiebe in flussen," *Sitzberichte der Akademie der Wissenschaften*, Wien, Austria, Sec. IIA, 133:199, 1925.
- Froelich, D. C., "Abutment Scour Prediction," Presentation, Transportation Research Board, Washington, D.C., 1989.
- Garcia, M., "Sedimentation and Erosion Hydraulics," in *Hydraulic Design Handbook*, (edited by L. W. Mays), McGraw-Hill, New York, 1999.
- Goldstein, S., "The Steady Flow of Viscous Fluid Past a Fixed Spherical Obstacle at Small Reynolds' Number," *Proceedings of the Royal Society of London*, Series A, vol. 123, 1929.
- Kennedy, J. F., "The Formation of Sediment Ripples, Dunes, and Antidunes," *Annual Review of Fluid Mechanics*, (edited by W. R. Sears), vol. 1, Annual Reviews, Inc., Palo Alto, California, pp. 147-168, 1969.
- Lagasse, P. F., F. Schall, F. Johnson, E. V. Richardson, and F. Chang, "Stream Stability at Highway Structure," Federal Highway Administration, U.S. Department of Transportation, Hydraulic Engineering Circular No. 20, Washington, D.C., November, 2001a.
- Lagasse, P. F., L. W. Zewenbergen, J. D. Schall, and P. E. Clapper, "Bridge Scour and Stream Instability Countermeasures," 2nd Edition, Federal Highway Administration, U.S. Department of Transportation, Hydraulic Engineering Circular No. 23, FHWA NHI 01-003, Washington, D.C., 2001b.
- Laursen, E. M., "Scour at Bridge Crossings," *Journal of the Hydraulics Division*, ASCE, vol. 86, no. 1142, 1960.
- Mays, L. W., and C. Carriaga, Aqua Fria River Sediment Transport Study, Final Report, Flood Control District of Maricopa County, Phoenix, Arizona, 1993.
- Meyer-Peter, E., and R. Müller, "Formular for Bed-Load Transport," *Proceedings*, International Association for Hydraulic Structures Research, 2nd Meeting, pp. 39-64, Stockholm, Sweden, 1948.
- Miller, C. R., "Determination of the Unit Weight of Sediment for Use in Sediment Volume Computation," U.S. Bureau of Reclamation, Denver, Colorado, 1953.
- Oseen, C., *Hydrodynamik*, Chapter 10, Akademische Verlagsgesellschaft, Leipzig, Germany, 1927.
- Pemberton, E. L., and J. M. Lara, "Computing Degradation and Local Scour," Technical Guideline for Bureau of Reclamation, Engineering Research Center, Denver, Colorado, January 1984.
- Prasuhn, A. L., *Fundamentals of Hydraulic Engineering*, Holt, Rinehart and Winston, New York, 1987.
- Richardson, E. V., and S. R. Davis, "Evaluating Scour at Bridges," 4th edition, Hydraulic Engineering Circular No. 18, Publication No. FHWA NHI 01-001, Federal Highway Administration, U.S. Department of Transportation, Washington, D.C., 2001.
- Richardson, E. V., D. B. Simons, and P. Y. Julien, "Highways in the River Environment," FHWA-HI90-016, Federal Highway Administration, U.S. Department of Transportation, Washington, D.C., 1990.
- Richardson, E. V., D. B. Simons, and P. F. Lagasse, "River Engineering for Highway Encroachments," Hydraulic Design Series No. 6, Publication No. FHWA/NHI 01-004, Federal Highway Administration, U.S. Department of Transportation, Washington, D.C., 2001.
- Schwab, G. O., R. K. Frevert, T. W. Edminster, and K. K. Barnes, *Soil and Water Conservation Engineering*, 3rd ed., Wiley, New York, 1981.
- Shen, H. W. and P. Y. Julien, "Erosion and Sediment Transport," in *Handbook of Hydrology*, (edited by D. R. Maidment), McGraw-Hill, New York, 1993.
- Shields, A., "Anwendung der Aechchkeits-mechanik und der turbulenz forschung auf die Gerschiebewegung," *Mitt Preussische, Versuchsanstalt für Wasserbau and Schiffbau*, Berlin, Germany, 1936.
- Shulits, S., "The Schoklitsch Bed-Load Formula," *Engineering*, London, England, June 21, 1935, pp. 644-646, and June 28, 1935, p. 687.
- Simons, D. B., and F. Sentürk, *Sediment Transport Technology*, Water Resources Publications, Littleton, Colorado, 1977.
- Strickler, A., "Beiträge zur Frage der Geschwindigkeitsformel und der Rauhgkeitszahlen für ströme, Kanäle und geschlossene Leitungen," *Mitteilungen des Eidgenössischen Amtes für Wasserwirtschaft* 16, Bern, Switzerland, 1923 (translated as "Contributions to the Question of a Velocity Formula and Roughness Data for Streams, Channels, and Closed Pipelines," by T. Roesgan and W. R. Brownie, Translation T-10, W. M. Keck Lab of Hydraulics and Water Resources, California Institute of Technology, Pasadena, California, January 1981).
- U.S. Army Corps of Engineers (USACE), "Scour and Deposition in River and Reservoirs, Users Manual," Hydrologic Engineering Center, Davis, California, 1991.
- U.S. Bureau of Reclamation, *Design of Small Dams*, U.S. Gov. Printing Office, Denver, Colorado, 1987.
- U.S. Department of Agriculture, Agricultural Research Service (USDA-ARS), "A Universal Equation for Predicting Rainfall-Erosion Losses," USDA-ARS Special Report 22-26, 1961.